ENEA

Ente per le Nuove tecnologie, l'Energia e l'Ambiente

Ministero dello Sviluppo Economico

RICERCA SISTEMA ELETTRICO

Analysis of the two-phase flow meters and densitometers with the reference to the SPES-3 facility

C. Bertani, M. De Salve, M. Malandrone, A. Mosetto, B. Panella

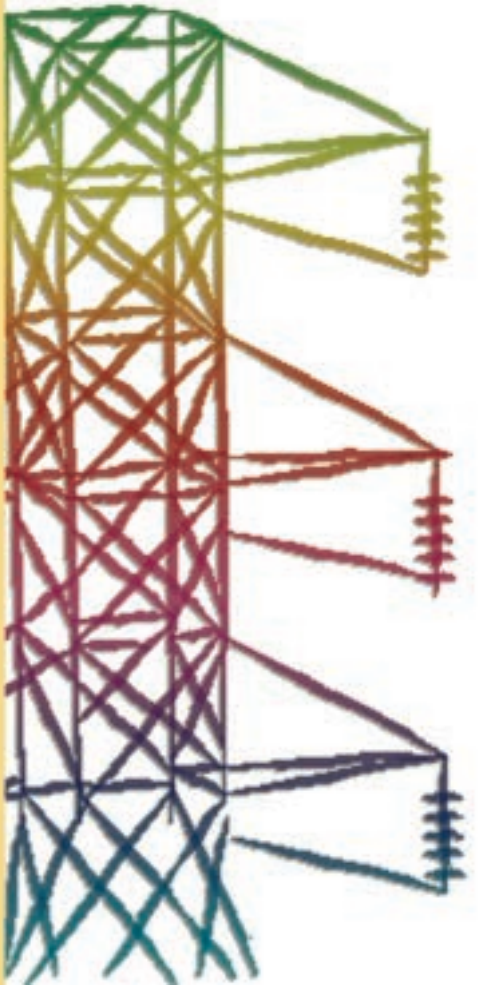

Report RSE/2009/74

Ente per le Nuove tecnologie,
l'Energia e l'Ambiente

Ministero dello Sviluppo Economico

RICERCA SISTEMA ELETTRICO

Analysis of the two-phase flow meters and densitometers with the reference to the SPES-3 facility

C. Bertani, M. De Salve, M. Malandrone, A. Mosetto, B. Panella

Report RSE/2009/74

ANALYSIS OF THE TWO-PHASE FLOW METERS AND DENSITOMETERS WITH THE REFERENCE TO THE SPES-3 FACILITY

C. Bertani, M. De Salve, M. Malandrone, A. Mosetto, B. Panella (CIRTEN)

Dicembre 2008

Report Ricerca Sistema Elettrico
Accordo di Programma Ministero dello Sviluppo Economico – ENEA
Area: Produzione e fonti energetiche
Tema: Nuovo Nucleare da Fissione
Responsabile Tema: Stefano Monti, ENEA

CIRTEN
CONSORZIO INTERUNIVERSITARIO
PER LA RICERCA TECNOLOGICA NUCLEARE

POLITECNICO DI TORINO
DIPARTIMENTO DI ENERGETICA

Analysis of the two-phase flow meters and densitometers with reference to the SPES facility

Analisi dei misuratori di portata e densità per i deflussi bifase con riferimento al circuito SPES

Cristina Bertani, Mario De Salve, Mario Malandrone, Annamaria Mosetto, Bruno Panella

CIRTEN CERSE-POLITO RL 1252/2008

PISA, Dicembre 2008

Lavoro svolto in esecuzione della linea progettuale LP2 punto L dell'AdP ENEA-MSE del 21/06/07 Tema 5.2.5.8 – "Nuovo Nucleare da Fissione".

INDEX

1. Introduction

This report is a summary of the master thesis *Two phase flow instrumentation for the simulation of the IRIS nuclear reactor*. It is focused on the choice of the best combination of two-phase flow instruments to provide the measurement of the mass flow rate in some locations in the SPES3 experimental facility. The SPES3 facility is a scaled model (on a 1/100 volume scale) of the IRIS (International Reactor Innovative and Secure) reactor.

The SPES3 facility has to prove that the thermodynamical coupling between the Reactor Vessel (RV) and the Containment can effectively stop the leak and guarantee a safe course in case of accident. The fluid flowing from the Reactor Vessel to the Containment and viceversa is mainly a two-phase mixture of steam and liquid. That is why the measurement of the two-phase flow rates in the SPES3 pipe lines is crucial to assess the effective efficiency of the IRIS integral structure.

The analysis is focused on the Lower Break LOCA, i.e. the break of the DVI (Direct Vessel Injection) lines. Those lines connect the Reactor Vessel to the tanks containing the water needed to guarantee a proper cooling of the core in case of accident.

In the SPES3 facility two DVI break lines are foreseen in order to simulate both the SPLIT break and the DOUBLE ENDED GUILLOTINE (DEG) break. Both the break lines need to be equipped with two phase flow instrumentation to provide the measurement of the two-phase mass flow rate. The mass flow rate and the void fraction expected during the DEG break of the DVI lines has been calculated through a simulation of the accident with the RELAP software. In the SPLIT break line (RV side of the break) a maximum void fraction around 0.56 is expected, while in the DEG break line the trend of the void fraction is highly oscillating between 0 and 1.

The void fraction variation in a wide range of values worsen the mass flow rate measurement process. For a proper calculation of the mass flow rate both the flow velocity and the density should be detected. Some types of densitometers (density measurement) can detect the void fraction with a reasonable uncertainty in these conditions, too, but the main problem is the interpretation of the signal from the flow meter (velocity measurement). The output of the meter needs to be related both to the

velocity of the gaseous phase and to the velocity of the liquid phase, basing on the different flow patterns.

In the next two sections a description of the most important flow meters and densitometers will be presented. In the last section the performances of each instrument will be judged according to the installation requirements in the SPES3 facility. The following figure shows the two phase flow instrumentation as it will be located on the DVI break lines.

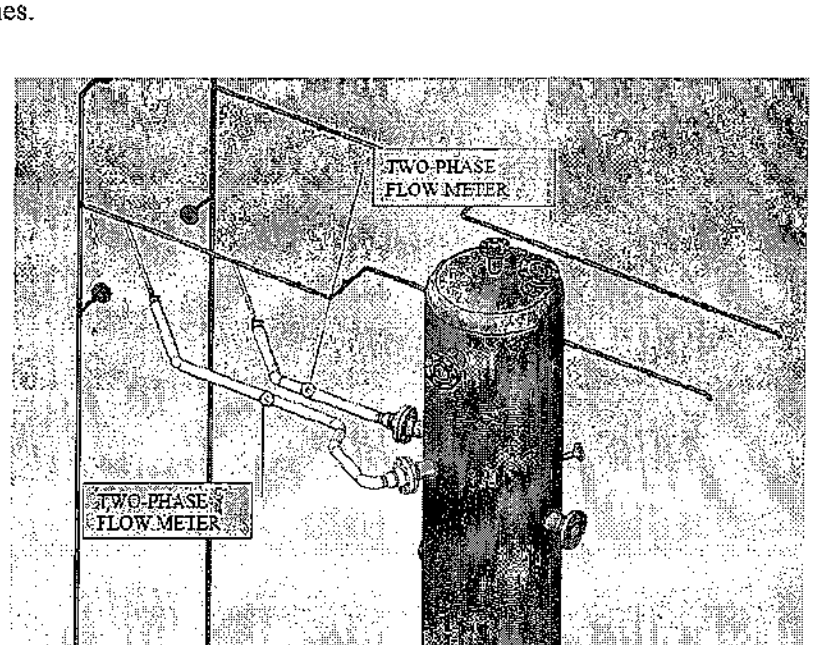

Figure 1: Two phase flow instrumentation position on the DVI break lines.

2. Flow meters

The second section is focused on the description of the flow meter devices capable of measuring the two-phase flow velocity. Firstly some criteria that each meter needs to satisfy are listed, then the performances of each device, related to each criteria, are described.

Flow meter selection criteria

The most important criteria that the flow-meter has to satisfy are listed below, with a brief explanation:

1. Two phase flow handling capability and easy modeling-Criteria 1
2. High Span (minimal number of parallel lines)-Criteria 2
3. Good Repeatability and Accuracy-Criteria 3
4. Minimal Installation Constraints (straight pipe length between the meter and the disturbance source)-Criteria 4
5. Simplicity of Calibration; effects of calibration and operation temperature differences (different fluid properties, flow-meter material expansion)-Criteria 5
6. Capability of Handling Different Flow Regimes (temperature range, pressure range)-Criteria 6
7. Transient Operation Capability (time response)-Criteria 7
8. Bi-directional Operation Capability-Criteria 8
9. Minimal Regulatory Requirements-Criteria 9
10. Suitable Physical Dimension-Criteria 10
11. Minimal Disturbance to the Flow-Criteria 11
12. Simplicity of Data Acquisition-Criteria 12
13. Capability of Operating in Different Assembling Orientation (horizontal, vertical, inclined)-Criteria 13

2.1. Differential-pressure meters

The basic model for the calculation of the mass flow rate is the following:

$$\dot{m} = C\sqrt{\rho_{TP}\Delta p_{TP}}$$

$$\rho_{TP} = \alpha\rho_g + (1-\alpha)\rho_l$$

$\dot{m}$	Two-phase mass flow rate [kgs^{-1}]
Δp_{TP}	Two-phase pressure drop [Pa]
ρ_{TP}	Two-phase mixture density [kgm^{-3}]
ρ_l	Liquid density [kgm^{-3}]
ρ_g	Vapor density [kgm^{-3}]
α	Two-phase mixture void fraction

The proportionality constant C can be extrapolated from single-phase flow literature (provided the meter is single-phase standard design) and tailored on the basis of preliminary in-situ testing. The calculation of the two-phase mixture density ρ_{TP} requires, in principle, the side measurement of the void fraction α (typically performed in academic research).

Some authors suggested two-phase flow correlation to correct the reading of a differential pressure flow-meter, usually applied just to the measurement of single-phase flow, in order to obtain the correspondent mass flow rate in two phase flow. Miller (1996) suggests the Murdock equation for two-phase flow both in an orifice meter and in a Venturi meter (Miller (1996), Murdock (1961)*).

Hewitt (1978) lists many other references for the study of the pressure drop across Venturi meters and orifice in two-phase flow (page 96,97).

2.1.1. Orifice plates

1. **Two phase flow handling capability and easy modeling-<u>Criteria 1</u>-** Simplicity and predictability is guaranteed (in single phase flow) only if the meter is used in the same condition in which the original data was obtained. The standards connected with this type of meter are ISO 5167-1(BN EN ISO 5167-1).

   To use an orifice plate with two phase flow, there are three approaches (Baker (2000)):

   - ✓ adjusting the value of density to reflect the presence of a second component.

- ✓ adjusting the discharge coefficient to introduce the presence of the second component
- ✓ relating two phase pressure drop to that which would have occurred if all the flow were passing either as a gas or as a liquid (suggested by (Miller, 1996)).

Most of the available correlations for two-phase flow are valid only for low (x<0.1) or very high (x>0.95) steam quality. For other references see paragraph 5.8, page 113, Baker (2000).

The wet-gas flow is defined (in Steven (2006)) as a two phase flow that has a Lockart-Martinelli parameter value (X) less or equal to 0.3, where X is defined as:

$$X = \sqrt{\left(\frac{dp}{dz}\right)_l \Big/ \left(\frac{dp}{dz}\right)_g},$$

where $\left(\frac{dp}{dz}\right)_k$, k=g,l represents the pressure gradients for single-phase gas and liquid flow as fractions of the total two-phase mass flow rate, respectively (Whalley (1987)).

Murdock derived a correlation to predict the behavior of an orifice plate in two-phase flow, horizontal mounting (Steven (2006a), Murdock (1962)*). The experimental data were not restricted to wet gas flow only. They ranged in the following intervals:

- ✓ 31.8 mm < pipe diameter < 101.6 mm
  - o bar < pressure < 63 bar
- ✓ 0.025 bar < pressure drop < 1.25 bar
- ✓ 0.11 < x< 0.98
- ✓ $0.2602 < \beta = \frac{d}{D} < 0.5$
- ✓ $13000 < \mathrm{Re}_g < 1270000$

The correlation is expressed as:

$$\dot{m}_g = \frac{\dot{m}_{g,Apparent}}{1+1.26X_m},$$

where $\dot{m}_{g,Apparent}$ is the uncorrected value of the gas mass flow rate as detected by the orifice and $\dot{m}_g$ is the corrected value. The constant (1.26)

is an empirical value. X_m is the modified Lockart-Martinelli parameter, defined as:

$$X_m = \frac{\dot{m}_l}{\dot{m}_g}\sqrt{\frac{\rho_g}{\rho_l}}\frac{k_g}{k_l},$$

where k_g and k_l are the gas and liquid flow coefficient, respectively. Each of them is the product of the velocity of approach, the discharge coefficient and the expansibility factor. The correlation is dependent only on X_m, while the influence of the flow pattern is not considered.

The pressure drop in single phase gas flow is lower than the pressure drop in two-phase, wet steam flow, so the value detected by the orifice meter, without correction, tends to overestimate the gas mass flow rate.

A possible correlation to obtain the ratio between the pressure drop across an orifice in two-phase flow and in single phase flow was studied by Chisholm (Hewitt (1978), Chisholm (1972)*).

Chisholm further developed the two-phase orifice plate meter theory between 1967 and 1977 (Chisholm (1967)*, (1977)*). He concluded that the orifice meter response to wet steam, two phase flow in horizontal mounting does not only depend on the modified Lockart-Martinelli parameter (Xm), but also on the gas-liquid density ratio (i.e. on the pressure). His model results in the following formula:

$$\dot{m}_g = \frac{\dot{m}_{g,Apparent}}{\sqrt{1+\left[\left(\frac{\rho_g}{\rho_l}\right)^{1/4}+\left(\frac{\rho_l}{\rho_g}\right)^{1/4}\right]X_m + X_m^2}},$$

where m_g, $m_{g,Apparent}$ and X_m have the same meaning as in the Murdock's equation and ρ_k, $k = g,l$ are the gas/liquid density.

The modern preference is to ignore the orifice meter as an instrument to measure the two-phase flow, since it acts as a dam for the liquid flow rate. It's advisable to use instead a Venturi flow meter instead as it is less likely to cause blockage to the liquid phase (Steven (2006a)).

2. **High Span (minimal number of parallel lines)**-**Criteria 2**-The typical span of this type of meter is 5:1 (table 3.1, page 48, Baker, 2000), so that an array of differential meters is required to fully cover SPES3 needs,

driven by an active control system to place in line the proper meter during the test and valve off all the others.

3. **Good Repeatability and Accuracy-Criteria 3**-The accuracy of the orifice plate for single phase flow is in the range 2%-4% full scale (http://www.engineeringtoolbox.com/orifice-nozzle-venturi-d_590.html, March 10, 2008).
4. **Minimal Installation Constraints (straight pipe length between the meter and the disturbance source)-Criteria 4**-A minimum straight pipe length is requested upstream and downstream of an orifice plate; ISO 5167 standard gives the complete information (one phase flow) of which an abstract is contained in table 5.1, page 103, Baker (2000). See Chapter 1, paragraph 4. In the table β is defined as the ratio d/D of orifice diameter to pipe internal diameter. The presence of bends and elbows in the pipe can influence the meter measurement: decrease in bends angle does not necessarily reduce the disturbing influence. Putting flow conditioners between the bend and the meter could not be always the right solution because it may introduce additional errors. Conditioner-flow-meter combinations should be calibrated as one unit, see figure 5.5, page 104, Baker (2000).
5. **Simplicity of Calibration; effects of calibration and operation temperature differences (different fluid properties, flow-meter material expansion)-Criteria 5**-The standards (ISO 5167-1(BN EN ISO 5167-1)) define precisely how to construct, install and use the orifice meter (for single phase flow).
6. **Capability of Handling Different Flow Regimes (temperature range, pressure range)-Criteria 6**-Not Available data (NA).
7. **Transient Operation Capability (time response)-Criteria 7**-Orifice plates and Venturi meters are typically designed for steady state applications. Fast transient response requires special care in the design and may require the correction of the signal on the basis of the modeling of the meter, which is doable but not straightforward.

   If the flow is not steady, but pulsating, the measurement error will increase because of different reasons (Baker, 2000):

- ✓ square root error
- ✓ resonance
- ✓ limitations in the pressure measurement device.

The first one is connected to the capability of a fast response of the pressure meter, the second to the possibility of a correspondence between the pulsating frequency and the resonance frequency of some components. Commercially available differential pressure transmitters are generally unsuitable for dynamic measurement (Baker (2000), Clark (1992))*. The response is highly influenced by the length of transmission pipe lines and the medium used (gas or liquid).

8. **Bi-directional Operation Capability-Criteria 8**-Differential meters are typically one-directional. Bi-directional capability can be obtained either with a modified design or with in-situ testing of a one-directional meter in reverse flow conditions.
9. **Minimal Regulatory Requirements-Criteria 9**-There are not particular regulatory requirements to install this type of flow-meter.
10. **Suitable Physical Dimension-Criteria 10**-The physical dimension of the flow-meter doesn't represent an issue because the plate is contained into the pipe.
11. **Minimal Disturbance to the Flow-Criteria 11**-The ISO standards provide an expression for pressure loss across an orifice plate (eq. 5.8, page 99, Baker (2000)). A typical value for the pressure loss is about $0.73\Delta p$, where Δp represents the differential pressure across the meter.
12. **Simplicity of Data Acquisition-Criteria 12**-The pressure transducers are capable of following the fast transients expected in the SPES3 facility.
13. **Capability of Operating in Different Assembling Orientation (horizontal, vertical, inclined)-Criteria 13**-The correlation available for the correction of the orifice meter reading in wet steam flow has been based on a experiment with a horizontal mounting orifice meter. It is advisable to use the correlation in conditions as closer as possible to the original experiment.

2.1.2. Venturi meters and standard nozzles

1. **Two phase flow handling capability and easy modeling-Criteria 1-** Some of the most important effects of the two-phase flow to the response of a Venturi meter are described by Steven (2006a):

- ✓ The meter reading increases as the liquid load increases (i.e. the Lockart-Martinelli parameter increases. The effect is higher if the gas/liquid density ratio is lower (see Figure 13, Steven (2006a)).
- ✓ The gas Froude number is defined as the square root of the ratio between the gas inertia (if the gas flows alone) and the gravity force on the liquid phase:

$$\checkmark \quad Fr_g = \sqrt{\frac{J_g^2 \rho_g}{gD\left(\rho_l - \rho_g\right)}},$$

where Jg is the superficial velocity of the gas phase, ρ_k, $k = g, l$ are the gas and liquid phase densities and D is the pipe diameter. If the gas Froude number increases, for fixed gas to liquid density ratio, the over reading increases. If the liquid density ratio and the Lockart-Martinelli parameters are fixed, the gas Froude number is higher if the superficial gas velocity is higher. With an increase in the gas superficial mass velocity the differential pressure across the meter is increasing, too. See Figure 16, Steven (2006a).

- ✓ Stewart presented the response of a Venturi meter to wet-gas flow for two fluids (nitrogen and kerosene) (Steven (2006a), Stewart (2003)*). The gas to liquid density ratio (i. e. the pressure) and the gas Froude number were fixed. Different sets of data were collected for different β ratio. The Venturi meter over reading decreases if β increases (see Figure 17, Steven (2006a)).
- ✓ The response of the Venturi meter in two-phase flow is likely to be influenced by the liquid properties. Reader-Harris tested a 4'' Venturi meter with two different values of gas to liquid density ratio (0.024 and 0.046). At low gas flow rates (i.e. at low gas Froude number) there was not significant liquid property effect, but at higher gas Froude number it was found that the water wet gas flow would have a lower increase in the

reading in comparison with kerosene wet gas flow under the same flow conditions (Steven (2006a), Reader-Harris et al (2005)*). Other experiments by Steven (2006b)* supported the results obtained by Reader-Harris. Steven also postulated that the different results obtained with different liquid property are a direct consequence of the flow pattern that can be different for similar flow parameters, but different liquid properties.

- ✓ Steven (2006a) indicated also a possible diameter effect on Venturi meter wet gas over reading. He presented the comparison of two data sets for two different Venturi diameters. The gas to liquid density ratio and the gas Froude number in the two experiments were very close to each other. The device with the bigger diameter registers the higher over reading. Steven concluded that the difference in the over reading is due to the different flow regimes established inside the pipes. The larger meter has more entrainment (is more in the annular mist region) than the smaller meter. These observations need to be confirmed by a more detailed testing of the Venturi meter with various diameters.

The application of Venturi meters and nozzles in two-phase flow was studied by Baker (1991). A correlation proposed by Baker (2000), de Leeuw (1997, cf. 1994)* is valid only for gas with a small amount of liquid (the Lockhart-Martinelli parameter has to be less than 0.3).

The correlation is based on the data from a 4'' diameter, Sch. 80, $\beta = 0.401$ Venturi meter with nitrogen and diesel oil. The de Leeuw study is based on the previous Chisholm's orifice plate work. The following equations show the correlation:

$$\dot{m}_g = \frac{\dot{m}_{g,Apparent}}{\sqrt{1 + CX + X^2}},$$

$$C = \left(\frac{\rho_g}{\rho_l}\right)^n + \left(\frac{\rho_l}{\rho_g}\right)^n,$$

$$n = 0.606\left(1 - e^{-0.746Fr}\right) \quad \text{if} \quad Fr \geq 1.5$$

$$n = 0.41 \quad \text{if} \quad 0.5 \leq Fr < 1.5$$

$\dot{m}_{g,Apparent}$ is the uncorrected value of the gas mass flow rate as detected by the meter, $\dot{m}_g$ is the corrected value and Fr is the gas Froude number. The difference between the de Leeuw formulation and the Chisholm

formulation for orifice plates is the values of the n exponent. This depends on the gas Froude number.

De Leeuw stated that the value of n is dependent on the flow regime. For stratified flow (i.e. for $Fr < 1.5$) n is constant and equal to 0.41. As the flow pattern changes from stratified to annular mist and on towards mist flow, the over reading for a set value of the quality will increase. He claimed that for that meter geometry, for a known value of the liquid flow rate and within the test matrix parameters of the data set used, this correlation is capable of predicting the gas mass flow rate with ±2% uncertainty.

Fincke (1999) shows that a Venturi meter used to measure two-phase flow, by the single-phase formulation, over predicts the effective flow rate. This is due to an increase in the pressure drop in two-phase condition, because of the interaction between the gas and the liquid phase.

The author also proves that the Murdock correlation (Fincke (1999), Murdock (1961)*) is not sufficient to adjust the apparent reading to the reference flow rate value; the gas flow rate evaluated with the correlation is affected by an error that can reach 20% of the reading.

It could be concluded that the application of the Murdock correlation to a data set detected by a Venturi meter is somewhat questionable, since Murdock's correlation has been firstly studied to be applied to orifice plate data set. The first correlation for the correction of a Venturi meter response to wet gas flow has been published in 1997 by de Leeuw.

Fincke (1999) obtained the following performance using an extended throat nozzle to measure the two-phase flow rate of low pressure (15 psi-1 bar) air-water mixtures and of high pressure (400 psi-27.6 bar, 500 psi-34.5 bar) natural gas-Isopar M mixtures:

- ✓ Accuracy of ±2%of reading for $m_l / m_g < 10\%$.
- ✓ Accuracy of ±4% of reading for $10\% < m_l / m_g < 30\%$.

The studied interval corresponds to $0.95 < \alpha < 1.0$. During measurement the ratio between the liquid flow rate and the gas flow rate was known.

Based on the Venturi meter measurements and derived set of equations, the gas flow rate was calculated.

2. **High Span (minimal number of parallel lines)-Criteria 2**-Typical spans of Venturi meters is 5:1 (see table 3.1, page 48, Baker (2000)), so that an array of differential meters is required to fully cover SPES3 needs, driven by an active control system to place in line the proper meter during the test and valve off all the others.
3. **Good Repeatability and Accuracy-Criteria 3**-The accuracy of the Venturi meter is usually around 1% of full range in one phase flow (http://www.engineeringtoolbox.com/orifice-nozzle-venturi-d_590.html, March 10, 2008).

   Steven (2002) compared the results of seven correlations for the correction of the Venturi meter response to wet gas flow:

   - ✓ Homogeneous model (see Steven (2002) for details)
   - ✓ Murdock correlation: it has been previously described in the section dedicated to the orifice plates.
   - ✓ Chisholm correlation: it has been previously described in the section dedicated to the orifice plates.
   - ✓ Lin correlation (Steven (2002), Lin (1982)*): it was originally developed for orifice meter, it considers the influence of the pressure and of the liquid mass content on the meter over reading.
   - ✓ Smith & Leang correlation (Steven (2002), Smith and Leang (1975)*): it was developed for orifice plates and Venturi meters, it introduces a blockage factor that accounts for the partial blockage of the pipe area by the liquid. The blockage factor is a function of the quality only.
   - ✓ the modified Murdock correlation: it was developed by Phillips Petroleum. The Murdock constant M has been replaced by a new value (1.5 instead of 1.26), to adapt the formula to Venturi meter over reading.

   Some of them (Murdock, Chisholm, Lin and Smith & Leang correlations) were actually studied for the orifice plate response in two-phase flow, but they were extensively used in the natural gas industry for Venturi meter applications. The modified Murdock and the de Leeuw correlations were instead studied for the Venturi meter reading correction.

The meter studied was an ISA Controls standard North Sea specification 6'', $\beta = 0.55$ Venturi and it was tested with a nitrogen and kerosene mixture. The experiment was conducted for three pressure values (20 bar, 40 bar and 60 bar) and four values of the volumetric gas flow rates (400 m^3/h, 600 m^3/h, 800 m^3/h and 1000 m^3/h).

The difference between the actual mass gas flow rate and the mass gas flow rate evaluated with the seven correlations was expressed as the root mean square fractional deviation:

$$d = \sqrt{\frac{1}{n}\sum_{i=1}^{n}\left(\frac{m_{g,\text{corrected},i} - m_{g,\text{experimental},i}}{m_{g,\text{experimental},i}}\right)^2}.$$

The data are listed in the following table (Table 1). The d value was calculated for the whole data set and then for each pressure value separately.

All pressures	d	40 bar	d
de Leeuw	0.0211	de Leeuw	0.0193
Homogeneous	0.0237	Homogeneous	0.0220
Lin	0.0462	Murd, M=1.5	0.0410
Murd, M=1.5	0.0482	Lin	0.0448
Murd, M=1.26	0.0650	Murd, M=1.26	0.0589
Chisholm	0.0710	Chisholm	0.0658
Smith & Leang	0.1260	Smith & Leang	0.1199
20 bar	d	60 bar	d
de Leeuw	0.0279	de Leeuw	0.0140
Homogeneous	0.0285	Homogeneous	0.0202
Lin	0.0449	Murd, M=1.5	0.0287
Murd, M=1.5	0.0677	Lin	0.0479
Chisholm	0.0793	Murd, M=1.26	0.0504
Murd, M=1.26	0.0823	Chisholm	0.0675
Smith & Leang	0.1159	Smith & Leang	0.1401

Table 1: Root mean square fractional deviation for the whole data set (all pressures) and for each individual pressure, Steven (2002), Table 2.

The most important observations are:

- ✓ de Leeuw correlation has the best performance and is the best choice for correcting the Venturi meter over reading in wet steam. It takes into account the influence of the pressure (gas to liquid density ratio), of the gas volumetric flow rate and of the flow patterns.
- ✓ The homogeneous model predicts the exact mass flow rate with a surprising little error in comparison to the other models. The

author deduced that the good agreement between this model and the actual mass flow rate should have been dictated by the similarity of the flow conditions in the experiment and the assumption of the model. The model performances are in fact increasing with the pressure and it is generally assumed that the greater the pressure, the larger is the amount of water in suspension in the gas flow (with a more homogenized flow pattern).

- ✓ The modified Murdock correlation, despite studied on purpose for the correction of the Venturi meter over reading, gives the worst agreement with the actual gas mass flow rate. This formula has been developed by Phillips Petroleum and the conditions in which it was validated are unknown.

4. **Minimal Installation Constraints (straight pipe length between the meter and the disturbance source)**-Criteria 4-The necessary values of straight tube between a bend (or more bends) and the meter are the same for Venturi and nozzles and are shown in table 6.2, page 136, Baker (2000). The data proposed by ISO standards have been reviewed by Baker (2000), NEL (National Engineering Laboratory) (1997a)*, that suggests longer straight pipe lengths (for single phase flow only).
5. **Simplicity of Calibration; effects of calibration and operation temperature differences (different fluid properties, flow-meter material expansion)**-Criteria 5-The meter is one of the oldest method of measuring flow and the design is extensively described in the standard ISO 5167-1 (for single phase flow). Hewitt (1978), Harris (1967)* shows that the calibration of a Venturi meter, for steam water mixtures, is affected by the geometry of the upstream pipework: the calibration equation that relate Δp and the flow rate is different depending on the different pipe configuration.
6. **Capability of Handling Different Flow Regimes (temperature range, pressure range)**-Criteria 6-Fincke (1999) tested a Venturi flow meter in annular and mist annular flow with a good accuracy, but for other flow patterns the applicability of a Venturi meter depends on the

homogenization of the mixture. If the flow is well homogenized, then it can be treated as a single phase flow with an average density of the gas and liquid $\left(\overline{\rho}=\alpha\rho_g+(1-\alpha)\rho_l\right)$. Fincke (1999) does not present test results for this latter situation.

Since the only available correlation (de Leeuw's correlation) to correct the reading of a Venturi meter in two phase flow is affected by the flow pattern, the meter is actually influenced by the distribution of the phases. The formula is valid only for wet steam and is used mainly in the natural gas production industry.

7. **Transient Operation Capability (time response)-Criteria 7**-Since the meter is based on the same physical principle of the orifice plate, the major issue is represented by the dynamic response of the pressure meter, that is influenced by the length of transmission and the medium used (gas or liquid). According to Ferri (Ferri (2008)), the dynamic response of the pressure transducers and transmitters is fast enough to measure the expected transients in SPES3.
8. **Bi-directional Operation Capability-Criteria 8**-Differential meters are typically one-directional. Bi-directional capability can be obtained either with a modified design (which could reduce the extrapolability of literature material) or with in-situ testing of a one-directional meter in reverse flow conditions.
9. **Minimal Regulatory Requirements-Criteria 9**-There are not particular regulatory requirements to install this type of flow-meter.
10. **Suitable Physical Dimension-Criteria 10**-The inlet diameter of the meter is the same as of the pipe, so no issues are expected about dimensions and weight.
11. **Minimal Disturbance to the Flow-Criteria 11**-The value of pressure loss across the Venturi meter is about 0.05-0.2 Δp, where Δp represents the differential pressure between the entrance and the throat, so it is much lower than the one for the orifice plates (based on the single phase flow only).
12. **Simplicity of Data Acquisition-Criteria 12**-The pressure transducers are capable of following the fast transients expected in the SPES3 facility.

13. **Capability of Operating in Different Assembling Orientation (horizontal, vertical, inclined)**-**Criteria 13**-The correlation available for the correction of the Venturi meter reading in wet steam flow has been based on a experiment run in a horizontal mounting Venturi meter. It is advisable to use the correlation in conditions as closer as possible to the original experiment.

2.2. Turbine meters

1. **Two phase flow handling capability and easy modelling-Criteria 1-** Turbine meters have been used for two-phase flow applications and turbine meter designs for wet gas metering are currently available. The basic model is the following:

$$\dot{m} = C\rho_{TP}\omega$$

$$\rho_{TP} = \alpha\rho_g + (1-\alpha)\rho_l$$

$\dot{m}$	Two-phase mass flow rate [kgs^{-1}]
ω	Rotational frequency [Hz]
ρ_{TP}	Two-phase mixture density [kgm^{-3}]
ρ_l	Liquid density [kgm^{-3}]
ρ_g	Vapor density [kgm^{-3}]
α	Two-phase mixture void fraction

The proportionality constant C can be extrapolated from single-phase flow literature (provided the meter is single-phase standard design) and tailored on the basis of preliminary in-situ testing. The calculation of the two-phase mixture density ρ_{TP} requires, in principle, the side measurement of the void fraction α (typically performed in academic research). Baker (2000), Baker (1991) lists some references relating to the use of the meter in multiphase flow. Baker (2000), Ohlmer and Schulze (1985) used turbine meter in experiments to model accident conditions in a nuclear plant. The instruments were just calibrated in a water-only or air-only loop with velocities up to 12 m/s and 100 m/s, respectively. The turbine meters presented a very good linearity down to 1% of the nominal range. The relation between the turbine meters reading and the mass flow rate was simply:

$$\dot{m} = A \cdot \overline{\rho} \cdot v_T ,$$

where $\dot{m}$ is the mass flow rate, v_T is the mixture velocity detected by the turbine, A is the cross sectional area of the pipe and $\overline{\rho}$ is the average mixture density detected by a two-beam gamma densitometer. The values obtained were compared to the mass flow rates measured by a reference

TMFM (True Mass Flow Meter, in fact a Coriolis flow-meter, see page 398-400, Baker (2000)) and showed a remarkably good agreement.

Two different types of tests were implemented: LB (large break) and SL (small leak) tests. During the first ones very high flow velocities (up to 100 m/s at the break location) occurred and the thermohydraulic transients were very strong; the second ones were characterized by lower flow velocities and much longer transients (one hour and more). However, the failure rate for the instrument used in the SL was higher, because the of the longer operation time at temperatures above 120°C (this value has been chosen as the discriminating parameter).

Baker and Deacon (1983) tested a turbine flow-meter in a vertical upward air-water flow up to $\alpha = 0.06$. They obtained in almost all cases a positive error (the flow rate measured by the turbine was bigger than the actual flow rate) with respect to the reference flow rate (previously measured with single phase flow instruments). The maximum error rises up to 20%. The flow patterns were mostly bubble and plug flow. A surprising hysteresis effect was noticed in the turbine output for $\alpha \cong 0.05$. According to Baker (2000): "The safe rule is to avoid using the meter in multiphase flow".

Chen and Felde (1982), reported some interesting result of the measurement of two phase mass flow at the ORNL THTF (Oak Ridge National Laboratory, Thermal-Hydraulic Test Facility) using two different spool pieces design:

- ✓ Thermocouple, absolute pressure tap, turbine meter for volumetric flow or velocity, single beam gamma densitometer for the average density, drag disk for the momentum flux.
- ✓ Thermocouple, absolute pressure tap, turbine meter for volumetric flow or velocity, three beams gamma densitometer for the average density, drag disk for the momentum flux.

They evaluated the error in using the homogeneous flux model and the Kamath and Lahey model (Chen and Felde, (1982), Kamath and Lahey (1977)*) to measure the mass flux in steady state, two phase flow regime and obtained uncertainty bands of less than ±50% of reading (95% confidence level) for both the models.

Hardy (1982) described the performance of a string probe and a turbine flow meter to measure steady two-phase flow (steam and entrained water) at the vent valve location of the Cylindrical Core Test Facility (CCTF) in Japan; 80% of all the measurements fall within ±30% of the known flow rate for velocities $>2\frac{m}{s}$, for lower flow rates the error rises to ±70%, because of the low sensitivity of the homogeneous model at low flow rates.

Hardy (1982) demonstrated that the turbine flow-meter response is sensitive to the variation in the flow pattern (see Figure 2). The dotted lines in the figure delimits the regions of the graph characterized by different flow patterns.

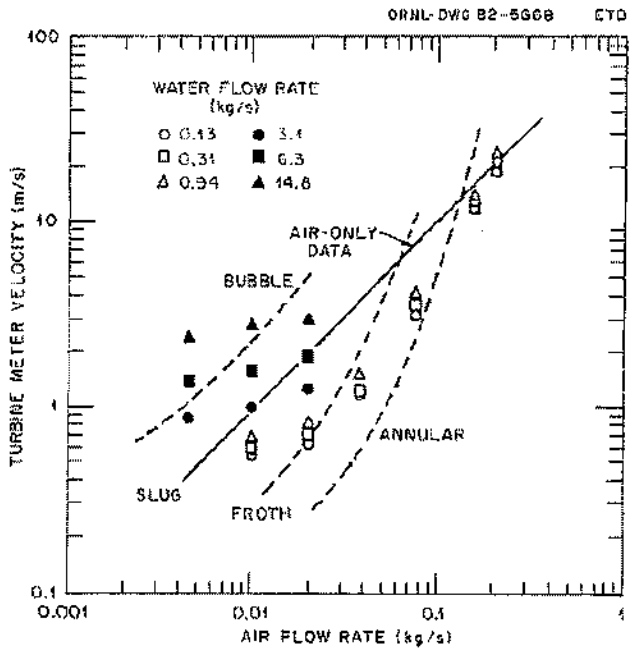

Figure 2: Turbine meter velocities as a function of the air flow rate in two-phase vertical upflow, Figure 16, Hardy (1982)

For the lowest values of liquid flow rate the turbine response is dominated by the water velocity: the introduction of liquid tends to slow down the flow-meter. For increasing values of the air flow rate, the turbine velocity approaches the air only line (empty symbols) and finally, in the case of annular-mist flow regime, the turbine response is dominated by the air

flow. At low air flows and high water rates the liquid phase is continuous and the turbine response is dictated by the water flow (black symbols).

Later on Hardy and Hylton (1983) confirmed that the response of a turbine flow-meter is likely to be more sensitive to the gas phase at high-void condition, while at low-void flows they tend to react more to the liquid phase. In intermediate void fraction condition, i.e. slug flow regime, their behavior is not well understood.

Hsu in Hetsroni (1982) lists some models developed to interpret the response of a turbine flow meter and relate it to the true mass flow rate:

- ✓ Volumetric model (Silverman and Goodrich, (1977)*)
- ✓ Aya model (Aya, (1975)*)
- ✓ Rohuani model (Rohuani, (1964)*)

According to Hsu (Hetsroni (1982)), some experiments at the Oak Ridge National Laboratory showed that the first model is working better for down flow with slip ratio<1, while Aya and Rohuani model predict the turbine velocity more accurately for horizontal flow or for down flow with slip ratio>1.

2. **High Span (minimal number of parallel lines)**-Criteria 2-Typical spans of turbine meters are 20:1-30:1, extendible in single-phase flow applications up to 100:1. In case more than one meter is required, they cannot share the same pipe, in order to protect the lower span turbine from rotor overspeed. The turndown ratio (span) is 10:1, but may be up to 30:1, for flow rates of 0.03-7000 m^3/h (Baker (2000)). All these values refer to single phase meter only.

   Chen and Felde (1982) used a turbine flow meter inserted in a spool piece for mass flux in the range 195-830 $\frac{kg}{m^2 s}$.

   Hardy (1982) reported the results from a turbine flow meter coupled with a string probe in the range of mass flow rates 0.1-16$\frac{kg}{s}$.

   Ohlmer and Schulze (1985) tested some turbine flow-meters in two different types of tests, Large Break and Small Leak tests. In the first one the fluid velocities in the intact loop remained below 10$\frac{m}{s}$ and decreased

under $1\frac{m}{s}$ at the end of the tests, while in the location closer to the break position they reached values around $100\frac{m}{s}$. In the Small Leak test the intact loop velocities were around $0.5\frac{m}{s}$.

3. **Good Repeatability and Accuracy-Criteria 3**-Without taking into account the bias error, the repeatability usually assumes the following values (Baker (2000)), for one phase applications:
   - ✓ ±0.05% for meters of less or equal to 50mm
   - ✓ ±0.02% for meters of greater than or equal to 75 mm

   Tests of a turbine flow meter and a string probe spool piece (Hardy (1982)) and comparison between the values calculated using the calibration equation and the actual mass flow rate obtained mass flux values to within ±30% at high rates $\dot{M} > 2\frac{kg}{s}$ and to within ±70% for flows $< 2\frac{kg}{s}$.

   Ohlmer and Schulze (1985) tested a turbine flow-meter (CENG) in water, after it has been used for 7 Small Leak tests and verified that the linear calibration curve remained unvaried for measurements above 10% of nominal flow rate, while in the lower region a mean deviation up to 25% of the reading was observed (the standard deviation was about 1% of the reading). The error increase was due to the bearing alterations.
4. **Minimal Installation Constraints (straight pipe length between the meter and the disturbance source)-Criteria 4**-Calibration of the flow-meter together with surrounding pipework and straighteners is recommended to eliminate the effect of upstream flow effect. ANSI/API suggested an upstream length of 20D and a downstream length of 5D. Table 10.2, page 230, Baker (2000) shows an example of suggested upstream spacing from manufacturer. See table 10.3, page 231, Baker (2000) for elbow and bends effects on installation. All these values refer to single phase meter only.

5. **Simplicity of Calibration; effects of calibration and operation temperature differences (different fluid properties, flow-meter material expansion)**-Criteria 5-Temperature differences between calibration and operation cause dimensional changes, viscosity changes, density changes and velocity pattern shift. Manufacturers may provide correction factors (Baker (2000), Gadsshiev et al. (1988)*). It's necessary to calibrate the instrument in the same direction in which it will be used in operation.

   Hardy (1982) calibrated a turbine flow-meter/string probe spool piece in a wide range of flow regimes, and he obtained two different fitting curves to approximate the response of the spool piece to the two-phase flow. The scatter of the data was remarkable (as previously discussed, in section 1).

6. **Capability of Handling Different Flow Regimes (temperature range, pressure range)**-Criteria 6-Temperature differences between calibration and operation cause dimensional changes, viscosity changes, density changes and velocity pattern shift. Manufacturers may provide correction factors (Baker (2000), Gadsshiev et al. (1988)*). The maximum applied pressure is 240-400 bar for threaded design, the maximum temperature is 310°C (Baker (2000)).

   Chen and Felde (1982) experiments were conducted in a pressure range of 5.5-13.8 MPa, very close to the pressure interval of interest for the SPES3 tests. They demonstrated (comparing the Kamath and Lahey model to the homogeneous model) that the variation of the correlation coefficients may lead to great changes in the mass flux evaluation, especially for fast transients. Chen and Felde, (1982), Kamath and Lahey (1977)*.

   Those coefficients depend on the flow regimes and are adjustment to homogeneous model input for non homogeneous flow effects.

   Also the variation of the slip ratio could cause great changing in the mass flux evaluation (the higher the slip ratio, the smaller the magnitude and the earlier is the peak in the mass flux).

   A good knowledge of the expected flow regimes is therefore necessary to calculate the mass flux with the lower uncertainty.

The quality range they observed during their experiments was 0.8-1.4 quality for steam and water. The steam quality is defined as:

$$x = \frac{i - i_l}{i_g - i_l},$$

where i is the enthalpy related to the liquid phase (l) or to the gas phase (g); a quality value greater than 1 is connected to the presence of superheated steam.

The authors advised that the applicability of their results to other flow regimes is questionable.

Ohlmer and Schulze (1985) used a model of turbine flow-meter studied at the CENG (Centre D'Etudes Nucleaires of Grenoble) to measure the two-phase flow in the LOCE (Loss of Coolant Experiments) test. The test facility reproduced the operation condition of a PWR reactor and the turbines had to face conditions of high pressure and temperature: pressure of 158 bar and coolant temperature up to 327°C.

Hardy (1982) tested a turbine flow meter coupled with a string probe for all the flow patterns from bubble to annular $(0 \le \alpha \le 1)$. The mass flow rate was obtained correlating the two-phase density from the string probe to the velocity sensed by the turbine with the following formula:

$$\dot{m} = \rho_{sp} v_T,$$

where ρ_{sp} is the density from the string probe and V_T is the velocity from the turbine. The data, represented in a graph that related the mass flow rate $(\dot{M})$ to the product $\rho_{sp} V_T$, shown a high scatter especially for $\dot{M} < 2\frac{kg}{s}$. The curve was fitted using two different exponential functions, one for $\dot{M} < 5\frac{kg}{s}$ and one for $\dot{M} > 5\frac{kg}{s}$.

Hewitt (1978) stated that the interpretation of the performance of a turbine flow meter in two phase flow is difficult for flow regimes other than those close to homogeneous. For example, the response in annular flow, for a certain mass flux and void fraction, is likely to be different from that for homogenized flow with the same characteristics (mass flow rate and void fraction).

7. **Transient Operation Capability (time response)-Criteria 7**-Turbine meters can effectively handle fast transients. The response time constant (with single phase fluid, water) is 0.005 to 0.05 sec for a flow rate step change of 50%, till 0.17 s for a step change of 63%.

   Chen and Felde (1982) obtained a good time response of at least 50 ms in their experiments, comparing the results from the homogeneous model with those from the Kamath and Lahey model (Chen and Felde, (1982), Kamath and Lahey (1977)*). Kamath and Lahey model introduce in the calculation the influence of some parameter that are excluded from the homogeneous model: non uniformity of the velocity, void profiles, imperfect guidance by the rotor blades, rotor inertia, slip ratio, bearing friction, windage losses. The rotor inertia influenced the response time, particularly in the faster transients: the Kamath-Lahely model precedes the homogeneous model by 50 ms in some portion of the transient, resulting in a significant mass flux difference.

   Hewitt (1978) suggests being very careful in evaluating the transient response of a turbine flow-meter, because of the inertia of the turbine rotor. Hewitt (1978), Figure 5.9, page 99, (based on Kamath and Lahey (1977)* calculations) shows the influence of the rotor inertia on the evaluation of the flow rate. The turbine tends to over predict the flow rate in the first part of the transient and to under predict it in the second part because of the increasing and decreasing of the angular momentum. The effect is more evident as the inertia increases.

8. **Bi-directional Operation Capability-Criteria 8**-Both one-directional and bi-directional designs are currently available, but a calibration for each flow direction is necessary.
9. **Minimal Regulatory Requirements-Criteria 9**-There are not particular regulatory requirements to install this type of flow-meter.
10. **Suitable Physical Dimension-Criteria 10-**

    Meter size:

    - ✓ threaded: 6-50 mm
    - ✓ flanged: 6-500 mm

    The meter has to fit the pipe dimensions.

11. **Minimal Disturbance to the Flow-Criteria 11**-The meter is designed to pass through the fluid without disturbing the flow. For these reason the most popular type of blade is twisted helically, thus obtaining the less disturbance to the flow. The support vanes are commonly used as flow straighteners to reduce swirl. The pressure losses (water as flowing medium) are 0.2 bar in 12 mm size to 0.25 bar in 200 mm size.
12. **Simplicity of Data Acquisition-Criteria 12**-There are different methods to obtain rotor speed (Baker 2000):
    - ✓ Inductive
    - ✓ Variable reluctance (the magnetic reluctance can be thought of as having an analogous function to resistance in an electrical circuit; is the resistance opposed by a certain material to the passage of the magnetic flux).
    - ✓ Radiofrequency.
    - ✓ Photoelectric.
    - ✓ Magnetic reed switch.

    The signal needs to be amplified and screened from external magnetic and voltage sources. There could be an influence due to a magnetic pickup device (referred presumably to type 1), 2) and 5)) on the velocity of the rotor due to the drag force; at 1/6 FDS (full-scale deflection) it provokes an error of 4% (Baker (2000), Ball (1977)*).

    Ohlmer and Schulze (1985) verified the slowing down effect of two types of pick off devices (magnetic pick-off and eddy current pick-off); they stated that the influence of the brake effect of the pick off system is evident just for velocities below 1% of the maximum velocity, when the turbine is given a certain rotational speed, and then is allowed to run freely in the stagnant air.
13. **Capability of Operating in Different Assembling Orientation (horizontal, vertical, inclined)-Criteria 13**-NA

2.3. Vortex shedding meters

1. **Two phase flow handling capability and easy modeling-Criteria 1-** Vortex shedding meters have been used for two-phase flow applications. The basic model is the following:

$$\dot{m} = C\rho_{TP} f$$

$\dot{m}$	Two-phase mass flow rate [kgs^{-1}]
f	Vortex shedding frequency [Hz]
ρ_{TP}	Two-phase mixture density [kgm^{-3}]
ρ_l	Liquid density [kgm^{-3}]
ρ_g	Vapor density [kgm^{-3}]
α	Two-phase mixture void fraction

$$\rho_{TP} = \alpha\rho_g + (1-\alpha)\rho_l$$

The proportionality constant C can be extrapolated from single-phase flow literature (provided the meter is single-phase standard design) and tailored on the basis of preliminary in-situ testing. There is an optimum for the length/width ratio of the shedding body that guarantees coherence and stability in the vortex production: the width has to be of a quarter to a third of the pipe diameter. The width is measured in the direction of the flow (this is true for single phase flow). An important parameter in the evaluation of the meter is the Strouhal number (see eq. 11.2, page253, Baker (2000)) that has to be constant in a certain range of variation of Re to guarantee the proper use of the meter. It is defined as:

$$S = \frac{f \cdot w}{v},$$

where f is the vortex shedding frequency, w is the width of the bluff body and v is the flow velocity. Some flows which seem to be perfectly steady actually have an oscillatory pattern that depends on the Reynolds number. Figure 3 represents the variation of the Strouhal number as a function of the Reynolds number for a wide range of values $\left(10 < \mathrm{Re} < 10^7\right)$. The Strouhal number is almost constant for a certain range of Re.

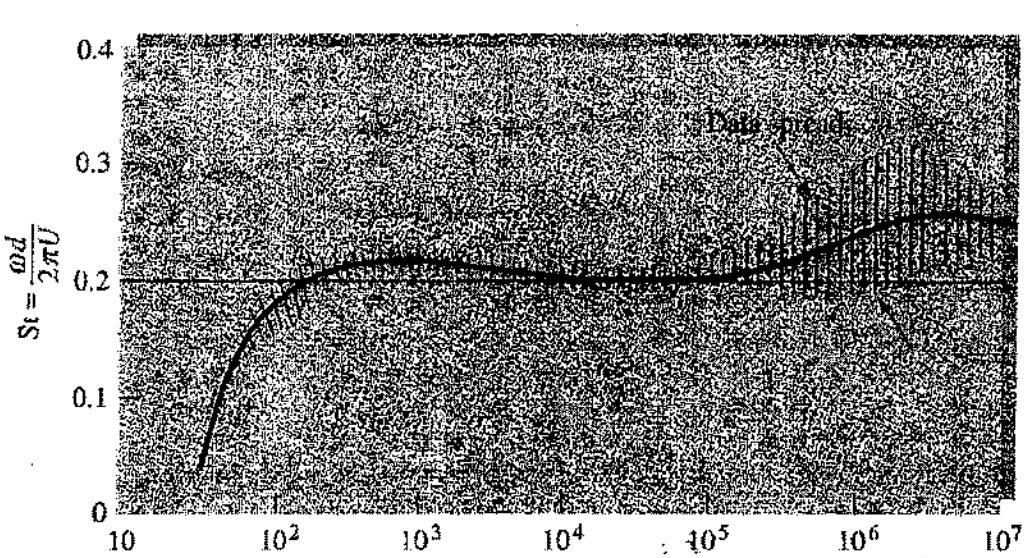

Figure 3: Variation of the Strouhal number as a function of the Reynolds number (White (1994), Figure 5.2 (b), page 270)

The calculation of the two-phase mixture density ρ_{TP} requires, in principle, the side measurement of the void fraction α (typically performed in academic research).

Application on two phase flow: Baker (2000), Hussein and Owen (1991)* found a correction factor for vortex meter for wet steam with a high steam quality, but the insertion of an upstream separator is highly recommended, indicating applicability for almost single phase flow.

There are some important problems connected with the use of a vortex-meter for two phase flow measurement.

One first important phenomenon is that the gas and the liquid phases could be separated by the vortex motion (Baker (2000), Hulin et al (1982), (1983)*). The authors studied the vortex emission in a vertical air-water upward two-phase flow.

The experiments demonstrated that:

- ✓ For $\alpha \leq 0.1$ the amplitude of the pressure oscillations induced by the vortex emission remains stable with time and it shows a very sharp peak for a particular frequency (the liquid volume flow rate is kept constant). For $\alpha > 0.1$ the oscillation amplitude decrease and it displays much broader peaks (the liquid volume flow rate is

fixed). Figure 4. The power spectrum amplitude describes how the power of a signal is distributed with frequency. In this particular case, it describes how evolves the amplitude of the pressure oscillations with frequency.

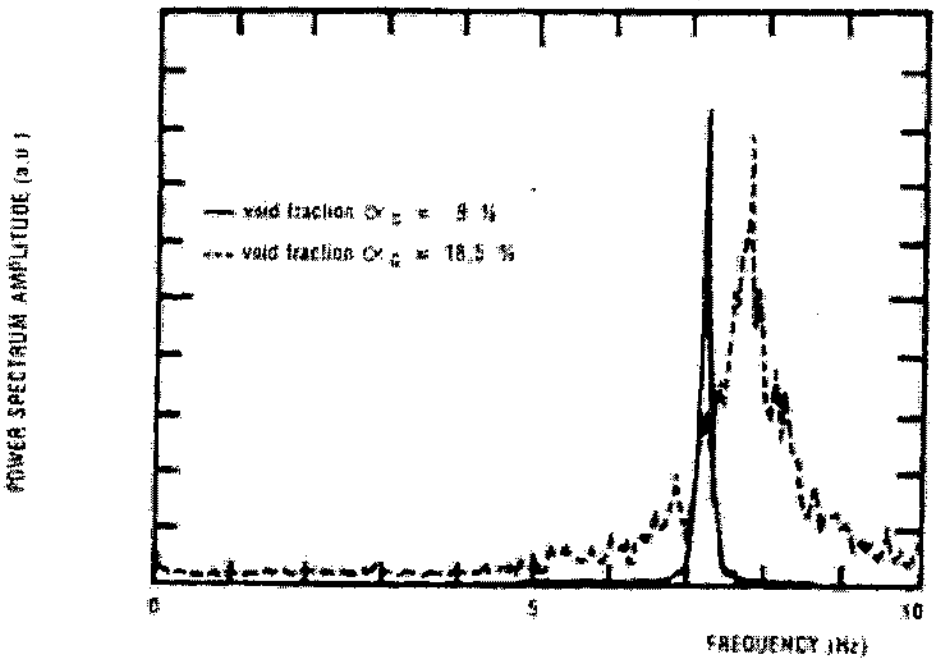

Figure 4: Power spectra of vortex induced pressure oscillations (the vertical scale is multiplied by 20 for the dotted curve α_G=18.5%), Hulin et al. (1982), Figure 3

- ✓ The authors measured the variation in the Strouhal number with the liquid volume flow rate and with α. They verified that it depends only slightly on the liquid volume flow rate and that is mainly influenced by the variation of the void fraction. See Figure 4, Hulin et al. (1982).
- ✓ The vortex emission becomes incoherent and displays erratic pressure fluctuations for $\alpha > 0.1$, especially for the higher values of liquid volume flow rates Q_L (see Figure 6, Hulin et al. (1982)).
- ✓ The pressure oscillations amplitude decreases with the increase of Q_L and of the void fraction (with leveling off after $\alpha = 0.1$).

All these phenomena can be explained by the bubble trapping inside the vortex core region. As the Bernoulli pressure gradient across the core

region and the external region of the vortex is increasing, more and more gas bubbles are pushed towards the central region.

The lower density due to the presence of the trapped gas causes a decrease in the measured pressure oscillations.

For increasing values of α, the difference in concentrations of bubbles inside and outside of the vortex core is decreasing. The increase of the density of bubbles between the various vortices is the cause of the vortex emission perturbation.

It could be concluded: the signal is stable only for void fractions up to 0.1 and sufficiently high flow rates. The transition between two regimes ($\alpha < 0.1$ and $\alpha > 0.1$) occurs when the vortex cores get saturated with bubbles and the void fraction between the various vortices start to increase, causing a major perturbation in the vortex emission.

A second issue connected with the measurement of two-phase flow with vortex shedding flow-meters is that bubbles may trigger certain sensors causing an error in the detection of the vortex shedding frequency (Baker (2000), Baker and Deacon (1983)):

- ✓ Very small diffused bubbles: it seems likely that calibration will be retained.
- ✓ Larger bubbles: these can occasionally trigger the electronics, introducing errors.
- ✓ Large quantities of air: they will eventually break the vortices build up mechanism and stop the shedding.

2. **High Span (minimal number of parallel lines)-Criteria 2**-Typical span of Vortex shedding meters is 20:1, but is possible to reach 200:1 (Doebelin (2003)).

   Coherence and stability of the shedding range (for single phase flow) has been achieved down to about Re=10000 (Baker (2000)). The constant of the K factor for a Re range of 1000:1 for air and water was demonstrated (Baker (2000), Zanker and Cousin (1975)*). Very good results were reported by Baker (2000), White et al. (1974)* that obtained a calibration curve for a 75 mm meter in air over a 360:1 turndown (span) with a scatter of ±1% over the range. A major problem related with these measurements is sensing the signal, because if velocity changes by 1:100, then the head

pressure will change by 10000:1, a very wide span for a pressure sensing device.

3. **Good Repeatability and Accuracy-Criteria 3**-Baker (2000) stated that typical current performances of that type of meter for one phase flow are: repeatability, about ±0.2% rate; linearity, better than ±1% for a turndown ratio (span) of up to 40:1 for liquids and 30:1 for gases. The accuracy of most vortex meters is 0.5%-1% of rate for Reynolds numbers over 30000. As the Reynolds number drops, metering error increases. At Reynolds numbers less than 10000, error can reach 10% of actual flow (http://www.omega.com/literature/transactions/volume4/T9904-09-ELEC.html#elec_3, March 10, 2008).
4. **Minimal Installation Constraints (straight pipe length between the meter and the disturbance source)-Criteria 4**-Table 11.2, page 265, Baker (2000) shows data for the change in uncertainty of the meters due to different straight pipe length between the meter and some typical fittings.
   Table 11.3, page 265, Baker (2000) compares the installation length for orifice plate and for vortex meters.
   Table 11.4, page 266, Baker (2000) compares installation requirements in manufacturers' literature and for orifice plates.
   Baker (2000), Cousins (1977)* states the effect of swirl in changing the meter performance. Pressure taps downstream should be 2D to 7D and temperature taps should be 1D to 2D downstream of the pressure one (Baker (2000)).
5. **Simplicity of Calibration; effects of calibration and operation temperature differences (different fluid properties, flow-meter material expansion)-Criteria 5**-Temperature variation could affect meter accuracy and compensation may be necessary.
6. **Capability of Handling Different Flow Regimes (temperature range, pressure range)-Criteria 6**-Temperature variation could affect meter accuracy and compensation may be necessary. Vortex may be affected by pulsatile flow particularly when the pulsatile frequency and its harmonics are close to the shedding frequency.
7. **Transient Operation Capability (time response)-Criteria 7**-Vortex shedding meters can effectively handle fast transients. With the proper

choice of the bluff body (small triangular shedder) is possible to obtain higher shedding frequencies for a given velocity and the jitter time (the time between the generation of two vortex) is reduced. With standard bluff bodies the vortex frequency at the maximum flow rate is in the range 200-500 Hz, while, with a body shape studied in order to have a short time response, the higher frequency is around 6000 Hz. The velocity measurement can then be updated after each pulse (one reading every 0.001 s for a 1000 Hz frequency, for example), Doebelin (2003).

8. **Bi-directional Operation Capability-Criteria 8**-Bi-directional capability might be obtainable with a proper selection of the cross sectional shape of the vortex generating element and the positioning of the sensors .
9. **Minimal Regulatory Requirements-Criteria 9**-There aren't particular regulatory requirements to install this type of flow-meter.
10. **Suitable Physical Dimension-Criteria 10**-The instrument is contained in the pipe and the physical dimensions and weight should not be an issue.
11. **Minimal Disturbance to the Flow-Criteria 11**-Since the only disturbance to the flow is the vortex shedding element spanning the pipe cross section, very low pressure drops and very limited flow disturbance can be expected.
12. **Simplicity of Data Acquisition-Criteria 12**-Many different types of methods has been used to sense the shedding frequency (Baker (2000)):
    - ✓ Ports in the side of a bluff body, leading to a transverse duct, which allows movement of fluid to be sensed by an internal hot wire or a thermistor.
    - ✓ Thermistor positioned on the upstream face of the bluff body to sense temperature changes.
    - ✓ Pressure sense by lateral diaphragm on the bluff body.
    - ✓ Flexure of the bluff body sensed by strain gages.
    - ✓ A shuttle ball in an internal cavity of the bluff body, with movement sensed by magnetic induction.
    - ✓ A beam of ultrasound modulated by the vortex shedding.
13. **Capability of Operating in Different Assembling Orientation (horizontal, vertical, inclined)-Criteria 13**-NA

2.4. Coriolis meter

1. **Two phase flow handling capability and easy modeling-Criteria 1-** Coriolis meters are in principle suitable for two-phase flow applications, but the literature on the subject is very limited. First approximated meter modeling is a problem, due to the highly sophisticated physics Coriolis meters rely on.

   The flow-meter is suitable for homogeneous two phase flow and for heterogeneous provided the phases are of similar density so that when vibrated the two phases behave as if rigidly connected (Baker (2000)). Baker (2000), Hemp and Sultan (1989)* published a theoretical paper about this topic. Baker (2000), Grumski and Bajura (1984) reported tests for air-liquid flows. They tested both a single tube and a dual tube Micro Motion Coriolis flow meters. The damping effect of the second phase (gas phase) on the tube vibrations causes a limit in the maximum void fraction that the meter can measure. The authors stated that as the void fraction is increasing, more and more energy is needed to make the tube vibrating. When the energy needed overcomes the maximum available energy from the magnetic drive coil, the meter stops working properly. They suggest to increase the number of tubes (and decrease the diameter of the tubes) within the meter body in order to decrease the amount of gas in each tube and reduce the damping effect.

12. **High Span (minimal number of parallel lines)-Criteria 2-**Grumski and Bajura (1984) tested the meters just for three values of water flow rate (22.7, 56.7 and 90.7 kg/min) and observed a high sensitivity for both the meter types at the lower flow rate.

    The single tube meter was not capable of giving results with less than 10% error on reading.

    The dual tube meter errors were from 10% to 40% for injected void fraction up to 0.35.

    All the following information is related to the one phase flow experience. The meters area available for flow ranges from 0-3 kg/h up to 0-680000 kg/h. Turndown ratio (span) is typically in between 20:1 and 100:1. Single

tube meters are available up to 75 mm diameter for flow rates from 15-1200 kg/h up to 1500-180000 kg/h.

3. **Good Repeatability and Accuracy-Criteria 3**-Baker (2000) stated that, for a commercial instrument of 20:1 turndown ratio (span), the typical performance is:
    - ✓ Uncertainty: ±0.25% rate+zero stability
    - ✓ Zero stability: ±0.05% FSD (full-scale deflection)
    - ✓ Repeatability: ±0.1% rate+zero stability/2

    For 100:1 turndown (span) the uncertainty is likely to be ±0.5-1%.

    Grumski and Bajura (1984) tested a single tube Micro Motion flow-meter and a dual-tube Micro Motion flow-meter. In the single tube design the reading change was about 2% for the maximum void fraction of 1.5%. In the dual tube design 2% accuracy was achievable for the maximum void fraction of 7.5%. Both values have been averaged and based on the results obtained in different operation conditions.
4. **Minimal Installation Constraints (straight pipe length between the meter and the disturbance source)-Criteria 4-**

    Installation constraints:
    - ✓ Orientation: vertical downward flow may result in partially empty tube. Pipework arrangements that might lead to trapped air or gas should be avoided (Baker (2000)).
    - ✓ Possible interference between the chosen frequency and an interference frequency (Baker (2000) Kiehl, (1991)*).
    - ✓ With a presence of a second phase the instrument could cause problems connected to the splitting of the flow and to the bubble coalescence (Baker (2000)).
    - ✓ No constrains connected with upstream flow effects are expected.
5. **Simplicity of Calibration; effects of calibration and operation temperature differences (different fluid properties, flow-meter material expansion)-Criteria 5**-Lack of symmetry on the tube and the sensors, changes due to density and viscosity (it is likely to be greater at low flow rates), unequal split of fluid may cause zero drift.

Capability of Handling Different Flow Regimes (temperature range, pressure range)-Criteria 6-Typical temperature range is -240°C to 200°C and certain high pressure versions are available up to 393 bar. For single tube meters temperature range is typically -25°C to 130°C. Special versions operational at PWR conditions are available (as special orders, M. Dzodzo,2007).

Grumski and Bajura (1984) demonstrated that the range of operation of a Coriolis meter in two-phase flow is limited by the failure condition of the meter. They tested two different types of Micro Motion Coriolis flow meters (the single tube and the dual tube type) and concluded that the range of void fraction of possible operation is 0-0.025 and 0-0.160 respectively (these are averaged values). The right values of these two intervals represent the break point for the meter. The break point has been defined by the authors as the ''void fraction reading when the slope of the curve (error-versus-void fraction) became large and the meter approaches the failure point''. See Figure 10, Grumski and Bajura (1984).

A better performance from the dual tube flow meter could be obtained by changing the inlet piping configuration in order to disperse the flow (by obtaining a more homogeneous flow pattern). Figure 15-3, Miller (1996) presents the influence of the void fraction variation on the meter percent error. For the void fraction up to 2.12% the maximum absolute error is 4%.

7. **Transient Operation Capability (time response)-Criteria 7**-The smoothing effect, due to the long time constants (caused by the length/volume of the U tubes), may cause errors to be introduced, paragraph 17.2.8 page. 410 (Baker (2000)).
8. **Bi-directional Operation Capability-Criteria 8**-Grumski and Bajura (1984) effectively tested two different Coriolis flow-meters (single and dual tube) with a reverse flow and demonstrated that there are not significant differences between the use in both directions.
9. **Minimal Regulatory Requirements-Criteria 9**-There are not particular regulatory requirements to install this type of flow-meter
10. **Suitable Physical Dimension-Criteria 10**-The weight range is: 8 kg-635 kg, the size range: 6 mm-200 mm. There could be problems connected to

the operation of this instrument type in narrow spaces because of the presence of bend pipes.

11. **Minimal Disturbance to the Flow-Criteria 11**-All the following information is related to the one phase flow experience. The pressure loss highly changes according to the different possible designs: figure 17.9, page 409, Baker (2000) shows the pressure drop for a straight tube design. The maximum value rises to 0.8 bar. Figure 17.10, page 411, Baker (2000) represents the pressure loss vs. mass flow rate for different designs of the meter.
12. **Simplicity of Data Acquisition-Criteria 12**-Sensor types (Baker (2000)):
    - ✓ a coil on one tube and a magnet on the other to generate an inductive voltage due to the relative velocity
    - ✓ optical method
13. **Capability of Operating in Different Assembling Orientation (horizontal, vertical, inclined)-Criteria 13**-Preferred orientation: vertical downward flow may result in partially empty tube. Pipework arrangements that might lead to trapped air or gas should be avoided (Baker (2000)).
    Grumski and Bajura (1984) did not notice a remarkable influence of the meter orientation on the meter performances.

2.5. Electromagnetic flow-meter

1. **Two phase flow handling capability and easy modeling-Criteria 1**-The principle of operation of this type of flow-meter is the electromagnetic induction. The simple law that in an ideal case regulates the phenomenon is:

$\Delta\phi_{EE} = B\square D\square v_m$,

where $\Delta\phi_{EE}$ [V] is the voltage between the electrodes, B[T] is the magnetic field, D[m] is the diameter of the pipe and v_m [m/s] is the mean velocity of the fluid in the pipe.

Usually the minimum conductivity necessary for the proper operation of the meter falls in the range $5-20\frac{\mu S}{cm}$ (www.omega.com (December 11, 2007)), but at least one manufacturer offers a meter capable of operation down to $0.05\frac{\mu S}{cm}$ (Baker (2000)).

The theory requests that:

- ✓ The magnetic field is uniform
- ✓ The velocity profile is axisymmetric

You can take into account the effects of distorted flow profiles using a weight function (Baker (2000), Shercliff (1962)*) and the effects of non uniformity of field defining the flow-meter sensitivity (eq. 12.3, page 285, Baker (2000)).

The flow-meter is composed by two elements:

- ✓ Sensor or primary element (metering tube with insulation, electrodes, coils to produce the magnetic field)
- ✓ Transmitter or secondary element

The primary device output resistance has to be of two or more orders of magnitude less than the input resistance of the secondary device (usually 20x10^6 ohms), so it's difficult to find an instruments that can work with pure water.

Baker (2000), Baker and Deacon (1983), experimented an electromagnetic flow-meter in air-water flow with errors of less than -1% for void fraction

up to 8%. They stated that an electromagnetic flow-meter in two phase flow could be affected by three types of error:

- ✓ shift from uniform velocity profile to a parabolic profile can produce 5% error, Baker and Deacon (1983), Baker (1973)*
- ✓ non uniform conductivity in the region of the fields and the electrodes (when the concentration of bubbles is higher on the pipe wall the authors calculated a signal change on the measurement of +0.7% with $\alpha_{wall} = 0.3$ and $\alpha_{axis} = 0$).
- ✓ If the liquid does not form a continuous conductive path, the output signal depends on how the secondary circuit of the meter reacts to the open circuit condition. This condition is realized when the void fraction is sufficiently high.

Baker (2000), Bernier and Brennen (1983), analyzed flow-meter performances for bubbly and churn flow: their data fall within ±2% of the prediction up to void fractions of 18%. The authors demonstrated analytically that the performances of a magnetic flow meter are almost independent of the fluid electrical conductivity, the velocity profile shape (provided that it is axisymmetric) and the flow pattern. They analyzed theoretically three different flow regimes (1. dispersed flow without relative phase motion, 2. annular flow with relative phase motion and 3. cylindrical voids parallel to the flow direction and with relative phase motion)

For all the three cases analyzed the collected data were laying on the same curve, without differences due to changing in the flow regimes.

It is important to remember that the results presented above are referred to the evaluation of the mean velocity of the conductive component (the liquid phase), but the meter cannot provide information about the mean velocity of the non conductive component, i.e. it is necessary to set a proper model to describe the slip ratio between the two phases.

Non uniformity of conductivity can change the flow-meter signal because there's a change in the shorting current. This could be a problem in two phase flow applications.

2. **High Span (minimal number of parallel lines)-Criteria 2**-100:1 turndown ratio (span) is the typical value for most of the meters available for single phase flow.

   More information about the operation range of different types of magnetic flow meters can be found in the following manufacturers' sites:

   - ✓ Omega (http://www.omega.com/prodinfo/magmeter.html)
   - ✓ Sparling (www.sparlinginstruements.com)
   - ✓ Dynasonics http://www.dynasonics.com/products/magnetic.php)
   - ✓ Foxboro (www.foxboro.com)

3. **Good Repeatability and Accuracy-Criteria 3**-The following values refers to single phase only. Repeatability is likely to be of order ±0.2% rate. Manufacturers' claims for uncertainty are shown in the following table (Paragraph 12.11, page 301, Baker (2000)).

Uncertainty	Flow range as % of full scale deflection
±1.5% of measured rate	5-2.5%
±1.0% of measured rate	15-5%
±0.5% of measured rate	50-15%
±0.3% of measured rate	100-50%

The percentage error of a magnetic flow-meter in two phase flow for two different volumetric liquid flow rates has been calculated by Baker and Deacon (1983). The air flow rate was gradually increased. The volumetric quality is defined as:

$$\beta = \frac{Q_g}{Q_g + Q_l},$$

where Q_l and Q_g are the volumetric flow rates for liquid and gas, respectively. In both cases the error was increasing with the void fraction increase.

In the first case the air was injected through a multiholed plate, the maximum error is around -3% for a volumetric quality β equal to 12.3%.

In the second case the air was injected through a 6 holed plate and the maximum error is around -1% for a volumetric quality β equal to 10.7%.

4. **Minimal Installation Constraints (straight pipe length between the meter and the disturbance source)-Criteria 4**-All the following data refer to single phase only. Installation constraints:
   - ✓ Effects on sensitivity of field and liner length (table 12.3, page 296, Baker (2000)).
   - ✓ Upstream flow distortion: table 12.4, page 297, Baker (2000) shows the effects of flow distortion generated by an eccentric orifice, the disturbance is minimum if its plane of symmetry is perpendicular to the electrode plane (Baker (2000), Al-Khazraji (1978)*). Table 12.5, page 298, Baker (2000) presents signal changes due to upstream disturbance.
   - ✓ Straight pipe necessary to decrease uncertainty: table 12.6, page 298 and 12.7, page 299,Baker (2000) lists straight pipe needed upstream of the flow-meter for the presence of a gate valve, a reducer, one or two bends.
5. **Simplicity of Calibration; effects of calibration and operation temperature differences (different fluid properties, flow-meter material expansion)-Criteria 5**-The response of the meter should not be affected by variation in liquid conductivity, provided that the conductivity is uniform over the region of the flow-meter (Baker (2000)). Temperature changes could affect the error connected with the measurements due to windings expansion. Baker (2000), Baker (1985)* obtained a maximum error of about -0.3%/100°C.
6. **Capability of Handling Different Flow Regimes (temperature range, pressure range)-Criteria 6**-Bernier and Brennen (1983) demonstrated theoretically that the meter response is independent of the flow regime (up to $\alpha = 0.18$). They tested a Foxboro electromagnetic flow-meter in a vertical upflow two-phase flow. The maximum water superficial velocity was 1.14 m/s, while the air injection rate was varied (with a maximum air superficial velocity of 1.138 m/s) to obtain different flow patterns (from bubbly flow to churn-turbulent flow). The authors monitored the variation of the ratio $\frac{\Delta\phi_{TP}}{(1-\alpha)\Delta\phi_{SP}}$ for different air injection rates and superficial

water velocities with a void fraction up to 18%. $\Delta\phi_{TP}$ is the differential voltage measured by the meter in two-phase flow; $\Delta\phi_{SP}$ is the differential voltage detected by an electromagnetic flow meter in single phase, water flow, placed upstream of the air injector. The authors verified that the ratio is almost independent of the air injection rate and of the water superficial velocity (i.e. it is independent of the flow pattern) and almost equal one. The experimental results fall within an error band of ±2% around the unity line (see Figure 3, Bernier and Brennen (1983)).

All the commercial flow-meters reviewed cannot tolerate the high pressure and temperature conditions of the SPES 3 facility.

7. **Transient Operation Capability (time response)**-Criteria 7-The time response of the transmitter is of order 0.1 s.
8. **Bi-directional Operation Capability**-Criteria 8-Some models of the magnetic flow-meter can effectively handle bidirectional flows, as it's stated by some manufacturer (Omicon, see http://www.onicon.com/pdfs/F-3100.pdf, 4 February, 2008 and AMS, see http://www.ferret.com.au/c/AMS-Instrumentation-Calibration/Bidirectional-magnetic-flowmeters-n726954, 4 February, 2008).
9. **Minimal Regulatory Requirements**-Criteria 9-No issues.
10. **Suitable Physical Dimension**-Criteria 10-No issues connected with physical dimensions.

    Minimal Disturbance to the Flow-Criteria 11-No disturbance to the flow is expected.
12. **Simplicity of Data Acquisition**-Criteria 12-Paragraph 12.4.2, page 289, Baker (2000) describes the most important characteristics of the transmitter (for single phase flow).
13. **Capability of Operating in Different Assembling Orientation (horizontal, vertical, inclined)**-Criteria 13-Some manufacturers prefer vertical installation with upward flow not to affect electrode contact because of entrained gases.

2.6. *Ultrasonic flow-meters*

There are three main types of ultrasonic flow-meter:

- ✓ Transit time flow-meter
- ✓ Doppler flow-meter
- ✓ Cross correlation flow-meter

The first type of ultrasonic flow meter have not been tested yet for two phase flow applications.

2.6.1. Doppler flow-meter

1. **Two phase flow handling capability and easy modeling-Criteria 1-**The **Doppler flow meter** depends on the Doppler velocity shift that occurs when sound bounces on a moving object. The sound wave is reflected by a particle or a disturbance moving with the flow.

   One of the major uncertainties in this measurement method is the ratio between the velocity of the reflecting object and the axial mean velocity. This method is thus sensing an average velocity in the volume defined by the intersection of the transmitted and the reflected beams. This punctual velocity could be calibrated to reconstruct the total volume flow rate, however the flow profile must be reproducible. The formula that gives the frequency shift in an ideal uniform profile velocity V is:

$$\Delta f = f_t - f_r = \frac{2 f_t \cos\theta}{c} v,$$

   where f_t and f_r are the transmitted and received frequency respectively, θ is the angle between the beam and the pipe axis and c is the sound velocity. This method is particularly applicable to two phase flow because it is based on measuring frequency shift in reflections from scatterers moving with the fluid.
2. **High Span (minimal number of parallel lines)-Criteria 2-**NA
3. **Good Repeatability and Accuracy-Criteria 3-**For **Doppler meters** uncertainty claims may be ±2% of the full scale, provided a good knowledge of the meter response in different flow condition (Baker (2000)).
4. **Minimal Installation Constraints (straight pipe length between the meter and the disturbance source)-Criteria 4-**For Doppler flow meters

one manufacturer (Baker (2000)) suggests 6D of straight pipe upstream and 4D of straight pipe downstream for single phase flow.

5. **Simplicity of Calibration; effects of calibration and operation temperature differences (different fluid properties, flow-meter material expansion)-Criteria 5**-The clamp on transducers are influenced by the changing in temperature that could lead to changes in the refraction angle (Baker (2000)) and to variation in the physical dimension (Doebelin (2003)).
6. **Capability of Handling Different Flow Regimes (temperature range, pressure range)-Criteria 6**-The temperature range for Doppler flow meters in single phase flow is -20 °C to 80 °C.
7. **Transient Operation Capability (time response)-Criteria 7**-NA

   Bi-directional Operation Capability-Criteria 8-The Doppler flow meter physical basics allow for the measurements of bidirectional flows. Some models of the Doppler flow meter can effectively handle bi-directional flows (www.rshydro.co.uk/doppler.shtml, April 1, 2008, Paul, (2008)).
8. **Minimal Regulatory Requirements-Criteria 9**-No issues.
9. **Suitable Physical Dimension-Criteria 10**-No issues.
10. **Minimal Disturbance to the Flow-Criteria 11**-Since the Doppler flow meter usually operates with clamp on transducers, it is causing no influence on the flow.
11. **Simplicity of Data Acquisition-Criteria 12**-The Doppler meter usually operates with clamp on transducers.
12. **Capability of Operating in Different Assembling Orientation (horizontal, vertical, inclined)-Criteria 13**-NA

2.6.2. Cross correlation flow-meter

1. **Two phase flow handling capability and easy modeling-Criteria 1-Cross correlation flow meters** take advantage of the modulation of the sound beams due to disturbances in the flow. If two beams cross the flow at a known distance apart L and the received signals are compared to find a similar pattern, the pattern for channel B will be displaced a time τ_m from that of channel A. It is easy to deduce that the flow has taken time τ_m to

move a distance L or $v = \frac{L}{\tau_m}$. This arrangement would measure a representative liquid phase velocity assuming that the voids travel at the same velocity as the liquid (this applicable only for homogeneous two phase flow). Baker (2000), King (1988)*, King et al (1988)* mentioned the development of an ultrasonic cross correlation flow meter for multiphase flow at National Engineering Laboratory, Scotland.

Olszowski et al. (1976) applied a cross correlation flow-meter to measure the velocity of an air-water flow. They used a sharp edged orifice plate of area ratio 0.5 to homogenized the flow upstream of the ultrasonic meter and obtain a measurement of the velocity, supposing that the flow was homogeneous. The orifice was mounted 15 D upstream of the ultrasonic meter. The two flow-meters were situated axially one pipe diameter apart.

Xu et al., (1986) studied a pulsed ultrasound cross correlation system in the volumetric flow rate of 0-960 ml/s for the liquid (water) phase and 0.08-50 ml/s for the gas (air) phase. The flow regime was classified as bubble flow with a uniform distribution of air bubbles in the sensing volume. The measurement section was made of a Perspex tube with an air/water mixture flowing vertical upwards. The authors were using the cross correlation measuring technique.

The two peaks found in the correlogram, that might correspond to two different sensed velocities, are interpreted as two different paths (i.e. two different flow noise sources) for the pulsed ultrasound.

The first peak is clearly correlated to the average air velocity, while the origin of the second peak seems to be connected to the variation in the bubble density and dimension and to the variation in the water velocity.

Figure 5 shows the relation between the first peak velocity and the gas velocity. The gas velocity has been calculated as:

$$v_g = \frac{Q_g}{\alpha A},$$

where $Q_g \left[\frac{m^3}{s}\right]$ is the air volumetric flow rate, $\bar{\alpha}$ is the mean void fraction measured by a differential u-tube manometer and A is the pipe cross-

section area. The void fraction range shown in the previous graph is from 0 to 0.15.

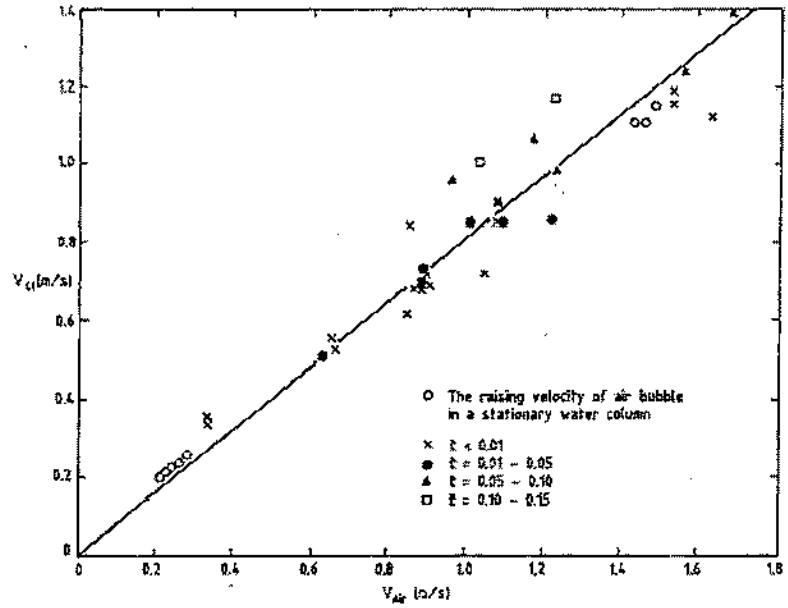

Figure 5: Relation between the air phase velocity and the velocity related to the first peak in the correlogram, Xu et al. (1986), Figure 9

Is important to underline that the signal obtained with the cross correlation method is strictly related to the distribution and the characteristics (density of bubbles, size of bubbles) of the gas phase, while no information is given about the velocity of the liquid phase.

2. **High Span (minimal number of parallel lines)-Criteria 2**-NA
3. **Good Repeatability and Accuracy-Criteria 3**-NA
4. **Minimal Installation Constraints (straight pipe length between the meter and the disturbance source)-Criteria 4**-Baker (2000), Paik et al (1994)* used clamp on transducers in some tests of installation effects in single phase flow. A complete data set of their result is shown in table 13.9, page 348, Baker (2000).
5. **Simplicity of Calibration; effects of calibration and operation temperature differences (different fluid properties, flow-meter material expansion)-Criteria 5**-NA
6. **Capability of Handling Different Flow Regimes (temperature range, pressure range)-Criteria 6**-Olszowski et al (1976) measured the velocity of the flow (air-water, homogeneous flow pattern supposed) in a void

fraction range (α) 0.6% to 43.6%, while the quality range (x) was 0.13×10^{-4} to 12.3×10^{-4}. The mixture velocity range was 1.6 to 4.1 m/s. The pressure varied between 1.1 to 2.1 bar. The experiment was performed using a translucent pipe and two clamp on transducers. When the cross correlation flow meter is applied at low volume ratio values ($\beta \leq 10\%$), the velocity detected by the cross correlation flow-meter is very close to the value obtained by the application of the homogeneous model to the single phase flow measurement.

When the volume ratio increased, the velocities indicated by the ultrasonic meter progressively exceeded the homogeneous velocity by a maximum of about 4% for volume ratio values up to 40%. This error is probably due to the increasing of the slip ratio.

It can be concluded that the instrument can positively measure the mixture flow rate (if the flow is supposed to be homogeneous) only if

- ✓ The mixture velocity is high enough to guarantee a proper mixing action by the orifice mounted upstream of the meter.
- ✓ The volume ratio is low enough to permit a proper mixing of the two phases. When the slug flow region has been reached, the mixing action of the orifice is suppressed.

7. **Transient Operation Capability (time response)-Criteria 7**-NA
8. **Bi-directional Operation Capability-Criteria 8**-The cross correlation technique can detect bi-directional flows.
9. **Minimal Regulatory Requirements-Criteria 9**-No issues.
10. **Suitable Physical Dimension-Criteria 10**-No issues
11. **Minimal Disturbance to the Flow-Criteria 11**-Theoretically the influence of the ultrasonic flow meter itself is almost unimportant, but if a homogenizing device like an orifice plate is needed, then it's necessary to take in account the induced pressure drop and the changes caused in the flow pattern.
12. **Simplicity of Data Acquisition-Criteria 12**-NA
13. **Capability of Operating in Different Assembling Orientation (horizontal, vertical, inclined)-Criteria 13**-NA

2.7. Wire mesh sensor (for velocity measurements)

7. **Two phase flow handling capability and easy modeling-Criteria 1**-The wire mesh sensor has been studied to provide the measurement of the void fraction of the two-phase mixture. However it is possible to use a combination of two sensors and the cross correlation technique to obtain the gas and the liquid velocities.

   Prasser et al. (2002) tested a couple of 24 x 24 probes to sense the gas phase velocity distribution in a 50 mm diameter pipe. The two sensors were positioned with an axial distance of 37 mm. The visualization of the distribution of the air velocity inside the pipe was obtained.

   The measurement of the liquid phase velocity could be feasible, but it has not been tested yet. It can be measured with the cross correlation technique if there are conductivity fluctuations in the liquid phase conductivity (Prasser (2008a)). These fluctuations could be caused by changes in the liquid temperature. Prasser stated that the liquid velocity measurement can be much more unreliable than the gas velocity measurement, but it can help increasing the information about the flow (Prasser (2006)). Schleicher suggested adding a liquid tracer (i.e. salt water bolun) to cause a detectable modification in the liquid conductivity (Schleicher (2008)).

2. **High span-Criteria 2**-The experiment (Prasser et al. (2002)) with the measurement of the gas phase velocity was performed in the superficial gas phase velocity (J_{air}) range from 0.037 m/s to 0.835 m/s, while the liquid phase velocity (J_{water}) was kept constant at 1.02 m/s. The probe has been used for the measurement of the void fraction distribution in the J_{air} range from 0 to 12 m/s and in the J_{water} range from 0 to 4 m/s (Prasser et al. (2002)).
3. **Good repeatability and Accuracy-Criteria 3**-NA
4. **Minimal installation constraints-Criteria 4**-No installation constraints are required. The meter causes a fragmentation of the bubbles, but this effect is not sensed by the sensor, since it measures the undisturbed upstream flow structure (Prasser (2006)).

5. **Simplicity of calibration; effect of calibration and operation temperature differences (different fluid properties, flow meter material expansion)-Criteria 5**-The linear dependence between the void fraction and the conductivity of the mixture needs for the knowledge of two limit values: the conductivity as measured with the pipe filled with liquid only and the conductivity measured with the pipe filled with gas only. The liquid conductivity is dependent on the temperature and the temperature is varying during the transient experiment in the SPES3 facility. It is therefore necessary to calibrate the instrument in order to take into account the changes in this limit value. Prasser (Prasser (2008b)) suggests two ways to proceed:
   - ✓ It is possible to perform a calibration of the sensor reading for a completely filled pipe as a function of the water temperature. A fast thermocouple mounted close to the sensor is then necessary to provide the correction of the limit value.
   - ✓ If there is a two-phase flow permanently present at each crossing point of the sensor, short-term PDFs (probability density functions) of the measured raw data can reveal the signal levels for liquid and gas without an explicit calibration. The position of the maxima in the PDF can be used as calibration values.
6. **Capability of handling different flow regimes (temperature range, pressure range)-Criteria 6**-The velocity of the gas phase has been sensed in the flow pattern range from bubble to slug flow $\left(J_{water}=1.02\,m/s;\ 0.037\,m/s<J_{air}<0.835\,m/s\right)$, Prasser et al. (2002). The meter has been used for the detection of the mixture void fraction in the flow pattern range from bubble to annular flow (Prasser et al. (2002)). The meter is capable of detecting the presence of bubbles whose dimensions are bigger than the wire pitch. The wire mesh probes previously tested had a wire pitch that ranged from 2 mm to 3 mm; the diameter of the pipe ranged from a minimum of 42 mm to a maximum of 195 mm (Prasser et al. (1998), Prasser et al. (2000), Prasser et al. (2002), Prasser et al. (2005), Pietruske and Prasser (2007)).

The probe is not influenced by the flow pattern because it simply registers the conductivity of the mixture, which is independent on the flow pattern. The maximum operation pressure for the probe is 7 MPa, while the maximum temperature is 286°C (Pietruske and Prasser (2007)).

7. **Transient Operation Capability (time response)-Criteria 7**-The maximum detection frequency is 10000 Hz for the 16 x 16 wire mesh design and 2500 Hz for the 64 x 64 wire mesh design.
8. **Bi-directional operation capability-Criteria 8**-The cross correlation technique allows for the detection of the reverse flow condition for the measurement both of the gas and the liquid velocity (Prasser (2008a)). Schleicher underlines that the detection of bi-directional flow is not a common use of the cross correlation technique (Schleicher (2008)).
9. **Minimal regulatory requirements-Criteria 9**-No issues.
10. **Suitable physical dimensions-Criteria 10**-The probe is inserted in the pipe cross section and the outer extension should not represent an issue.
11. **Minimal disturbance to the flow-Criteria 11**-The probe was presented with two different designs by Prasser et al. (1998):
    - ✓ Wire mesh sensor with 16 x 16 measuring points; 0.12 mm diameter wires.
    - ✓ Lentil shaped rods sensor with 8 x 8 measuring points or 16 x 16 measuring points.

    The first design is characterized by 96% of free cross section for one grid; the pressure drop coefficient (K) is about 0.04 (single grid). The second design has a 73% of free cross section for one grid and the pressure drop coefficient (K) is around 0.2 (single grid). The pressure drop (single phase flow) is then calculated as:

    $\Delta p = K \rho v^2$,

    where ρ is the density and v is the velocity. In water flow with $v = 1 m/s$ the pressure drop would be 40 Pa for the wire mesh design and 200 Pa for the lentil shaped rods design (Prasser et al. (1998)).

    The sensor is likely to slightly influence the flow pattern, since it causes a fragmentation of the bubbles.

12. **Simplicity of data acquisition-Criteria 12**-It is possible to store the data in the internal memory of the probe and then transfer them to a hard disk later on. Each measuring point value needs 12 bit of memory. For the 16 x 16 sensor this results in 384 bytes per frame. With the maximum frequency of 10 kHz, the total amount of memory necessary to store 1 s of measured data is 3750 kbytes. Since the internal memory of the probe is 4Gbytes, it is possible to measure about 18 minutes. Then is necessary to download the data to a hard drive. For the lowest available frequency (100 Hz), is then possible to store up to 30 hours of measured data in the internal memory (Schleicher (2008)).
13. **Capability of operating in different assembling orientation-Criteria 13**-The meter was tested both in horizontal (only one experiment, Prassser et al. (1998)) and vertical direction (Prasser et al. (1998), Prasser et al. (2000), Prasser et al. (2002), Prasser et al. (2005), Pietruske and Prasser (2007)). Almost all the available data are related to the vertical orientation.

2.8. *References

Al-Khazraji, Y. A., Al-Rabeh, R. H., Baker, R. C., and Hemp, J., (1978)*, Comparison of the effect of a distorted profile in electromagnetic, ultrasonic and differential pressure flow-meters, *FLOMEKO 1978 – Proc. Conf. on Flow Measurements of Fluids,* Groningen, The Netherlands (Amsterdam: North-Holland Publishing Co.): 215-22.

Arnold, R. M., and Pitts, R. W., (1981)*, Fluid flow meter for mixed liquid and gas, *US patent 4,272,982, June16.*

Aya, I., (1975)*, A model to calculate mass flow rate and other quantities of two phase flow in a pipe with a densitometer, a drag disk and a turbine meter, *Oak Ridge National Laboratory.*

Baker, R. C., (1973)*, Numerical analysis of the electromagnetic flowmeter, Proc. IEE, Vol. 120, 1039-1043.

Baker, C. R., and Deacon, J. E., (1983), Tests on turbine, vortex and electromagnetic flow-meters in two-phase air-water upward flow, *Int. Conf. Physical Modeling of Multi-Phase Flow*, Coventry, England: BHRA Fluid Engineering, Paper H1:337-52.

Baker, C. R., (1991) Response of bulk flow meters to multiphase flow, *Proc. I. Mech. E. Part C: J. Mech. Eng. Sci.*, 205:217-29.

Baker, C. R., (2000), Flow measurement handbook, *Cambridge University Press.*

Ball, J. M., (1977)*, Viscosity effects on the turbine flowmeter, *Proc. Symp. On flow Measurements in Open Channels and Closed Conduits,* NBS, Gaithersburgh, MD: 847-69.

Bernier, R. N., and Brennen, C. E., (1983), Use of the electromagnetic flow-meter in a two-phase flow, *Int. J. Multiphase Flow,* 9:251-7.

Brown, G. J., (1996)*, Oil flow performance of ultrasonic flow meters, *Norht Sea Flow Measurement Workshop*, Kristiansand, Norway, Paper 33.

Chen, N.C. J., Felde, D. K., (1982), Two phase mass flux uncertainty analysis for thermal-hydraulic test facility instrumented spool pieces, *ORNL.*

* The references signed with * refer to publications that were not directly consulted.

Chisholm, D., (1967)*, Flow of incompressible two-phase mixtures through sharp-edged orifices, *Journal of Mechanical Engineering Science*, Vol. 9, No.1.

Chisholm, D., (1972)*, The compressible flow of two-phase mixtures through orifices, nozzles and venturimeters, *Naional Engineering Laboratories UK*, Report No 549, 66-79.*

Chisholm, D., (1977)*, Research note: two-phase flow through sharp-edged orifices, *Journal of Mechanical Engineering Science*, Vol. 19, No.3.

Clark, C., (1992)*, The measurement of dynamic differential pressure with reference to the determination of pulsating flow using DP devices, *J. Flow Meas. Instrum. 3:145-50.*

Cousins, T., (1977)*, Vortex meters, *Transducer 77 Conf.*

de Leeuw, H., (1994)*, Wet gas flow measurements by means of a venturi meter and a tracer technique, *North Sea Flow Measurement Workshop,* Peebles, Scotland.

de Leeuw, H., (1997)*, Liquid correction of venturi meters reading in wet gas flow, *North Sea Flow Measurement Workshop,* Kristiansand, Norway, Paper 21.

Doebelin, E. O., (2003), Measurement system, application and design, *International edition.*

Ferri, R., (2008), E-mail communication, 26th February, 2008.

Fincke, J. R., Ronnenkamp, C., Kruse, D. Kroque, J., Householder, D. (1999), Performance characteristics of an extended throat flow nozzle for the measurement of high void fraction multi-phase flow, INEEL, *4th International Symposium Fluid Flow Measurement*, Denver.

Gadshiev, E. M., Grigor'yants, S. E., Gusein-zade, K. P., and Smirnov, V. P., (1988)*, Metrological support to hot-water meters in use and during production, *Meas. Technique,* 151-4.

Gerrard, D., (1979)*, Measure viscous flow over 150:1 turndown by PD meter techniques, *Control Instrum.*, 11(4):39-41.

* The references signed with * refer to publications that were not directly consulted.

Gold, R. C., Miller, J. S. S., and Priddy, W. J., (1991)*, Measurement of multiphase well fluids by positive displacement meter, *Offshore Europe Conf.*, Aberdeen, Scotland: SPE, Paper 23065.

Grimley, T. A., (1996)*, Multipath ultrasonic flow meter performance, *North Sea Flow Measurement workshop,* Peebles, Scotland: NEL.

Grunski, J. T., and Bajura, R. A., (1984), Performance of a coriolis-type mass flow-meter in the measurement of two-phase (air-liquid) mixtures, *Mass Flow Measurements ASME Winter Annu. Meet.*, New Orleans.

Hardy, J. E., (1982), Mass flow measurements under PWR reflood conditions in a downcomer and at a core barrel vent valve location, *ORNL*

Hardy, J. E. and Hylton , J. O., (1983), Electrical impedance string probes for two-phase void and velocity measurements, *ORNL, Int. J. Multiphase Flow,* Vol. 10, No. 5, pp. 541-556.

Hemp, J., and Sultan, G., (1989)*, On the theory and performance of coriolis mass flow-meters, *Mass Flow Measurement Direct and Indirect, Proc. Int. Conf. Mass Flow Measurement,* London, IBC Publications.

Hetsroni, G., (1982) Handbook of multiphase systems, *Hemisphere,* Washington.

Hewitt, G. F., (1978), Measurement of two phase flow parameters, *Academic Press.*

Hulin, J-P., Fierfort, C., and Condol, R., (1982), Experimental study of vortex emission behind bluff obstacles in a gas liquid vertical two-phase flow, *Int. J. Multiphase Flow,* 8:475-90.

Hulin, J-P, and Foussat, A. J. M., (1983)*, Vortex flow-meter behavior in liquid-liquid two-phase flow, *Int. Conf. Physical Modeling of Multi-Phase Flow*, Coventry, England: BHRA Fluid Engineering, Paper H3:377-90.

Hussein, I. B., and Owen, I., (1991)*, Calibration of flowmeters in superheated and wet steam, *J. Flow Meas. Instrum.*, 2:209-16.

Kamath, P. S., and Lahey, R. T., (1977)*, A turbine meter evaluation model for two phase transients, *Rensselaer Polytechnic Institute,* NES-459.

* The references signed with * refer to publications that were not directly consulted.

Kegel, T., (2003), Wet gas measurement, *4th CIATEQ Seminar on Advanced Flow Measurement,* Colorado Engineering Experiment Station, Inc.

Kiehl, W., (1991)*, Difference measurements using coriolis mass flow-meters, *J. Flow Meas. Instrum.,* 2:135-8.

King, N. W., (1988)*, Multi-phase flow measurement at *NEL, *Proc. North Sea Flow Measurement Workshop,* Norwegian Society of Chartered Engineers.

King, N. W., Sidney, J. K. and Coulthard, J., (1988)*, Cross correlation measurement in oil air mixtures, *2nd Int. Conf. on Flow Measurement,* London: BHRA.

Lin, Z. H., (1982)*, Two phase flow measurement with sharp-edged orifices, *International Journal of Multi Phase Flow* 8 (6), 683-693.

Miller, R. W., (1996), Flow measurement engineering handbook, *McGrawHill*

Murakami, M., Maruo, K., and Yoshiki, T., (1990), Development of an electromagnetic flowmeter for studying gas-liquid, two-phase flow, *Int. Chem. Eng.,* 30(4):699-702.

Murdock, J. W., (1961)*, Two phase flow measurement with orifice, ASME, Paper 61-WA-27.

Murdock, J. W., (1962)*, Two phase flow measurement with orifice, *Journal of Basic Engineering,* Vol. 84, pp 419-433.

NEL, (1997a)*, Installation effects on Venturi tubes, *Flow Measurement Guidance Note,* East Kilbride, Scotland: National Engineering Laboratory, No. 6.

NEL, (1997b)*, Ultrasonic meters for oil flow measurements, *Flow Measurement Guidance Note,* East Kilbride, Scotland: National Engineering Laboratory, No. 6.

Nicholson, S., (1994)*, Coriolis mass flow measurement, *FLOMEKO '94 Conf. on Flow Measurement in the Mid 90s,* Scotland, NEL.

Ohlmer, E., and Schulze, W., (1985), Experience with CENG full-flow turbine meters for transient two-phase flow measurements under loss-of-

* The references signed with * refer to publications that were not directly consulted.

coolant experiments conditions, *BHRA 2nd Int. Conf. on Multi-phase flow,* London, England, Paper H1: 381-95.

Olsozowski, S. T., Coulthard, J. and Sayles, R. S., (1976), Measurement of dispersed two-phase gas liquid flow by cross correlation of modulated ultrasonic signals, *Int. J. Multiphase Flow*, V. 2, pp. 537-548.

Paik, J. S., Mim, C. H. and Lee, D. K., (1994)*, Effect of variation of pipe velocity profile in the ultrasonic cross correlation flow meters, *FLOMEKO '94 Flow Measurements in the Mid-90s,* Glasgow, Scotland: NEL, Paper 7.1.

Pavlovic, V., Dimitrijevic, B., Stojcev, M., Golubovic, Lj., Zivkovic, M. and Stamenkovic, Lj., (1997)*, Realisation of the ultrasonic liquid flow meter based on the pulse-phase method, *Ultrasonic*, 35:87-102.

Paul, J. C., (2008), E-mail communication, 1st April, 2008.

Pietruske, H. and Prasser H.-M., (2007), Wire-mesh for high-resolving two-phase flow studies at high pressure and temperatures, *Flow Measurement and Instrumentation*, 18, 87-94.

Prasser, H. -M., Böttger, A. and Zschau, J., (1998), A new electrode-mesh tomograph for gas–liquid flows, *Flow Measurement and Instrumentation*, Volume 9, Issue 2, Pages 111-119.

Prasser, H.-M., Krepper, E., Lucas, D., Zschau, J., Peters,D., Pietzsch,, G., Taubert, W., Trepte, M., (2000), Fast wire-mesh sensors for gas-liquid flows and decomposition of gas fraction profiles according to bubble size classes, *2nd Japanese-European Two-Phase Flow Group Meeting*, Tsukuba, Japan

Prasser, H.-M., Zschau, J.,Peters, D., Pietzsch, G., Taubert, W., Trepte, M., (2002), Fast wire-mesh sensor for gas-liquid flows – Visualisation with up to 10000 frames per second, *ICAPP 2002*, Hollywood, Florida, Paper #1055.

Prasser, H.-M., Misawa, M. and Tiseanu, I., (2005), Comparison between wire-mesh sensor and ultra-fast X-ray tomograph for an air-water flow in a vertical pipe, *Flow Measurement and Instrumentation,* Volume 16, Issues 2-3, Pages 73-83.

* The references signed with * refer to publications that were not directly consulted.

Prasser, H.-M., (2006), E-mail communication, 26th September, 2006.

Prasser, H.-M., (2008a), E-mail communication, 20th March, 2008.

Prasser, H.-M., (2008b), E-mail communication, 31th March, 2008.

Priddy, W. J., (1994)*, Fields trial of multiphase metering systems at Prudoe Bay, Alaska, *SPE 69th Annu. Tech. Conf. Exhib.*, New Orleans, LA: 531-43.

Reader-Harris, M., et al., (2005)*, Venturi meter performance in wet gas using different test fluids, *National Engineering Laboratories*, UK.

Rouhani, S., (1964)*, Application of the turbine type flow meters in the measurement of steam quality and void, *Symposium of in core instrumentation, Oslo, Norway.*

Schleicher (2008), E-mail communication, 28th March, 2008.

Shercliff, J. A., (1962)*, The theory of electromagnetic flow measurement, *Cambridge: Cambridge University Press.*

Silverman, S. and Godrich, L. D., (1977)*, Investigation for vertical, two-phase steam-water flow for three turbine models, *Idaho National Engineering Laboratory presented at NRC Two-phase flow instrumentation meeting at Silver Spring, Maryland.**

Smith, R. V., and Leang, J. T., (1975)*, Evaluation of correlations for two phase flowmeters three current-one new, *Journal of Engineering for Power*, 598, 594.

Stefani, S., Garg, V. K., Green, L, McShane, J., Roidt, R. M., Ruddy, F., (1995) Instrumentation techniques for high temperature two-phase flow, *Westinghouse STC.*

Steven, R., (2002) Wet gas metering with a horizontally mounted Venturi meter, *Flow Measurement and Instrumentation*, Vol. 12, Issues 5-6, page 361-372.

Steven, R, (2006a), Wet gas metering with gas meter technologies, *CIATEQ*, Colorado Engineering Experiment Station, Inc.

Steven, R., (2006b)*, Liquid property and diameter effect in Venturi meters used with wet gas, *International Symposium of Fluid Flow Measurement*, Mexico.

* The references signed with * refer to publications that were not directly consulted.

Stewart, D., (2003)*, Applications of differential pressure meters to wet gas flow, *SE Asia Hydrocarbon Flow Measurement Workshop*, Kuala Lumpur.

Szebeszcyk, J. M., (1994)*, Application of clamp on ultrasonic flow meter in industrial flow measurements, *J. Flow. Meas. Instrum.*, 5:127-31.

Taitel, Y, and Duckler, A. E., (1976)*, A model for predicting flow regime transition in horizontal and near horizontal gas-liquid flows, AIChE (American Institute of Chemical Engineers) Journal, Vol. 22, No. 1.

Vaterlaus, H-P., (1995)*, A new intelligent ultrasonic flowmeter for closed conduits and open channels, *ASCE Waterpower-Proc. Int. Conf. on Hydropower*, 2:999-1008.

Whalley, P. B., (1987), Boiling, condensation and gas-liquid flow, *Clarendon Press, Oxford*

White, D. F., Rodely, A. E., and McMurtie, C. L., (1974)*, The vortex shedding flow-meter, *Measurement and Control in Science and Industry*, Pittsburgh, PA, Instrument Society of America, 1(2):967-74.

White, F. M., Fluid mechanics, (1994), McGRAW-HILL.

Xu, L. A. Green, R. G., Beck, M. S. and Plaskowski, A., (1986), A pulsed ultrasound cross correlation system for velocity measurement in two component flow, Int. Conf. Flow Meas. in Mid 80's, *paper 2.1, vol. 1, NEL*, East Kilbride, Scotland.

Zanker, K. J., and Cousins, T. (1975)*, The performance and design of vortex flow-meter, *Conf. on Fluid flow Measurement in the Mid 1970s*, East Kilbride, Glasgow, Scotland: National Engineering Laboratory, Paper C-3.

www.wikipedia.org (December 11, 2007)

www.omega.com (December 11, 2007)

http://www.omega.com/prodinfo/magmeter.html, 4 February, 2008

www.sparlinginstruements.com, 4 February, 2008

http://www.dynasonics.com/products/magnetic.php, 4 February, 2008

www.foxboro.com, 4 February, 2008

http://www.onicon.com/pdfs/F-3100.pdf, 4 February, 2008

* The references signed with * refer to publications that were not directly consulted.

http://www.ferret.com.au/c/AMS-Instrumentation-Calibration/Bidirectional-magnetic-flowmeters-n726954, 4 February, 2008

http://www.engineeringtoolbox.com/orifice-nozzle-venturi-d_590.html, March 10, 2008

http://www.omega.com/literature/transactions/volume4/T9904-09-ELEC.html#elec_3, March 10, 2008

www.instrunat.com, March 13, 2008

www.engineeringtoolbox.com, April 1, 2008

www.rshydro.co.uk, April 1, 2008

http://www.engineeringtoolbox.com/ultrasonic-doppler-flow-meter-d_495.html, April 29, 2008

3. Densitometers

The third section is dedicated to the description of the main devices capable to detect directly or indirectly the two-phase density. Firstly some criteria that each meter needs to satisfy are listed, then the performances of each device, related to each criteria, are described. The criteria chosen for the analysis of the densitometers performances are:

1. **Results: accuracy and characteristics of the response-Criteria 1**
2. **Installation constraints-Criteria 2**
3. **Dependence of the results on the phase distribution (flow regimes analyzed in the experiment)-Criteria 3**
4. **Temperature range and pressure range-Criteria 4 and Criteria 5**
5. **Time response-Criteria 6**
6. **Regulatory requirements-Criteria 7**
7. **Disturbance to the flow-Criteria 8**
8. **Shape of the probe and configuration of the experimental circuit**

When two devices (one flow meter and one densitometer) are used together to monitor the mass flow rate, some important points need to be discussed (Hewitt (1978)):

- ✓ The response of a meter in two-phase flow tends to be high sensitive to the flow pattern and to the upstream configuration and flow history.
- ✓ The best practice is to calibrate the instruments with known phase flow rates and with an exact simulation of the upstream pipework.
- ✓ The flow pattern is likely to be also time dependant in transient tests.
- ✓ Though the ideal is to use in situ calibration, the more usual method is to interpret the measurement from an instrument in terms of a theory whose validity is tested by conducting separate experiments. Very often these experiments are conducted for very different flow conditions and fluids: instruments used for steam/water flows are frequently calibrated using air/water flows.
- ✓ The response of a flowmeter may be different in transient situation and it is better to find a way to correct for this.

3.1. Gamma densitometer

All the following information is derived from Hetsroni (1982) and Bergles et al. (1981).

When a beam of monochromatic and collimated photons transverses a substance of thickness z, it has an emerging intensity given by the following attenuation law:

$$I = I_0 \exp\left[-\left(\frac{\mu}{\rho}\right)\rho z\right],$$

where $I\left[\frac{\text{photons}}{m^2 s}\right]$ is the beam intensity as it emerges from the material, I_0 is the initial intensity and $\frac{\mu}{\rho}\left[\frac{m^2}{kg}\right]$ is the specific absorption coefficient for the material.

The void fraction calculation is influenced by the distribution of the void fraction inside the channel. When liquid and steam exist in layers parallel to the beam, the chordal void fraction R_{GI} is then obtained using the following formula:

$$R_{GI} = \frac{I - I_L}{I_G - I_L},$$

where I_G represents the attenuated intensity with the channel full of gas and I_L the attenuated intensity with the channel full of liquid (Hewitt (1978), Petrick and Swanson (1958)*). In the opposite case, when liquid and steam exist in layers perpendicular to the beam, R_{GI} is obtained from:

$$R_{GI} = \frac{\ln(I/I_L)}{\ln(I_G/I_L)}.$$

The choice of the radiation could be dictated by different aims. Two main sources have been used: ^{170}Tm, which has an energy of 84 keV, a half life of 127 days, and a linear absorption coefficient in water (μ) of 0.18 cm^{-1} at room temperature, and ^{137}Cs, with an energy of 662 keV, a half life of 30 years and a linear absorption coefficient in water of 0.086 cm^{-1} at room temperature. The first one is the most strongly absorbed in water and the change in signal between a channel filled with water and one filled with

gas is greater with this source. The mass absorption coefficient for water decrease as a function of the incident beam energy (see Figure 15.1, page 457, Bergles et al. (1981)). With Cesium there is less attenuation, but the absorption law can be linearized avoiding the problems connected with the averaging. Furthermore, if the source strength is large enough, more photons will be counted in the same time interval and the statistical error due to photon emission fluctuation can be reduced.

Constraints due to the contrast (different absorption of the beam in the water and in the gas) and to the photon emission statistic nature have opposite effect on the choice of photon energy and beam intensity. In this respect X-rays have beam intensity 10^3 to 10^4 higher than gamma rays.

3.1.1. Thermal-Hydraulic test facility instrumented spool pieces-gamma densitometers (Chen and Felde (1982))

1. **Results: accuracy and characteristics of the response-Criteria 1**-The authors applied the homogeneous model to the analysis of the steady state data obtained from the spool pieces. They combined the signals from the turbine flow meter and from the drag disk to the one from the gamma densitometers (1 beam and 3 beams) to calculate the mass flow rate in four different ways
   - ✓ turbine flowmeter-1 beam gamma densitometer (TBM-GAM)
   - ✓ turbine flowmeter-3 beams gamma densitometer (TBM-GAM3)
   - ✓ drag disk-1 beam gamma densitometer (DD-GAM)
   - ✓ drag disk-3 beams gamma densitometer (DD-GAM3)

   The values obtained were compared to the reference mass flow rate measured at the inlet of the facility in single phase flow. Uncertainty bands increase from ±50% for the TBM-GAM3 model to ±80% for the TBM-GAM. Similar results are observed for the DD-GAM model, but the uncertainty bands are ⊔ 10% higher than for the DD-GAM3 model. These results confirm that the use of a single beam gamma densitometer in the model results in significantly higher uncertainties.
2. **Installation constraints-Criteria 2**-The use of a radiation source require the presence of a radiation screen. The dimension of the gamma densitometer could represent a mounting issue.
3. **Dependence of the results on the phase distribution (flow regimes analyzed in the experiment)-Criteria 3**-There are different models to calculate the average cross section density using a three beam gamma densitometer. In this experiment the authors used a three region annular model (Chen and Felde (1982), Turnage and Jallouk (1978)*). The pipe density is obtained from an area-weighted average of the three region densities.

   The most frequent flow pattern expected for this type of experiments at high quality (0.8-1.4) is dispersed flow.

   The authors did not refer directly to the influence of the variation of the flow regime on the gamma densitometer response, but they observed that a change in the liquid phase distribution coefficient could result in a major change in the mass flow rate measurement. The liquid phase distribution coefficient takes into account the effects of the distribution of both the void fraction and the velocity profile inside the pipe.

Also the variation of the slip ratio could lead to a major change in the mass flow rate measurement..

4. **Temperature range and pressure range-Criteria 4 and Criteria 5**-The initial temperature and the pressure at the test section outlet are 15 MPa and 593 K.
5. **Time response-Criteria 6**-The gamma densitometer has been used in fast depressurization transients, its response time, although not directly defined by the authors, is at least 50 ms, because this is the time delay characteristic of a particular effect of the turbine meter and it could be detected by the gamma densitometer.
6. **Regulatory requirements-Criteria 7**-The handling of radiation sources is strictly regulated and the procedure to obtain the authorization to install the densitometer could be troublesome.
7. **Disturbance to the flow-Criteria 8**-No disturbance to the flow is caused by the gamma densitometer.
8. **Shape of the probe and configuration of the experimental circuit**-the Thermal Hydraulic test facility (THTF) has been built with the specific aim of testing the thermal hydraulic conditions after a hypothetical accident in a PWR. It has been equipped with two different types of spool pieces:

   Spool pieces constituted by a turbine flow-meter, a drag disk and a single beam gamma densitometer positioned between the turbine flow-meter and the drag disk. The densitometer has an uncertainty of $\pm 104 \frac{kg}{m^3}$ with 95% confidence bands.

   Spool pieces constituted by a three beams gamma densitometer, a turbine flow meter and a drag disk. The gamma densitometer is positioned upstream with respect to the other devices in order to reduce their influence on the density measurements.

3.1.2. In-bundle gamma densitometer for subchannel void fraction measurement (Felde (1982))

1. **Results: accuracy and characteristics of the response-Criteria 1-**

   Some tests were implemented on the ion chambers in order to characterize current leakage effects with temperature. The leakage current approaches the order of magnitude of the ionization-generated current starting from ⌊ 589K; remarkable effects of hysteresis where also detected during heat up and cooldown experiments.

   The measured data obtained during the Upflow Film-Boiling Tests were compared to the signal obtained from a gamma densitometer installed at the outlet of the test section. The data show a good agreement until the 589K temperature is reached. Since that time the values from the in-bundle gamma densitometer show apparently non physical behavior and seem to follow the temperature measurements in the bundle. The apparently strange behavior of the probe can be explained introducing piezoelectric effects due to the thermal expansion of the connection cables. Another explanation could be the slight modification of the probe geometry during the experiments, resulting in a significant change in the received signal.

   Useful data from the operation of the in-bundle gamma densitometer were not obtained, but the design of the probe seems to be promising to measure the void fraction inside a rod bundle. Improvements in the insulation of the device have to be studied in order to overcome the temperature influence on the signal.

2. **Installation constraints-Criteria 2**-The use of a radiation source usually requires the presence of a radiation screen, but in this special case it was not necessary, since the gamma densitometer was positioned inside the fuel bundle and the outer portion of the installation already provided adequate shielding. The dimension of the gamma densitometer could represent a mounting issue.
3. **Dependence of the results on the phase distribution (flow regimes analyzed in the experiment)-Criteria 3**-NA
4. **Temperature range and pressure range-Criteria 4 and Criteria 5**- the initial temperature and the pressure at the test section outlet are 15 MPa and 593 K (the operation condition for the primary side in the SPES3 facility are 626 K and 17.5 MPa).
5. **Time response-Criteria 6**-NA

6. **Regulatory requirements-Criteria 7**-The handling of radiation sources is strictly regulated and the procedure to obtain the authorization to install the densitometer could be troublesome.
7. **Disturbance to the flow-Criteria 8**-No disturbance to the flow is caused by the gamma densitometer.
8. **Shape of the probe and configuration of the experimental circuit**-The Thermal Hydraulic test facility (THTF) has been built with the specific aim of testing the thermal hydraulic conditions after a hypothetical accident in a PWR. A heated rod bundle simulates the reactor core. Two gadolinium oxide (Gd_2O_3) sources are placed in two instrument rod position, each source is annular shaped. Two correspondent ion chambers detect the signal and reconstruct the in-bundle two-phase density. The ^{153}Gd emits 100 keV gammas.

   The calibration of the densitometer assumes an exponential attenuation of the gamma sources, that is verified just in ideal conditions: monoenergetic, collimated beam. Practically the calibration equation is:

$$\overline{\rho} - \rho_e = K \ln \frac{V_e}{V},$$

   where $\overline{\rho}$ is the average density of the mixture, ρ_e is the density relative to an empty bundle, V is the densitometer output voltage in the measuring condition and V_e is the densitometer output voltage for an empty bundle. The output voltage is proportional to the beam intensity revealed by the ion chambers. The data related to subcooled flow provide the other endpoint necessary to evaluate K.

3.2. Tomography

Tomography is an imaging technique that reproduces sections of the scanned object. It's based on a tomographic reconstruction algorithm to elaborate the images from the intensity of the radiation beams that reach the detectors.

The physical phenomenon on which the technique is based is the absorption of a radiation beam, as it passes through a material. The main difference with respect to the gamma densitometer is that the tomography can reproduce a cross section image of the whole pipe and the phase distribution inside it, while the gamma densitometer provides only an average value of the void fraction along the projection line. In the tomographic reconstruction the radiation source is made rotating around the object or many sources with different emission directions are employed at the same time. In this way the radiation beam is oriented in different directions and it is possible to obtain information from all the points on the monitored section.

When a radiation beam cross a material, its intensity is attenuated according to the absorption law. The absorption coefficient (μ) is space dependent. The differential intensity reduction on the $y = y_1$ direction can be written as:

$$dI = -I\mu(x, y_1)dx,$$

where I is the initial intensity.

The projection function for the line $y = y_1$ is then defined as:

$$p(y_1) = -\ln\left(\frac{I}{I_0}\right) = \int_{y=y_1} \mu(x, y_1)dx.$$

If the projection line is not parallel both to the x and to the y axis, it can be expressed as a function of x and y (see Macovsky (1983)) and the resulting general equation to calculate the projection function is:

$$p_\theta(t) = \int_{line(\theta,t)} \mu(x, y)ds = \int_{-\infty}^{+\infty} \mu(t\cos\theta - s\sin\theta, t\sin\theta + s\cos\theta)ds,$$

where t is the distance between the projection line and the axis origin, s is the coordinate along the projection line and θ is the inclination of the projection line (see Macovsky (1983)). The previous integral is the line integral of the function $\mu(x, y)$ along the line s and is called Radon transform of the $\mu(x, y)$ function.

The projection function is the value that is effectively sensed by the beams detectors and that need to be elaborated to obtain the image. The aim of the image reconstruction algorithms is to construct $\mu(x,y)$ from $p_\theta(t)$.

The Back Projection algorithm is just one of the available reconstruction algorithms. The main characteristic of this procedure are described in Macovsky (1983).

3.2.1. Fast X-ray CT (computed tomography) for transient two phase flow measurement (Misawa et al. (1998))

1. **Results: accuracy and characteristics of the response-Criteria 1-**

The spatial resolution of the tomograph was investigated analyzing the reconstructed image of phantoms A and B. All the 1 mm voids were not detected and all the 2 mm voids were not clearly visible in the image, therefore the authors concluded that the spatial resolution of the tomograph lied between 1 and 2 mm.

In order to calculate the void fraction based on a gray scale image, it was necessary to define a threshold level. The choice of the threshold was very important since the resulting void fraction value was highly sensitive on its variations. Two methods were proposed:

- ✓ The threshold level is placed at the point where the maximum attenuation gradient is found. This method tends to underestimate the void fraction, and this effect is as greater as the voids diameter is increasing.
- ✓ The threshold level is chosen manually in order to match the actual voids diameter. The threshold levels found with this method were used to calculate a calibration curve that relates the diameter value to the best threshold value.

Even if the second method was more accurate, it is applicable only for flows with similar sizes of void expected.

The axial resolution of the tomograph was investigated analyzing the reconstructed images of phantoms C and D. They were moved in the scanning zone at constant velocities ranging from 0.2 to 1.5 m/s.

When the phantoms were moving at the maximum velocity, two problems arose:

- ✓ The tomograph cannot detect a sudden contraction or expansion in the cross section of the scanned object.
- ✓ The tomograph cannot detect objects that are crossing the scanning zone in a time interval shorter than the one necessary to the tomograph to capture the signals from all the sources.

Two different air volumetric flow rates were introduced in the pipe. Bubbly flow pattern was observed with the smaller one and slug flow pattern with the bigger one. The bubbles were traveling at a velocity of 0.9 m/s and their average thickness was around 3 mm. Within 3.6 ms they moved 3.2 mm in the axial direction. Since the

beam thickness is 3 mm, the whole external surface of the bubbles could not be detected. Higher scanning rates would be necessary to obtain a complete imaging.

The area averaged void fraction was monitored for a 2 s time interval both for bubbly and slug flow (see Figure 6).

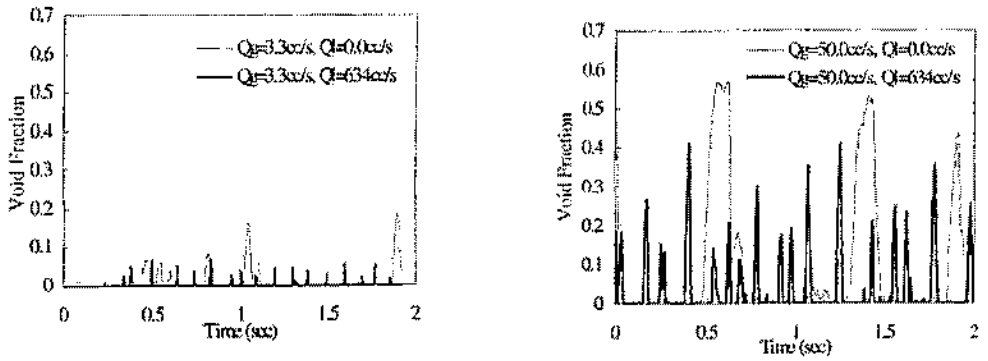

(a) Area averaged void fraction (bubbly)

(b) Area veraged void fraction (slug)

Figure 6: Void fraction changes for bubbly and slug flow as a function of time (Misawa et al. (1998), Figure 14)

The void fraction fluctuations well reflect the number of bubbles or slugs passed through the scanning region, as can be assessed by the comparison with a video tape.

2. **Installation constraints-Criteria 2**-The radiation sources need to be screened. The tomography device usually has big dimensions.
3. **Dependence of the results on the phase distribution (flow regimes analyzed in the experiment)-Criteria 3**-The flow regimes analyzed in the experiment were bubbly and slug flow.
4. **Temperature range and pressure range-Criteria 4 and Criteria 5**-NA
5. **Time response-Criteria 6**-The bias grids were employed to activate the X-ray sources sequentially. A time interval of 200 μs was necessary to switch the grid disarming, then the total time to complete a sequence of 18 X-ray generations was 3.6 ms.Finally the total time necessary to complete a scan was 4 ms, translating to a maximum scan rate of 250 scan/s.
6. **Regulatory requirements-Criteria 7**-The handling of radiation sources is strictly regulated and the procedure to obtain the authorization to install the densitometer could be troublesome.
7. **Disturbance to the flow-Criteria 8**-No disturbance to the flow is caused by the tomography.

Shape of the probe and configuration of the experimental circuit-the X-ray CT was constituted basically by 18 X-ray sources and 122 detectors. The sources were mounted in a semicircular assembly facing the detectors (see Figure 7). The scanned object was positioned in the centre of the assembly. The sources were sequentially activated. The radiation coming from each beam was sensed by 32 of the 122 total detectors.

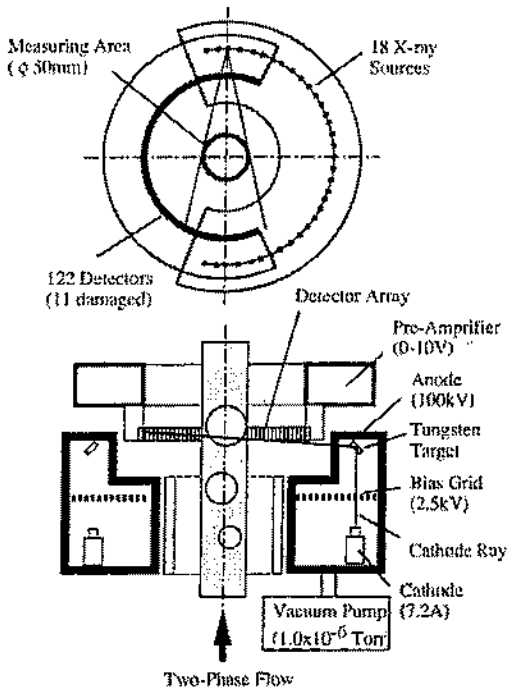

Figure 7: Schematic diagram of the sources and detector positions and diagram of electron beam switching X-ray CT system, Misawa et al. (1998), Figure 1

Two different types of scanned object were employed in the experiments:

- ✓ 4 types of acrylic resin phantoms; two of them (phantoms A and B) were used to examine the spatial resolution and the other two (phantoms C and D) to examine the axial resolution. The data collected from the phantoms experiments were employed for the calibration of the tomograph.
- ✓ Air-water two-phase mixture flowing into a 42 mm inner diameter pipe. The water velocity was 0.46 m/s. The air was introduced from a 8 mm diameter nozzle at a small (3.3 cm^3/s) and medium (50 cm^3/s) flow rate.

3.3. Drag plates

The drag plate is a very simple device capable of measuring the force exerted by the fluid flow on a portion of the pipe cross section. A body immersed in a flowing fluid is subjected to a drag force given by:

$$F_d = \frac{C_d A \rho v^2}{2},$$

where C_d is the drag coefficient and A is the cross section area of the pipe.

The drag coefficient is almost constant in a wide range of Re; Hunter and Green (1975)* demonstrated that the variation in C_d over a Re number range of 2000-250000 is from about 0.97 to 1.93.

The force sensed by the meter is proportional to the square of the velocity for Re>4000; in the laminar regime the results are not so predictable (Baker (2000), Ginesi (1991)*).

The force exerted on the plate is usually measured pneumatically or with electrical strain gauges.

One manufacturer (Target Flowmeter, Venture measurement Co. LLC, Spartanburg, SC, www.aaliant.com, 5 May 2008) offers devices for pipe sizes from 0.5 inches to 60 inches diameter (1.27 cm to 152.4 cm). The drag body size for the 0.5 inches diameter pipe is 0.4 inches diameter (1.016 cm) and the drag coefficient is around 4.5. It produces about 2 lb (8.9 N) of drag force at maximum flow. Drag bodies for larger pipe sizes take up a smaller fraction of the pipe cross section and have a drag coefficient of about 1.5; the maximum drag force is about 10 lb (44.5 N).

Uncertainty is between 0.5% and 2% of full scale. (Ginesi (1991)*). A commercial device is claimed to measure water flow rates in the range 0.4-1350 m^3/s and air flow rates in the range 12-40500 m^3/s with an uncertainty of 3% FSD. The turndown ratio is approximately 15:1 (www.engineeringtoolbox.com/target-flow-meters-d_497.html, 22 February 2008).

If the drag body is made symmetrical, bidirectional flow can be measured.

3.3.1. Measurement of two phase flow momentum using force transducers (drag plates), (Hardy and Smith (1990))

1. **Results: accuracy and characteristics of the response-Criteria 1-**

The Drag body was installed in order to monitor the momentum passing in both directions through the tie plate. The results were compared to the Δp measured across the plate, which is likewise proportional to flow momentum. Almost all the data fell in the uncertainty band ±20%. The scatter was due to the low sensitivity of the differential pressure device for values of Δp around 20 mm of water

A second comparison was performed with the momentum flux evaluated from the known input flow rates:

$$\frac{F}{A}=\alpha\rho_g v_g^2+(1-\alpha)\rho_l v_l^2.$$

The data showed a good agreement (see Figure 8).

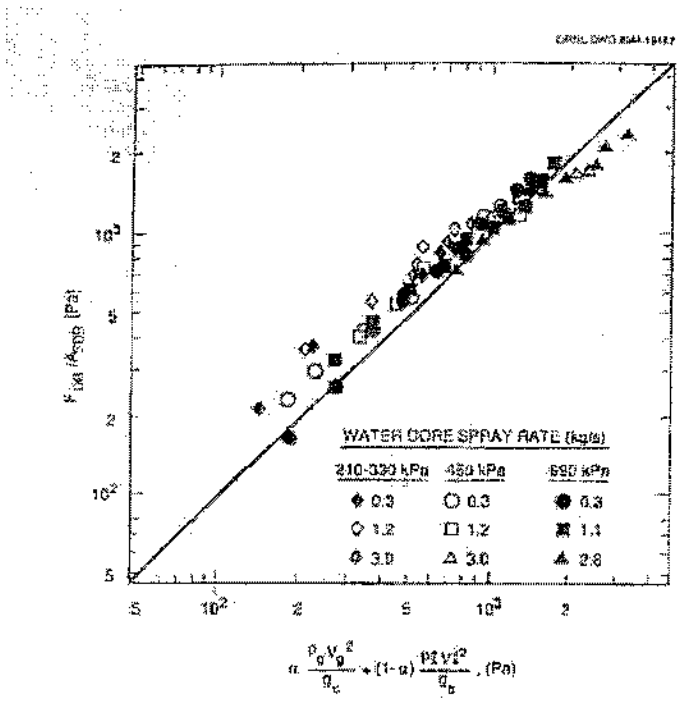

Figure 8: Comparison of momentum flux measured by the drag body with momentum flux calculated from measured data, Hardy and Smith (1990), Figure 9

In order to calculate the two-phase mass flow rate, the momentum measured with the drag plate was combined with the velocity detected by a turbine flow-meter:

$$\dot{m}=\left(\frac{(\rho v^2)_{DP}}{v_T}\right)\rho v,$$

where DP indicates the Drag plate data and T the turbine flow-meter data. The results are showed in Figure 9. The data provide a good estimate of the mass flow rate; almost all the data fell in an error band ± 20%.

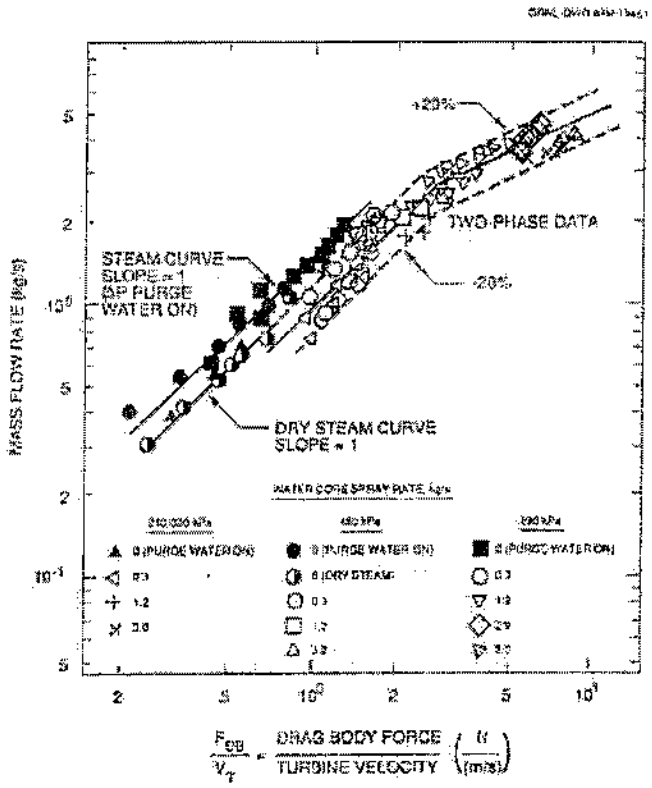

Figure 9: Comparison of mass flow rate from measured inputs with a mass flow model combining drag body and turbine meter measurement, Hardy and Smith (1990), Figure 10

2. **Installation constraints-Criteria 2**-No issues connected with the installation constraints.
3. **Dependence of the results on the phase distribution (flow regimes analyzed in the experiment)-Criteria 3**-No information are given by the authors about the flow pattern expected during the test, but, since the drag meter can span a certain fraction of the flow cross section area, it can be assumed that it is sensing an average momentum value. The velocity can be related to the average velocity of the two-phase flow.
4. **Temperature range and pressure range-Criteria 4 and Criteria 5**-the environmental conditions of the test facilities were: pressure up to 2.1 MPa and temperature up to 300°C. Thermal transients up to 40°C/s where expected.
5. **Time response-Criteria 6**-both the drag plates and the breakthrough detectors have a high resonant frequency in order to provide a fast dynamic response during the

transients. They have an average resonant frequency of ⊔ 70 Hz and 48 Hz, respectively.

6. **Regulatory requirements-Criteria 7**-No issues related to the regulatory requirements.
7. **Disturbance to the flow-Criteria 8**-The pressure drop caused by a drag plate has been calculated for the maximum mass flow rates expected in the DVI SPLIT and the DVI DEG break line, using the following formula (Miller (1983), Table 6.3, page 6-32):

$$\Delta p = 7.79\times10^{-5}\frac{\rho v^2}{(1-\beta)^{2.75}},$$

where ρ is the density, v is the average velocity and β is the ratio between the diameter of the drag plate and the pipe diameter. The flow rate is supposed single phase liquid and the associated value of the density is the liquid density. The value of β has been fixed at 0.5 to easily compare the pressure loss obtained for the drag plate to the pressure loss caused by an orifice (whose common β ratio is 0.5). The pressure drop related to the maximum mass flow rate in the DVI SPLIT break line is 0.14 kPa; the pressure drop related to the maximum mass flow rate in the DVI DEG break line is 0.028 kPa.

8. **Shape of the probe and configuration of the experimental circuit**-The drag body had to measure the bidirectional flow passing through a holed plate (tie plate of the end box). The force range was 0.9 to 220 N with a resolution of 0.1% of full scale (FS). The allowable uncertainty was 5% FS, included thermal and transient condition effects.

   The force was picked up by a full bridge configuration of four active strain gauges. These mounting allowed for temperature effects compensation.

   The Drag body was tested under load cycles from 25% to 100% of the rated load and to thermal shock from 220 °C to 25 °C with no significant shift in zero.

   The apparent strain due to thermal effects was measured at various temperatures under no load condition. The average thermal output was ±0.02 N/°C. This correspond to an uncertainty for thermal effects of ±0.1% FS.

   The combined effect of nonlinearity, hysteresis and repeatability was less than ±0.02% FS.

The Drag body was calibrated in air, steam and water single phase flow condition. The signal is effectively proportional to the square of the velocity with a scatter of the data equal to □ 10%.

3.3.2. Thermal-Hydraulic test facility instrumented spool pieces-drag disk measurements (Chen and Felde (1982))

1. **Results: accuracy and characteristics of the response-Criteria 1-**

The mass flux was evaluated combining the measurements from the drag disk, the turbine flow-meter and the gamma densitometer (single beam or three beam) assembled in each spool piece.

The drag disk was combined both with the turbine flow-meter (TBM-DD) and with the three beam gamma densitometer (DD-GAM3). The resulting mass fluxes, at the outlet of the test section in a horizontal pipe (spool piece BO1), are compared to the known inlet mass fluxes in Figure 10 (the equilibrium quality is varying), in Figure 7, Chen and Felde (1982) (the pressure is varying) and Figure 10, Chen and Felde (1982) (the reference inlet mass flux is varying). The TBM-DD and the DD-GAM3 values are included within ±30% of the reference mass flux.

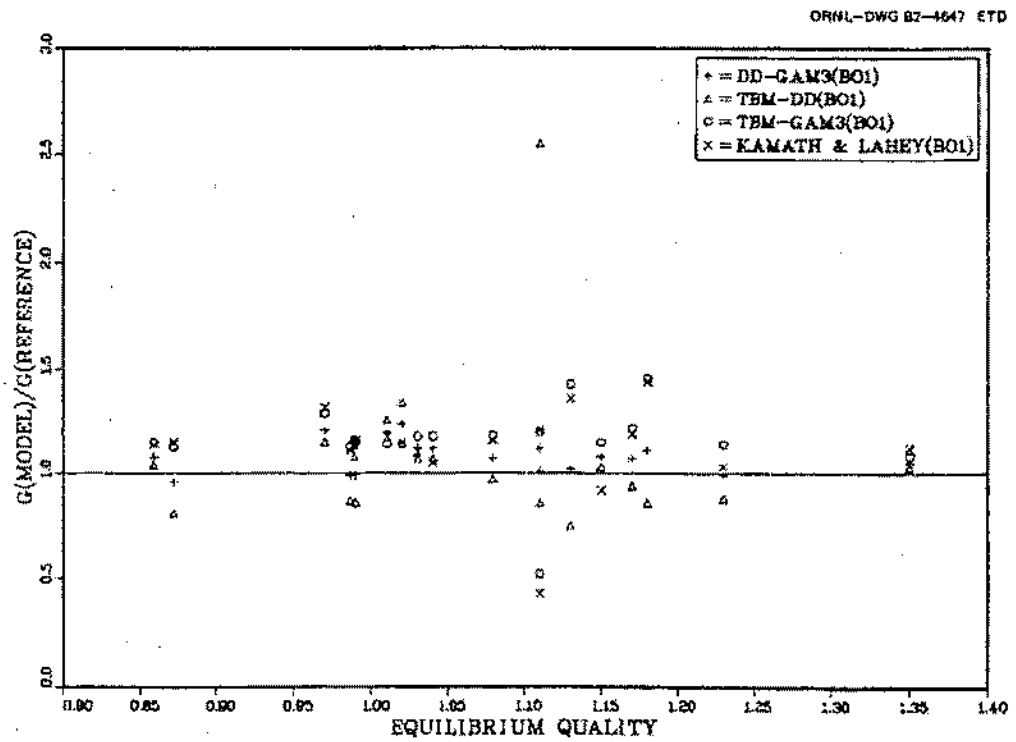

Figure 10: Comparison of mass flux models vs equilibrium quality at BO1 spool piece, Chen and Felde (1982), Figure 8

Figure 11 shows the comparison between the mass fluxes evaluated with DD-GAM and TBM-DD and the known mass fluxes in a vertical spool piece at the test section outlet (spool piece SV0). The uncertainty for DD-GAM is □ +70% and for TBM-DD is □ +140%.

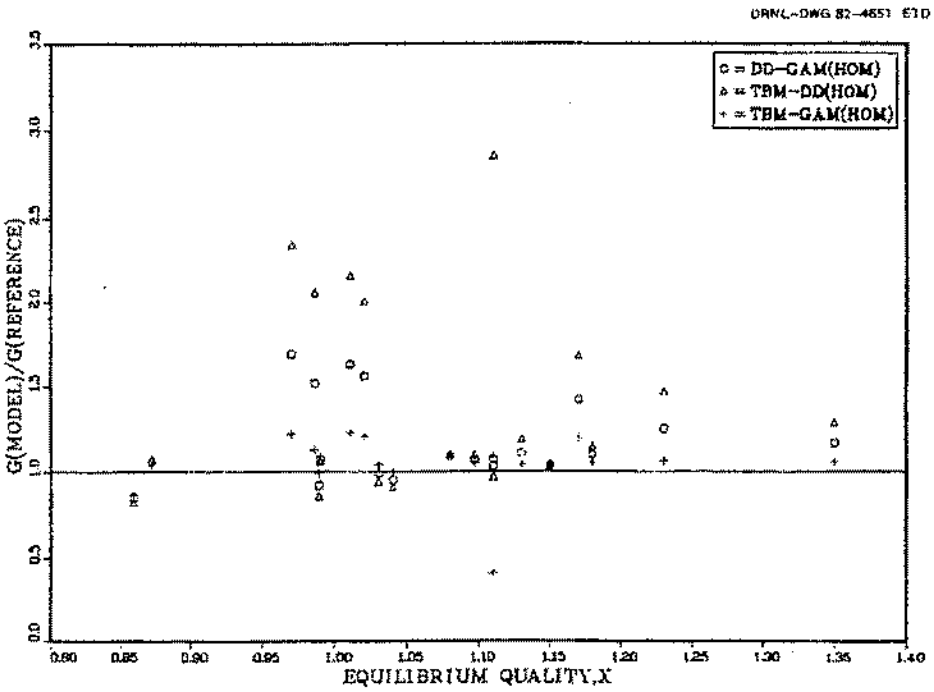

Figure 11: Comparison of mass flux model vs equilibrium quality at SV0 spool piece, Chen and Felde (1982), Figure 12

Figure 12 compares the DD-GAM and TBM-DD results in the horizontal spool piece positioned at the outlet of the test section (spool piece SH0). The uncertainty is □ –20% for DD-GAM and □ –35% for TBM-DD.

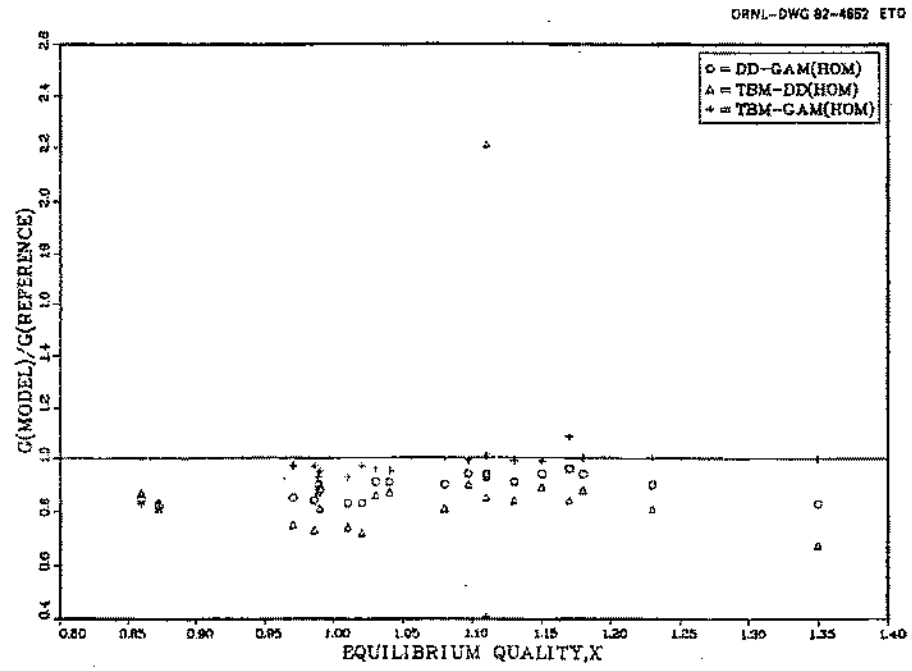

Figure 12: Comparison of mass flux models vs equilibrium quality at SH0 spool piece, Chen and Felde (1982), Figure 13

The authors stated that the higher uncertainties in the vertical spool piece have not to be necessarily ascribed to regime or orientation effects; based on their previous experience, they affirmed that the drag disk is the least reliable instrument in the spool piece in term of repeatability and consistency of the response to the fluid conditions.

2. **Installation constraints-Criteria 2**-No issues connected with the installation constraints.
3. **Dependence of the results on the phase distribution (flow regimes analyzed in the experiment)-Criteria 3**-The equilibrium quality was in the range 0.8-1.4, ($\alpha > 1$ is supposed to indicate superheated steam), while the mass flux was in the range 195-830 kg/m^2s. The flow pattern expected was dispersed flow.
4. **Temperature range and pressure range-Criteria 4 and Criteria 5**-the drag disk was used in steady state, two-phase flow experiment in a pressure range of 5.5-13.8 MPa. The initial temperature in the test section was 593 K.
5. **Time response-Criteria 6**-The data were collected with a time interval of 0.05 s.
6. **Regulatory requirements-Criteria 7**-No issues related to the regulatory requirements.
7. **Disturbance to the flow-Criteria 8**-The pressure drop caused by a drag plate for the maximum flow rates in the DVI SPLIT break line and in the DVI DEG break line have been calculated in paragraph 3.3.
8. **Shape of the probe and configuration of the experimental circuit**:
   The drag disk is a Ramapo Mark V model with a three bladed target (see Figure 13). The uncertainty for subcooled water flow condition is:
   - ✓ ±56% of reading for < 10% full scale
   - ✓ ±19% of reading for 10%-100% full scale

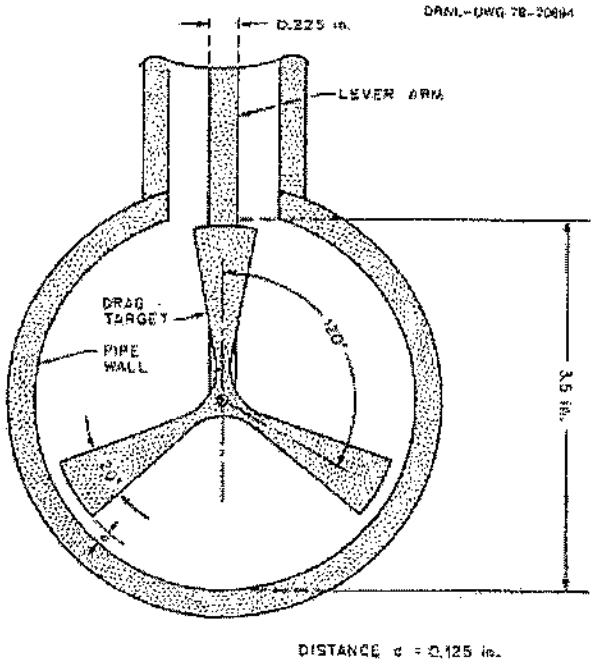

Figure 13: Appearance4 of three bladed drag target in pipe. View is looking downstream, Chen and Felde (1982), Figure 5

3.4. *Impedance gauges*

Another way of measuring the density of a two phase flow mixture is by monitoring its impedance and deriving from this value the related density, using models for different types of the liquid and gas flow distribution.

All the following information is derived from Hetsroni (1982).

In a two-phase flow the impedance depends on the distribution and concentration of the phases. Depending on the particular configuration, the impedance can be dominated by capacitance (C), conductance $\left(G=\frac{1}{R}\right)$, or both. It's better to operate at high frequencies to obtain capacitance domination, because the liquid conductivity can change by orders of magnitude with the temperature and the ion concentration, whereas the dielectric constant varies less. The relation between the conductivity σ and the conductance G for a conductor of length l and cross sectional area A is:

$$G=\sigma\frac{A}{l}.$$

The formula that relates the dielectric constant (or relative permittivity) ε and the capacitance C for a parallel plate capacitor with a surface area A and the distance between the plates equal to d is:

$$C\approx\varepsilon\frac{A}{d},$$

provided that $A \square\ d^2$.

Unfortunately one of the main problems related to the use of the impedance probe is the sensitivity to flow pattern. The relation between the admittance of the mixture and the void fraction is not bijective and for a single admittance value there could be different void fraction values, based on different flow patterns.

Five different models can be applied to the situation of two phase flow (Javorek (2004), Bruggeman (1935)*). These models calculate the equivalent permittivity of the mixture:

1) plate voids placed perpendicularly to the electrodes, which can be reduced to two capacitances connected in parallel.
2) plate voids placed parallel to the electrodes, which can be reduced to two capacitance connected in series.
3) a continuous medium (water) with cylindrical voids placed parallel to the electrodes, which could be a model for annular flow

4) a continuous medium medium with spherical voids, that could be a model for bubble flow:
5) for un-ordered plate voids Bruggeman (1935)*, Jaworek (2004) suggests a formula for the permittivity as a geometric mean of 2) and 3)

In Figure 14 is represented the effective relative permittivity of the precedent models as a function of the void fraction. The models 1), 3) and 4) gives similar results up to about $\alpha = 20\%$, while 2) and 5) the change in permittivity at low void fraction is very high.

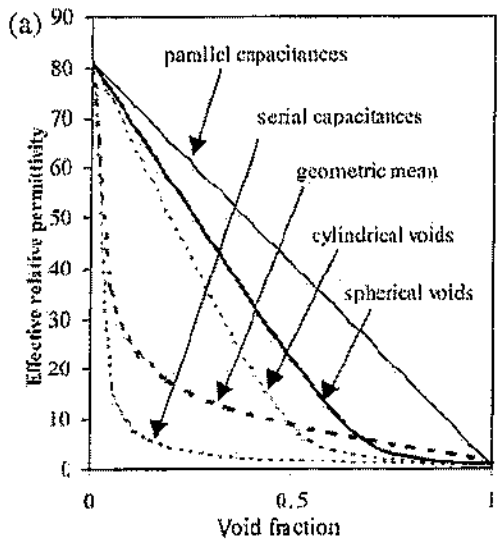

Figure 14: Effective relative permittivity as a function of the void fraction (Jaworek (2004), Figure 2 (a))

Many different types of electrodes configuration where studied; one of the most interesting to overtake the problem of non homogeneous configuration of the flow pattern was studied by Hetsroni (1982), Merilo et al. (1977)* (see Figure 10.2.6, page 10-32, Hetsoni (1982)

3.4.1. Mass flow measurement under PWR reflood conditions in a downcomer and at a core barrel vent valve location, based on the combination of a string probe with a drag disk or a turbine flow-meter (Hardy (1982)).

1. **Results: accuracy and characteristics of the response-Criteria 1-**

The drag disk-string probe combination was calibrated for both air only flow or water only flow, in a velocity range of, respectively, 2.6-31.0 m/s and 0.095-0.85 m/s, respectively.

The same combination was then calibrated for two phase flow measurements. Two correlations were required to fit the data obtained from the calibration facilities. The most important parameter to choose one correlation over the other is the flow pattern: the transition from droplet mist to froth flow seems to dictate different responses from the drag disk-string probe device. Other effects are also probable, such as the flow disturbances and variation in the slip ratio (see Figure 15).

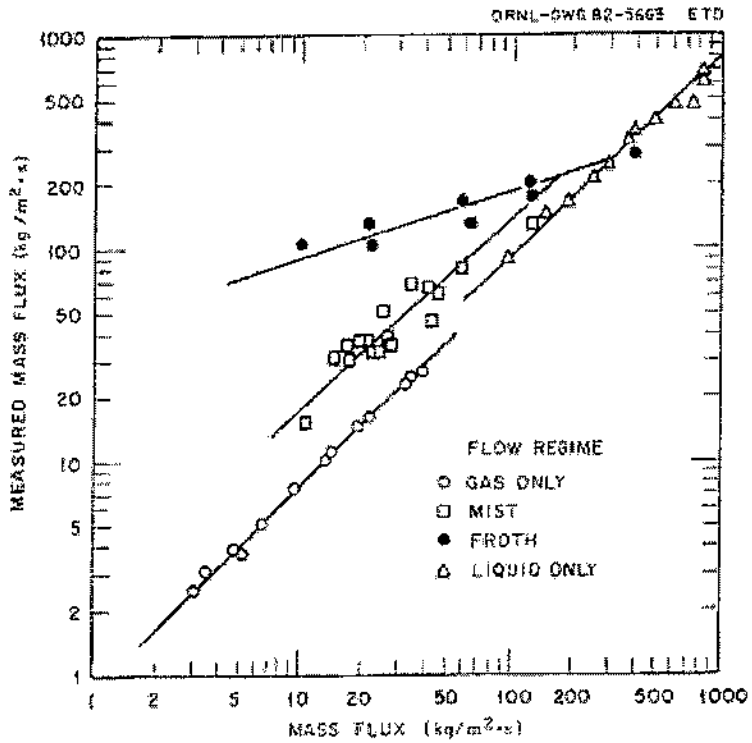

Figure 15: Drag disk and string probe data vs actual the mass flow rates for both single phase and two-phase flow (Hardy (1982), Figure 10)

The correlations evaluate the actual mass flux to within +40% and -30% for 85% of the data. The selection of the right correlation depends on the location of the sensor in the downcomer and on the flow regime (see Figure 11, Hardy and Smith (1982)).

The comparison between the values from the string probe and those from the gamma densitometer show a good agreement for $0.4 < \beta < 0.85$ $(0.15 < \alpha < 0.6)$. For liquid fraction $\beta < 0.4$ $(\alpha > 0.6)$ the string probe underestimates the results from the gamma densitometer; then the two values seem to converge again, and finally diverge for $\beta < 0.01$ $(\alpha > 0.99)$ (see Figure 16). For condition of $\beta > 0.4$ $(\alpha < 0.6)$ the flow is slug or bubble: in both cases the bubbles distribution is almost homogeneous, and the values from the gamma densitometer and the string probe correspond fairly well. For liquid fraction $\beta < 0.4$ and $\beta > 0.1-0.2$ the flow regimes are froth or annular and both tend to collect a film of water close to the pipe wall. The three beam gamma densitometer averages the entire cross section, where the string probe is more influenced by the high void fraction central region. For $\beta \approx 0.01-0.02$ $(\alpha \approx 0.98-0.99)$ the annular-mist flow regime occurs and the film on the wall is no more continuous, resulting in a more uniform distribution of voids. Finally the limit of the sensitivity of the three beam gamma densitometer is reached near $\beta \approx 0.01$ $(\alpha \approx 0.99)$ and below that value a scatter in the data is evident.

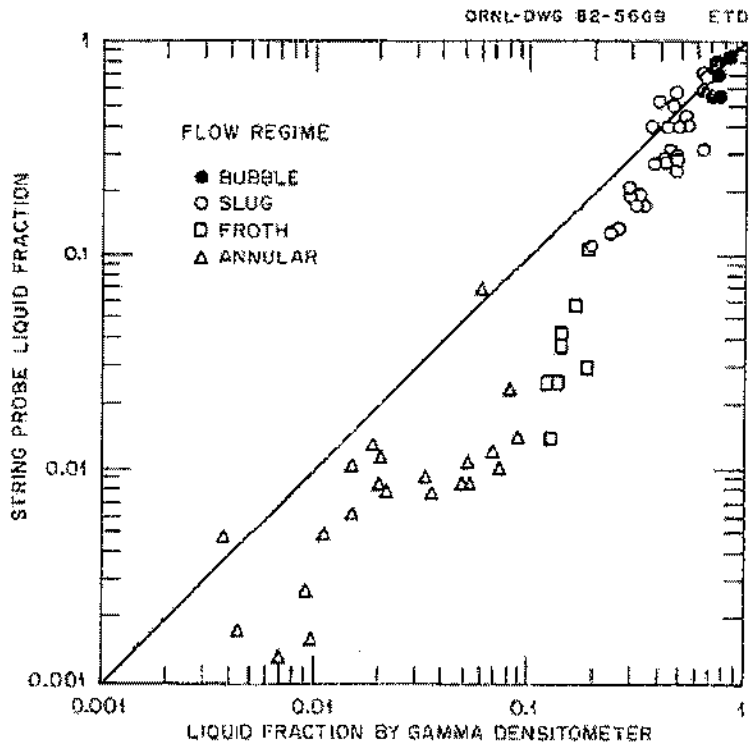

Figure 16: Comparison of liquid fraction from string probe and three beam gamma densitometer (Hardy (1982), Figure 17)

In order to obtain a value for the mass flow, the homogeneous model was adopted:

$$\dot{M} = \rho_{sp} V_T ,$$

where ρ_{sp} is the density detected by the string probe (based in the measured void fraction α and an assumption of homogeneous flow) and V_T is the velocity obtained from the turbine flow-meter. Two curves were fitted to the data (see Figure 17), above and below a break point equivalent to 5.0 kg/s for the mass flow rate:

- ✓ For the mass flow points >5 kg/s nearly all the data fell within ±30% of the calculated curve.
- ✓ For the mass flow points <5 kg/s the scatter was remarkable and only two thirds of the data fell within ±30% of the calculated curve.

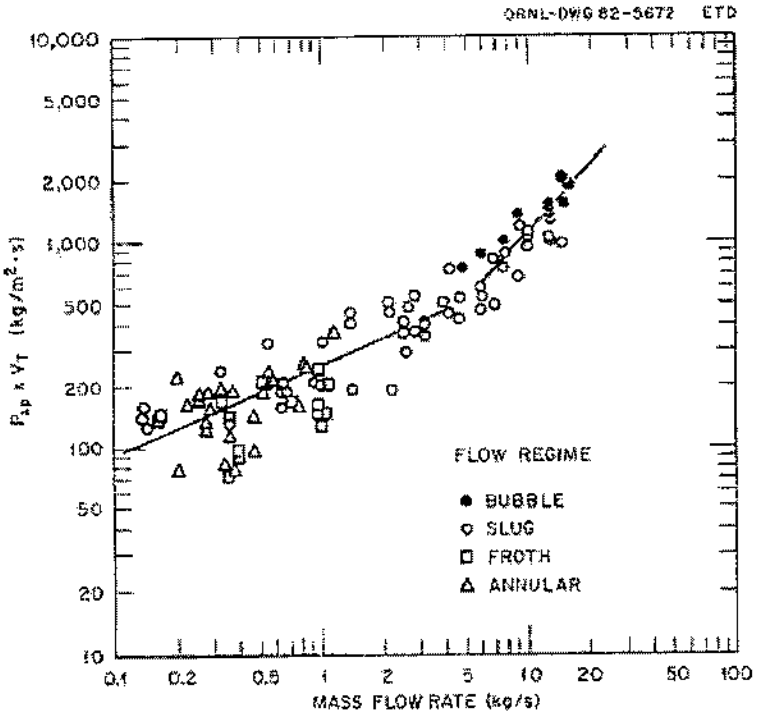

Figure 17: Actual mass flow rate compared with the mass flow rate calculated with the homogeneous model (Hardy (1982), Figure 20)

These two calibration equations were used to convert all the measurements obtained from the turbine flow-meter/string probe combination into the mass flow rate (see Figure 21, Hardy (1982)). For mass flows > 2 kg/s, 80% of the data fell within ±30% of actual mass flow rate. Below 2 kg/s, considerable scatter appear: the data fell within ±70% of the actual flow rate.

2. **Installation constraints-Criteria 2**-No issues connected with the installation constraints.

3. **Dependence of the results on the phase distribution (flow regimes analyzed in the experiment)-Criteria 3-**

   ✓ The drag disk-string probe combination was calibrated in three different types of air-water facilities. The first calibration was performed for the void fraction range $\alpha > 0.9$ (mist flow) and well homogenized conditions. The next calibration test was performed in the range $0.6 < \alpha < 1$. Finally the drag disk only was inserted in a rig simulating the liquid oscillations in the downcomer, in order to monitor the response of the disk. The calibration was implemented in order to obtain the calibration constant C:

   $$\dot{M} = C\left(\rho_{sp}\left(\rho V^2\right)_{DD}\right)^{0.5},$$

   where $\dot{M}$ is the mass flow rate, ρ_{sp} is the two phase density obtained by the string probe and $\left(\rho V^2\right)_{DD}$ is the flow momentum from the drag disk measurements.

   ✓ The liquid fraction (complement of the void fraction) determined by the string probe, was compared with that from a three beam gamma densitometer located 86 cm downstream of the string probe. The experiment span was $0 < \alpha < 1$.

4. **Temperature range and pressure range-Criteria 4 and Criteria 5-**not available
5. **Time response-Criteria 6-**NA
6. **Regulatory requirements-Criteria 7-**No issues related to the regulatory requirements.
7. **Disturbance to the flow-Criteria 8-**No data related to the disturbance to the flow are provided by the authors, but, since the design of the string probe is very similar to the design of the wire mesh sensor (described in 3.4.3), it is assumed that the pressure drop is of the same order of magnitude.
8. **Shape of the probe and configuration of the experimental circuit-**Two different types of experiments were conducted in the Slab Core Test Facility (SCTF) and in the Cylindrical Core Test Facility (CCTF):

   ✓ Installation of a drag disk-string probe combination in different locations of the STCF in order to monitor the void fraction trend during the last phases of the blowdown and the refill and reflood phases of a LOCA.

   The string probe consisted of a stainless steel frame with two stainless steel wires strung to form eight pairs of electrodes across the frame. The wires were isolated from the frame by cermet.

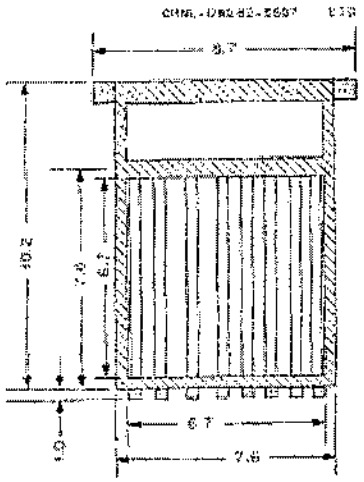

Figure 18: String probe (all dimensions in cm), Hardy (1982), Figure 4

The electrical impedance across the electrodes was measured and its signal converted in an output voltage. Using water-only and air-only calibration points and the magnitude and phase of the impedance signal, the capacitative portion of the impedance can be determined. One of the available models to reconstruct the void fraction of the mixture is to connect linearly the variation in the capacitance with the variation in the void fraction. The same type of string probe was used by Hardy and Hylton (1983).

- ✓ A string probe of the same type described in the previous paragraph, and a turbine flow-meter were installed at a vent valve location in the CCTF in order to monitor the mass flow rate passing through the valve. The combination of the two instruments measured only the 7% of the total volumetric flow (covering only the 7% of the cross section area), so to calculate the total mass flow rate the measured flow has to be multiplied by a suitable factor; assuming that the flow is well homogenized.

3.4.2. Double-layer impedance string probe for two-phase void and velocity measurements (Hardy and Hylton (1983)).

1. **Results: accuracy and characteristics of the response-Criteria 1-**

Void fraction measurements:

The values obtained from the string probe positioned in the first experimental facility were compared with the measurements of a three beam gamma densitometer (that had an accuracy of ±5% of reading). The data from both the upper and the lower level of the probe agreed quite well with the densitometer measurement. The string probe void fraction slightly overpredicted the densitometer in the range from $\alpha = 0.5$ to $\alpha = 0.95$ (up to 0.1 at $\alpha_{\gamma\,dens} = 0.58$, up to 0.3 at $\alpha_{\gamma\,dens} = 0.86$).

The probe was also tested in the second experimental facility and the obtained data were compared with the values from a gamma densitometer. There was a good agreement for α between 0.70 and 0.98. The string probe consistently measured a higher void fraction with respect to the gamma densitometer because of its position in the facility. The probe inspected the central part of the upper plenum (where the void fraction was higher), while the densitometer gave an average of the void fraction from the vessel centerline to the wall, assuring a value more coherent with the real situation (water tended to collect on the side surfaces).

Velocity measurements:

The values obtained from the probe placed in the first experimental facility were compared to the ones measured by a turbine meter. The turbines are more sensitive to the gas phase velocity at high void fractions and to the liquid velocity at low void fractions, at intermediate void fractions some theories have been studied, but none of them is widely accepted.

The string probe measures a gas phase velocity in low void fraction and a liquid phase velocity in high void fraction. The comparison between the values sensed by the string probe and the turbine flow-meter is therefore difficult. As the velocity increases (dispersed flow), the agreement becomes quite good because the string sensor is monitoring the droplets velocity and the turbine is sensing mainly the gas velocity, but the flow is almost homogenized and so the slip ratio approaches 1.

Other observations based on the analysis of the string probe velocity measurements confirm the theory that the string is approaching the turbine flow meter values at high and low velocities because the slip ratio in both cases is almost 1 (see Figure 19)

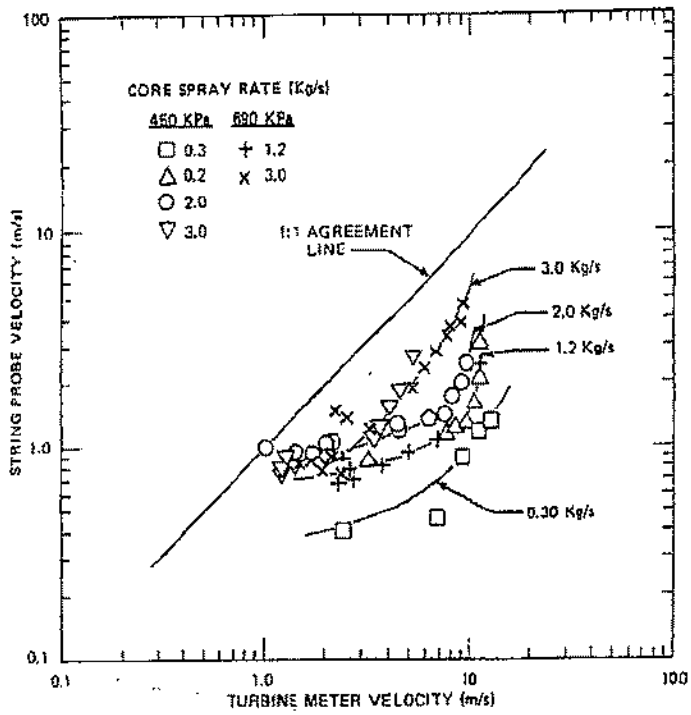

Figure 19: Velocity comparison of the string probe and turbine meter (Hardy and Hylton (1983), Figure 13)

The probe is able to measure a large range of flow velocities (1-17 m/s) and void fraction (0.25-0.99), with a good repeatability.

2. **Installation constraints-Criteria 2**-No issues connected with the installation constraints.
3. **Dependence of the results on the phase distribution (flow regimes analyzed in the experiment)-Criteria 3**-The formula to evaluate the void fraction is based on model 1) of the total permittivity (plate voids perpendicular to the electrodes):

$$\alpha \propto \frac{\varepsilon_l - \varepsilon_e}{\varepsilon_l - \varepsilon_g},$$

where ε_g is the permittivity of the gaseous phase, ε_l the permittivity of the liquid phase and ε_e is the permittivity measured between the electrodes. This linear relation is not always valid because it is affected by the presence of different flow regimes. The effect of the conductance on the impedance phase angle was used to estimate the distribution of the liquid phase (and therefore the flow pattern) and hence its influence on the capacitance-void fraction relationship. A correction is applied to the value of the relative capacitance according to the flow regime present. For a more detailed

description of this method see Hardy et al (1983), Hylton and Muller (1980)*, Hylton and McGill (1981)*.

The probes were also used to detect the velocity of the two phase mixture, using a technique of analysis of random signal from two spatially separated impedance probes. The flow disturbances can be sensed at the two locations with a time delay τ. In pure bubble flow the method will measure an average bubble velocity (so the velocity of the gas phase), in droplet flow an average droplet velocity will be detected, but in slug or froth flow the gas-liquid interface velocity are not necessarily the phase velocities. In annular-mist flow both the velocities of droplets and waves will be detected. A good knowledge of the existing flow pattern is therefore necessary to interpret correctly the results obtained with the velocity measurements.

4. **Temperature range and pressure range-Criteria 4 and Criteria 5**-three different experimental loops were tested:
   - ✓ A test rig that operated at pressure up to 10 bar and temperature up to 170°C with a wide range of steam and water flow rates.
   - ✓ A full scale vertical section of an upper plenum to measure void fraction in air-water mixtures (temperature and pressure range is not available).
   - ✓ A steam-water circuit that operated in the pressure range 2-7 bar (the temperature range is not available).

   The probe was designed and fabricated to operate under severe thermohydraulic conditions: temperature up to 350°C and thermal transient of 300°C/s.
5. **Time response-Criteria 6**-NA
6. **Regulatory requirements-Criteria 7**-No issues related to the regulatory requirements.
7. **Disturbance to the flow-Criteria 8**-No data related to the disturbance to the flow are provided by the authors, but, since the design of the string probe is very similar to the design of the wire mesh sensor (described in 3.4.3), it is assumed that the pressure drop is of the same order of magnitude.
8. **Shape of the probe and configuration of the experimental circuit**-The probe consist in a pair of steel wires (electrodes) strung back and forth across a rectangular stainless steel frame. There are two electrodes layers to allow the measurement of the velocity. They are characterized by an axial spacing of 1.90 cm and an electrode to electrode spacing of 0.25 cm (see Figure 1, Hardy and Hylton (1983)). Two wires are

strung per layer, creating a pair of electrodes. The wires were electrically insulated from the frame by a cermet (ceramic-metal material).

3.4.3. Wire mesh sensor for gas-liquid flow visualization with up to 10000 frames per second (Prasser et al. (1998), Prasser et al. (2002), Prasser et al. (2000)) (void fraction, average local gas velocity, transition from bubble to annular flow)

1. **Results: accuracy and characteristics of the response-Criteria 1**-Prasser et al. (1998) firstly compared the response from the two different types of impedance sensors to the signal obtained from a single beam gamma densitometer. The volumetric gas fraction was averaged over time and diameter. The agreement between the heavy sensor with rods and the gamma densitometer is very good, while there is a systematic error of up to 8% for the wire mesh sensor compared to the gamma densitometer (see Figure 6, Prasser et al. (1998)).

   In their first experiment with the 24x24 wire mesh sensors, Prasser et al. (2002) studied the transition from bubble to plug flow with a time resolution of 0.4 ms (2.5 kHz). They fixed the superficial water velocity and varied the superficial air velocity. They reconstruct the air velocity profile in the pipe for different values of the superficial air velocity. The profiles follow qualitatively the classical turbulent liquid velocity profile with an offset due to the bubble rise velocity. The central maximum of the velocity increases as the void fraction maximum shifts from the periphery to the center of the pipe (Figure 20 and Figure 11, Prasser et al. (2002)).

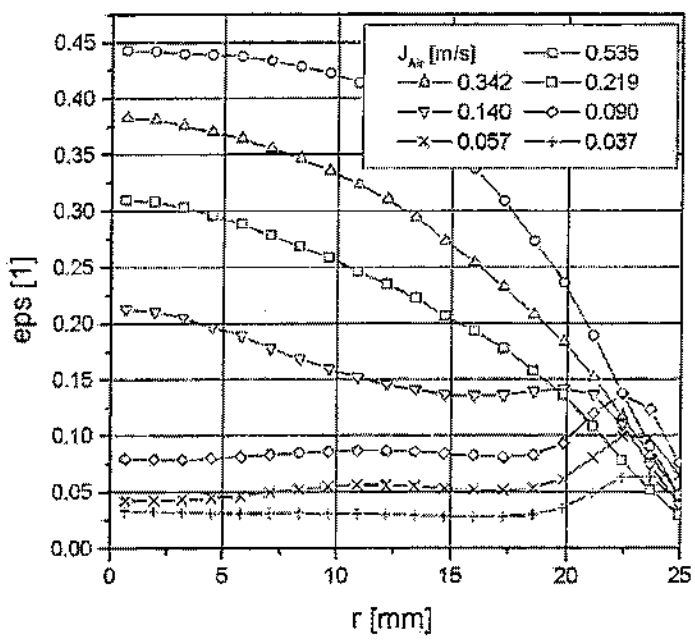

Figure 20: Radial gas fraction for superficial air velocity equal to 1.02 m/s and varied superficial gas velocities, Prasser et al. (2002), Figure 10

In the second experiment with the 16x16 wire mesh sensor, the authors visualized the transition from bubble to annular flow. The high frequency of the data detection (10000 Hz) permitted to identify precisely the plug-like periodic structures in the transition region between bubble and annular flow (see Figure 22).

In both experiments (Prasser et al. (2002)) the results presented the flow structure in the vertical cross sections. The images were assembled from the consecutive results in the horizontal cross sections. They are obtained by calculating the void fraction distribution along the pipe diameter for each time step and by stacking the different frames as colored bars in a vertical sequence. (Figure 21).

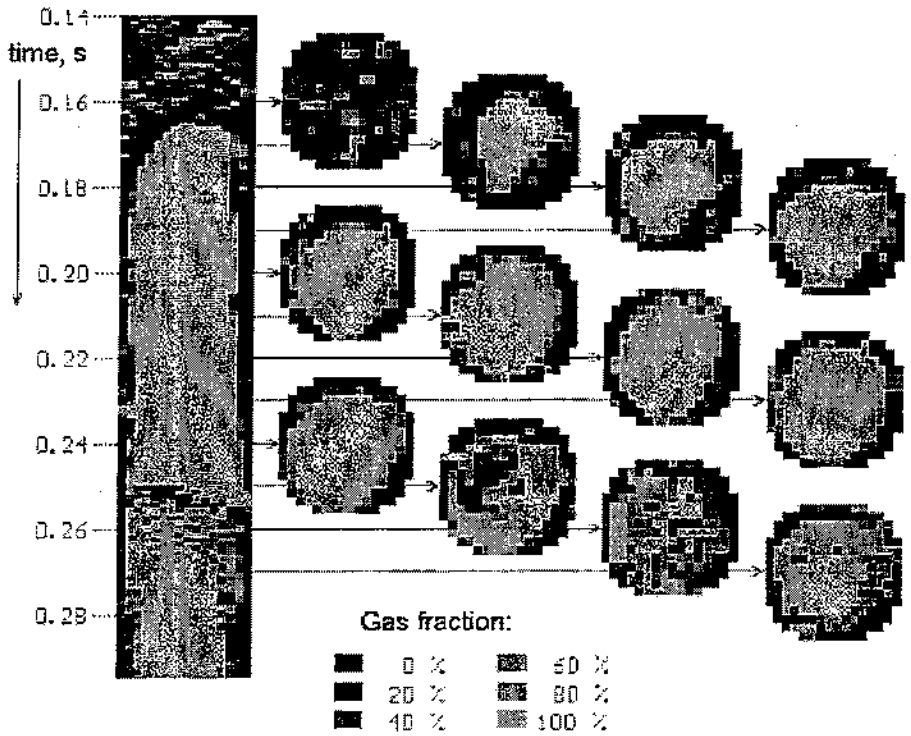

Figure 21: Sequences of local instantaneous gas fractions obtained in a vertical slug flow, Prasser et al. (2002), Figure 6

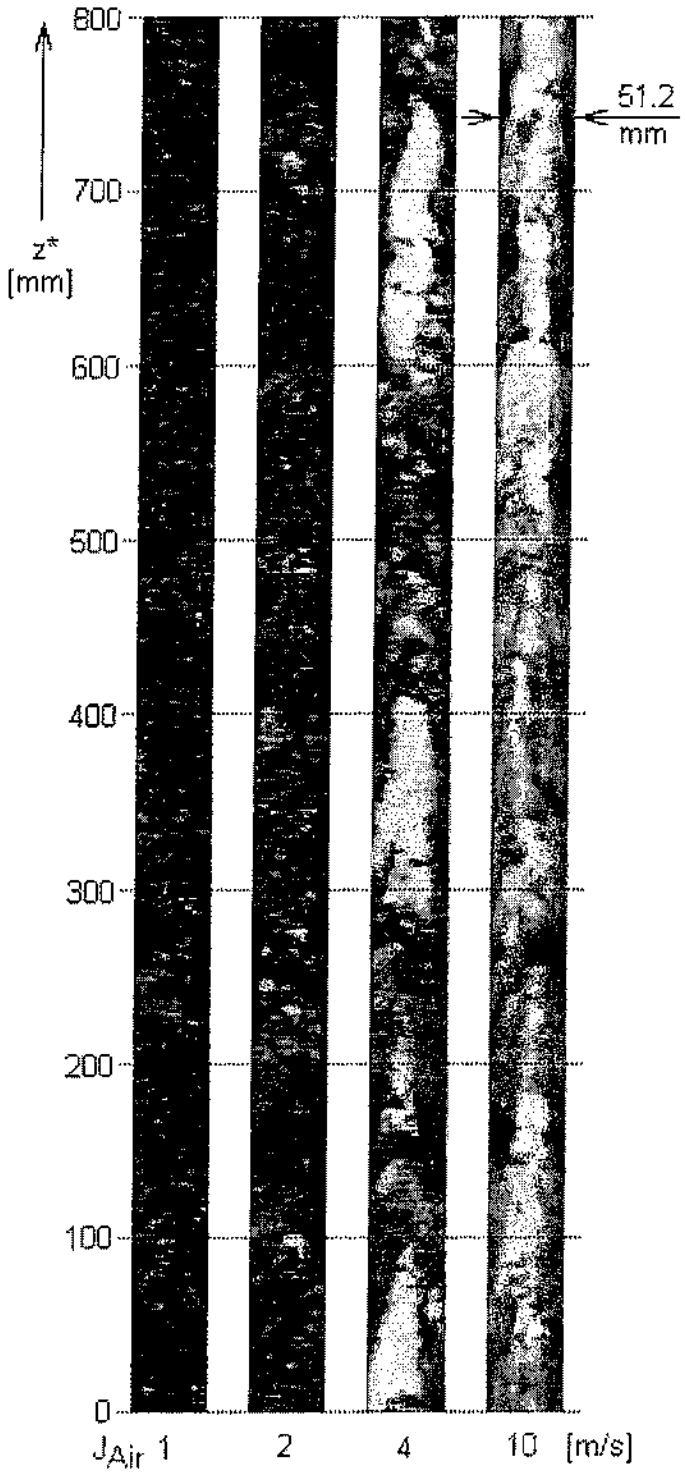

Figure 22: Virtual sectional views with superficial water velocity equal to 4 m/s, recorder with the wire mesh sensor at 10000 Hz; churn-turbulent flow, Prasser et al. (2002), Figure 14

In case of steady flow condition, the vertical time axis can be converted in a virtual z (height) axis by scaling it with the average phase velocity of the gaseous phase. If this

(v_{air}) cannot be measured, it can be approximated using the superficial air velocity (J_{air}) and the averaged void fraction $\overline{\alpha}$:

$$z^* = \overline{v_{air}} \cdot t \cong \frac{t \cdot J_{air}}{\overline{\alpha}}.$$

2. **Installation constraints-Criteria 2**-No issues connected with the installation constraints.
3. **Dependence of the results on the phase distribution (flow regimes analyzed in the experiment)-Criteria 3**-in the 1998 experiments the superficial velocity of water was kept constant at 1 $\frac{m}{s}$, while the superficial velocity of air was varied in the range 0.14-12 $\frac{m}{s}$. The flow regime evolved from bubble flow $\left(J_{air} = 0.14\frac{m}{s}\right)$ to annular flow $\left(J_{air} = 12\frac{m}{s}\right)$. $J\left[\frac{m}{s}\right]$ represents the superficial velocity.

   In the experiment with the two 24x24 wire mesh sensors described by Prasser et al. (2002) J_{water} was kept constant $\left(1.02\frac{m}{s}\right)$. J_{air} varied in the range 0.037 $\frac{m}{s}$-0.835 $\frac{m}{s}$. The flow regimes observed in this range started from bubble flow and evolved to plug flow.

   In the second experiment with only one 16x16 wire mesh sensor (Prasser et al. (2002), the minimum value for J_{water} was $1\frac{m}{s}$, while the maximum value was $4\frac{m}{s}$. J_{air} was increased from $1\frac{m}{s}$ to $10\frac{m}{s}$. The flow regime in this case changed from bubble to annular.
4. **Temperature range and pressure range-Criteria 4 and Criteria 5**-the maximum fluid pressure and temperature for the sensor with lentil-shaped rods are respectively 7 MPa and 80°C, but a sensor for higher pressure and temperature (16 MPa and 350°C) was under development at that time (Prasser et al. (1998)).
5. **Time response-Criteria 6**-the time resolution for the probes in the 1998 experiments was 1024 frames per second.

   The second experiment described by Prasser et al. (2002) applied a new design of the data acquisition digital circuit with a time resolution of 10000 frames per second for).

The authors also presented the result of another experiment with a time resolution of 2500 frames per second.

6. **Regulatory requirements-Criteria 7**-No issues related to the regulatory requirements.
7. **Disturbance to the flow-Criteria 8**-In the 1998 experiments two different probe designs were tested:
   - ✓ The wire mesh sensor for lab application is characterized by a percentage of free cross-section area of 96% (for one grid) and a pressure drop coefficient (k) equal to 0.04 for a single grid (based on equation $\Delta p = k\rho v^2$).
   - ✓ The sensor with enforced rods for high mechanical loads is characterized by a percentage of free cross section area (for one grid) of 73% and a pressure drop coefficient of 0.2 (for a single grid)

   The authors assumed that the pressure drop coefficients for the two grids can be added.
8. **Shape of the probe and configuration of the experimental circuit-**

   In 1998 two new different types of probes were introduced by the author:
   - ✓ Wire mesh sensor for lab application: it consists of two planes of 0.12 mm diameter wire grids with 16 wires each. This type of probe showed a limited mechanical stability. The distance between the two planes is 1.5 mm. The sensor is characterized by 16x16=256 cross points (measuring points). See Figure 23.

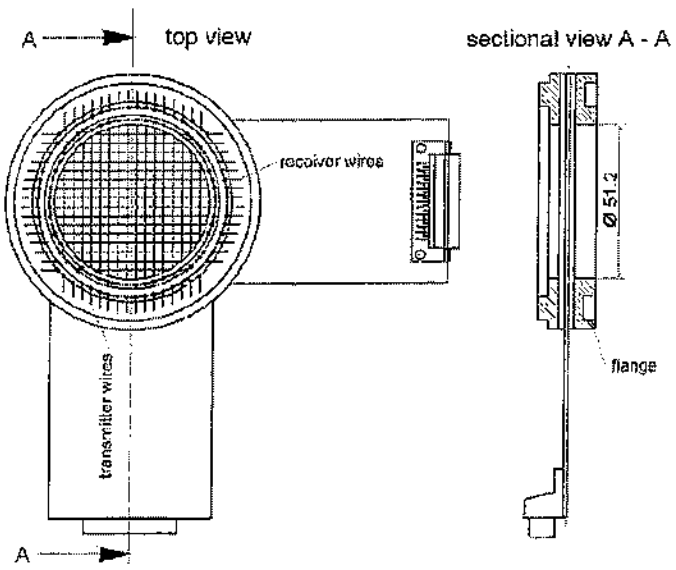

Figure 23: Wire mesh sensor for lab applications (16x16 sensitive points), Prasser et al. (1998), Figure 3.

- ✓ Sensor with enforced electrode rods for high mechanical loads. This type of sensor was manufactured in two different versions:
  - 8 electrodes in each plane (64 measuring points) for a 50 mm diameter pipe.
  - 16 electrodes in each plane (256 measuring points) for a 100 mm diameter pipe.

The rods are lentil-shaped in order to reduce the pressure drop across the sensor. In the design by Prasser et al. (1998), two planes of wires formed an angle of 90° and the impedance is measured between a wire of the first plane (transmitter) and a wire of the second plane (receiver). The related void fraction is the value referred to the volume near the crossing point between the two wires. During the measuring cycle the transmitter electrodes are activated by a circuit in a successive order. A two dimensional matrix of values of current measured between the transmitters and the receivers is stored. It is related to the conductivities between all the crossing points. To convert the conductivity values into void fraction values, a calibration with the pipe filled with liquid and filled with gas was performed. A linear dependence between gas fraction and conductivity is assumed:

$$\alpha = \frac{\sigma - \sigma_l}{\sigma_g - \sigma_l};$$

σ is the measured conductivity, σ_l is the conductivity with the channel full of liquid and σ_g is the conductivity with the channel full of gas.

A part of the driving current could flow from the activated transmitter to the neighboring transmitters and from these to the receivers, causing a blurring (loss of spatial resolution) of the acquired images. In order to avoid this cross-talk phenomenon, both the outputs of the transmitters and the inputs of the receiver were designed with impedance significantly lower than the impedance of the fluid. In this way the potential of all the wires, except that one of the activated transmitter, cannot depart from zero.

The experiments (Prasser et al (1998)) were realized in a 51.2 mm vertical pipe with air-water flow.

The main structure of the sensor described by Prasser et al. (2002) is analogue to the first one presented (the new wire mesh probe for lab application introduced in 1997), but it has a different number of wires.

The 24x24 wire mesh sensors were employed to visualize the transition from bubble to slug flow in a 51.2 mm diameter pipe with vertical air-water flow. Thus, the electrode pitch is 2 mm. The two layers (transmitters layer and receivers layers) are placed at an axial distance of 1.5 mm. The two sensors were positioned with a small axial distance (37 mm or 52.5 mm) in order to sense the average local gas velocity by means of the cross correlation technique.

An additional test (Prasser et al (2002)) was performed with only one 16x16 wire mesh sensor to study the transition from bubble to annular flow in a 51.2 mm diameter pipe with air-water flow. The electrode pitch is 3 mm. The two layers (transmitters layer and receivers layers) are placed at an axial distance of 1.5 mm.

3.4.4. Comparison between wire-mesh sensor and ultra-fast X-ray tomograph for air-water flow in a vertical pipe (Prasser et al. (2005)).

1. **Results: accuracy and characteristics of the response** Criteria 1 the first type of comparison involved both cross section images and virtual section images reconstructed plotting time sequences of void distributions over the diameter (see Figure 24 and Figure 25).

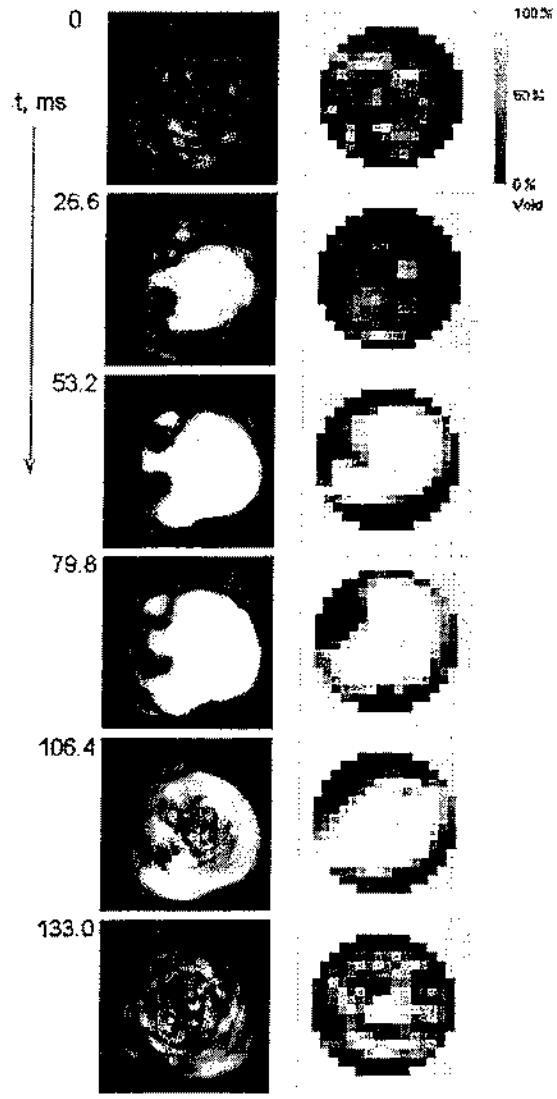

Figure 24: Time series of selected void fraction distributions during the passage of a gas plug with superficial water velocity equal to 0.24 m/s and superficial air velocity equal to 0.3 m/s; left X-ray scanner, right wire-mesh sensor, Prasser et al. (2005), Figure 6

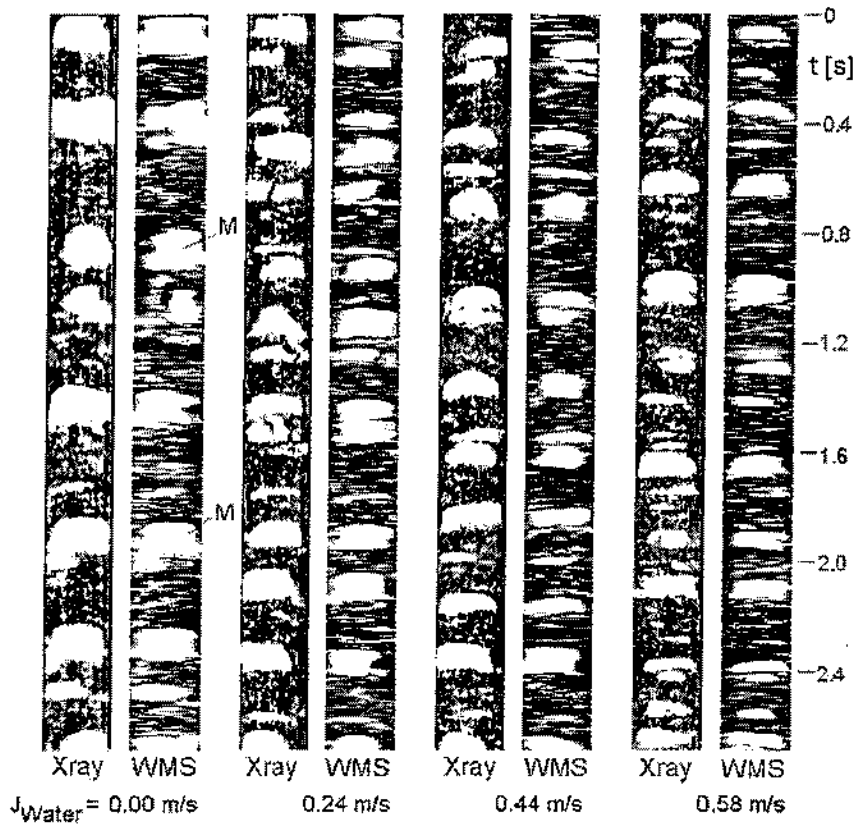

Figure 25: Virtual sectional view of the void fraction distributions measured by X-ray tomography and wire mesh sensor for superficial air velocity equal to 0.3 m/s, M indicates distorted mushroom-like bubbles at stagnant liquid), Prasser et al. (2005), Figure 7

The agreement between the measuring methods is very good. However two problems were emerging:

- ✓ At low liquid velocities the wire-mesh sensor tends to modify the typical shape of Taylor bubbles (www.glossary.oilfield.slb.com, 5 May 2008) into a mushroom-like shape (big bubbles as in slug flow).
- ✓ The image reconstruction from the X-ray system was unsatisfying in the case of a bubbly flow, because the tomograph operates at a frequency that is too low to catch the movements of a small bubble in all the 18 recorded positions. Consequently the algorithm that reconstructs the real image, based on the recorded data, fails in monitoring the rapid bubble movements.

All the available data were used to calculate average values of the void fraction over the entire cross section and measuring period. The absolute deviation between the two

methods is of the order of magnitude of 10% for both the gas injections devices (see Figure 11, Prasset et al. (2005)).

In order to avoid the second type of error described above (due to the reconstruction algorithm), a simple exponential model for the absorption of the X-rays in the water was implemented; it contains some improvements to overcome errors due to the:

- ✓ Sensitivity of the X-ray detectors decreases with time, and
- ✓ Intensity of the X-ray source is not constant.

The averaged cross sectional void fraction from the X-ray device, using the exponential model, was then compared with the correspondent value obtained from the wire mesh sensor. The most important conclusions are:

- ✓ The agreement between wire-mesh and X-ray tomography is good for the bubbly flow at the beginning of measurement. Despite using a correction for the changes in the X-ray detectors sensitivity, after 1-2 s a growing deviation was found (Lower portion of Figure 14, Prasser et al. (2005)).
- ✓ In the case of large Taylor bubble, the qualitative agreement is generally quite good (Figure 15, Prasser et al. (2005)). The passage of the bubbles is recorded. However, the void fraction during the passage of large Taylor bubbles is underestimated by the wire-mesh sensor, because of a film of water entrained in the wake of the first plane of wires (upper portion of Figure 14, Prasser et al. (2005) and Figure 15, Prasser et al. (2005)).

The comparison of the void fraction averaged over the cross section and for the first second of measurements gave the following results:

- ✓ A very good correspondence is verified between wire-mesh sensor void fraction and X-ray scanner void fraction for bubbly flow (the greatest deviation from the line of ideal correspondence reaches about 1%)
- ✓ For the plug flow the agreement is less good because of the underestimation of the local void fraction inside the large Taylor bubbles. The discrepancy rises up to 4%.

2. **Installation constraints**-Criteria 2-No issues connected with the installation constraints.
3. **Dependence of the results on the phase distribution (flow regimes analyzed in the experiment)**-Criteria 3-The test was performed in an air-water mixture, for superficial

gas velocity in the range 0.02-0.4 m/s, while the liquid velocity varied from 0 to 0.69 m/s. Both bubbly and slug flow were reproduced using two different types of injectors.

4. **Temperature range and pressure range-Criteria 4 and Criteria 5**-The tests were performed with a mixture of air and water at ambient temperature and pressure.
5. **Time response-Criteria 6**-The wire-mesh sensor used in this experiment operates at a 1053 Hz frequency, while the X-ray tomography reaches a frequency of 263 Hz.
6. **Regulatory requirements-Criteria 7**-No issues related to the regulatory requirements.
7. **Disturbance to the flow-Criteria 8**-The pressure drop caused by the wire mesh sensor is of the same order of magnitude of the one described in paragraph 3.4.3.
8. **Shape of the probe and configuration of the experimental circuit**-The tests were carried out in a vertical acrylic glass pipe of 42 mm inner diameter supplied with air-water mixture.

   The authors suggest low attenuation wall materials such as beryllium or carbon composites for the measurement region in high pressure and temperature conditions.

   The X-ray computer tomography (CT) machine has a framing time of 3.8 ms. 18 X-ray sources are placed along a circle of diameter 120.5 mm. Each source is activated in a successive order by an electronic control. The radiation penetrating the object is measured by a ring of 256 CdTe detectors. The radiation of each source reaches a sector of 60 pixels (detectors) located opposite to the given X-ray focus. A complete set of projections is captured in 3.8 ms, so a scanning rate of 263 Hz can be attained.

   The wire-mesh sensor used in this experiment is of the same type of the one described in 3.4.5. It's equipped with 16 receiver and 16 transmitter wires of 120 μm diameter. The measuring matrix has consequently the dimension 16x16. The sensor operates at a frequency of 1053 Hz. Its inner diameter is equal to the diameter of the test pipe (42 mm), the lateral pitch of the wires is 2.6 mm (42/16=2.6 mm), the distance between the two grids (the two wire layers) is 1.7 mm.

   The two instruments were positioned 15 cm apart in the same pipe, the wire mesh sensor was downstream of the X-ray device in order not to influence the flow. The data were recorded for 4 s. The sampling frequencies for the wire-mesh sensor and the fast X-ray CT were set at 1053 Hz and 263 Hz respectively.

3.4.5. Wire-mesh sensors for two phase flow studies (Pietruske and Prasser (2007))

1. **Results: accuracy and characteristics of the response-Criteria 1-**

Two identical 50 mm sensors were placed at a distance of 63 mm in the test section in order to obtain a velocity profile for the gaseous phase using a cross correlation method. The superficial gas velocity at the sensor location was calculated by an integration of the void fraction distribution and the gas velocity profile over the cross section. The results obtained are shown in Figure 14, Pietruske and Prasser (2007).

The superficial velocity of the gaseous phase for the 195 mm probe was calculated directly from the injected steam flow rate, because a second sensor to realize a cross correlation was not available. The results related to the bigger probe are shown in Figure 26.

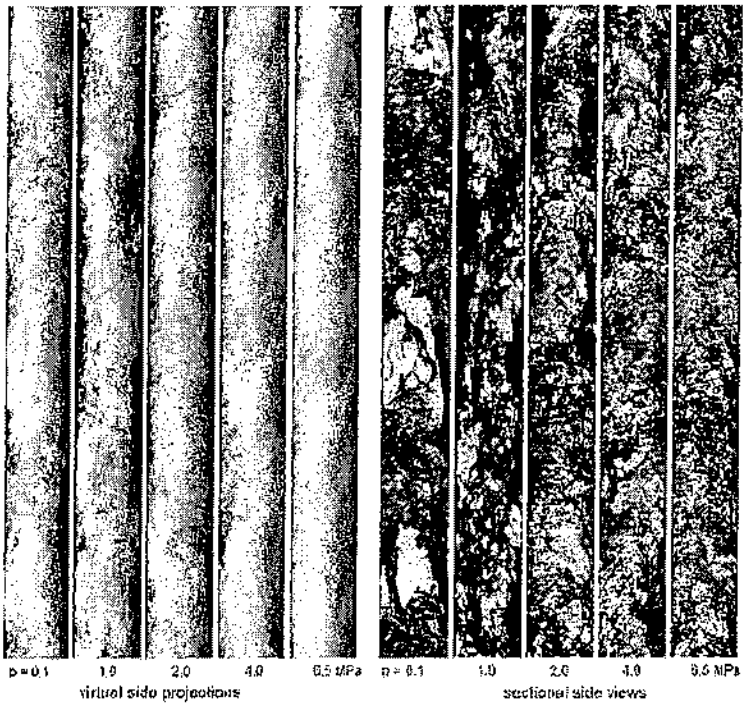

Figure 26: Vizualisation of wire-mesh sensor data obtained for the 195.3 mm diameter pipe, superficial air velocity = 0.84 m/s, superficial water velocity = 1 m/s, L/D = 39.7, Pietruske and Prasser (2007), Figure 15

The superficial velocity of the liquid phase was 1 m/s in both experiments, while the gas superficial velocity is almost always constant and change around 1 m/s (from 0.76 to 1.34 m/s).

2. **Installation constraints**-Criteria 2-No issues connected with the installation constraints.
3. **Dependence of the results on the phase distribution (flow regimes analyzed in the experiment)**-Criteria 3-The experiments were realized for both the sensors trying to maintain the same superficial velocities for both the gaseous phase and the liquid phase and changing the pressure. The flow patterns visualized are characterized by a sluggish flow at the minimum value of pressure (0.1 MPa); the slugs dissolve and the flow pattern moves towards churn turbulent structure with increasing pressure.
4. **Temperature range and pressure range**-Criteria 4 and Criteria 5-the tests were performed at 1, 2, 4 and 6.5 MPa (the maximum pressure allowed is 7 MPa) and at 180, 212, 250 and 280°C correspondingly (the maximum temperature allowed is 286°C).
5. **Time response**-Criteria 6-up to 10 kHz.
6. **Regulatory requirements**-Criteria 7-No issues related to the regulatory requirements.
7. **Disturbance to the flow**-Criteria 8-The pressure drop caused by the wire mesh sensor is of the same order of magnitude of the one described in paragraph 3.4.3.
8. **Shape of the probe and configuration of the experimental circuit**-the type of probe tested is the same described in 3.4.3 A complete two dimensional conductivity distribution is obtained (Figure 1, Pietruske and Prasser (2007)).

   Two probes were tested:

   - ✓ The bigger one has an inner diameter of 195 mm with a matrix of 64x64 measuring wires of 120 μm diameter. The electronic is able to register 2500 samples per second.
   - ✓ The smaller one has an inner diameter of 50 mm with a 16x16 matrix of measuring wires. The electronic is able to register samples up to a frequency of 10 kHz.

   The production process of both the sensors is very complicated because they have to compensate temperature dilatation of the wires and to provide a simple mechanism for the substitution of broken wires. The construction has also to withstand rapid temperature transients.

3.4.6. Conductance probe to measure the liquid fraction in two-phase flow (Fossa (1998))

1. **Results: accuracy and characteristics of the response** Criteria 1-The tests were conducted with a two-phase air-water mixture, measuring the resistive component of the flow.

   The void fraction measurements were compared with the theoretical formulas from Fossa (1998), Coney (1973)*, Tsochatzidis et al (1992)*, for the prediction of the conductance of a two phase flow characterized by the presence of a liquid film. Fossa (1998), Maxwell (1882)* and Breuggeman (1935)*, studied the analytical formulas to connect the void fraction and the conductivity in a uniformly dispersed two phase flow (used for bubbly flow).

   A preliminary set of experiments was carried out to find some reference values for the conductance (e.g. the conductance of the pipes filled with water).

   The conductance was measured for different flow patterns and probe geometry and then normalized with respect to the conductance of the pipes full of liquid. The data collected were plotted against the mean liquid fraction and compared to the theoretical formulas. The mean liquid fraction was obtained using a method based on differential pressure measurements.

   For the section A under stratified conditions the scatter between the theoretical data (Fossa (1998), Coney (1973)*) and the measured value is within 8%. The agreement increased with a bigger spacing between the electrodes (24 mm instead of 14 mm). See Figure 27.

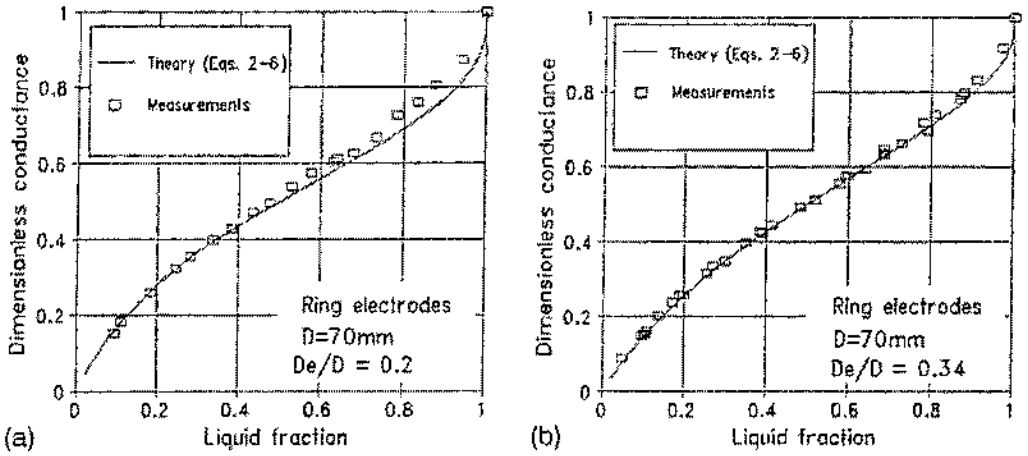

Figure 27: Measured and theoretical dimensionless conductance for two different electrode spacing, ring electrodes under stratified flow conditions, Fossa (1998), Figure 3

The same analysis was conducted on the data obtained from section A, under bubbly flow regime, for void fraction from 0.74 to 1. Fossa (1998), Maxwell (1882)* equation corresponds almost perfectly with the data obtained from the two electrodes positioned 24 mm apart, while the data from the 14 mm spaced electrodes shown a worse agreement. See Figure 28.

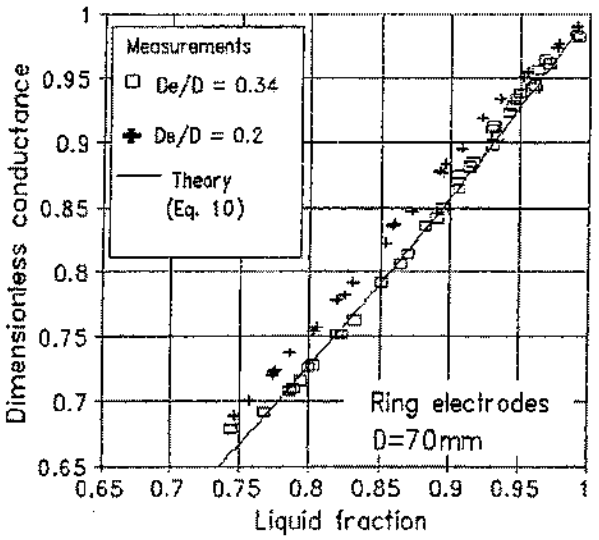

Figure 28: Measured and theoretical dimensionless conductance for two different electrode spacing, ring electrodes under bubbly flow conditions. De indicates the distance between the electrodes, Fossa (1998), Figure 4

The response under annular flow conditions was evaluated using both section A and B. Section A presents results that follows the predicted trends (Fossa (1998), Tsochatzidis et al (1992)*) with a maximum error of 10%. The theory can take in account differences in the electrodes spacing. Section B (ring electrodes) is analyzed under the same condition and shows a scatter of the measured data of 15% with respect to the theoretical values (Fossa (1998), Coney (1973)*, Tsochatzidis et al (1992)*).

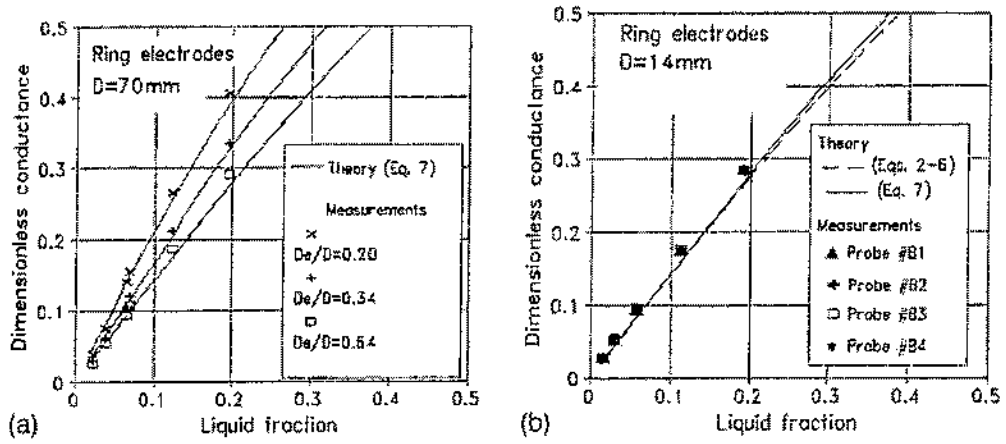

Figure 29: Measured and theoretical dimensionless conductance for two probe geometries: (a) ring electrodes D=70 mm, (b) ring electrodes D=14 mm. De indicates the distance between the electrodes, annular flow, Fossa (1998), Figure 5.

This validates the procedure of introducing the adequate ratio (higher) between De (ring electrode spacing) and D (pipe diameter) to describe properly the influence of the distance between the plates in the theoretical analysis.

No analytic formulas are available for the investigation of the behavior of plate electrodes, so just a comparison with the response from ring electrodes was performed; the plate electrodes show a great sensitivity to the changes in liquid fraction and are frequently affected by the presence of surface pollutants (e.g. air bubbles), so calibration is strictly recommended before a set of measurements.

2. **Installation constraints-Criteria 2**-No issues connected with the installation constraints.
3. **Dependence of the results on the phase distribution (flow regimes analyzed in the experiment)-Criteria 3**-three different flow patterns were analyzed: bubble, stratified and annular.
4. **Temperature range and pressure range-Criteria 4 and Criteria 5**-Not available
5. **Time response-Criteria 6**-The signal sampling rate is 300 Hz.

6. **Regulatory requirements-Criteria 7**-No issues related to the regulatory requirements.
7. **Disturbance to the flow-Criteria 8**-No data related to the disturbance to the flow are provided by the authors. The probes tested were built in two different designs: ring electrodes and plate electrodes. In both cases their shape was very thin and they were positioned on the inner side of the pipe, adherent to the surface. It can be supposed that the influence on the flow is very little.
8. **Shape of the probe and configuration of the experimental circuit**-two different configurations for the test section were used. The first one (A) is a pipe made of Plexiglas, 70 mm internal diameter, 480 mm long, equipped with three flush ring electrodes located 14 mm and 24 mm apart.

   The second one (B) is a cylinder made of PVC, 14 mm internal diameter, 70 mm long, used only for annular flow. It's equipped with two ring electrodes (width 1 mm, located 9 mm apart) and two plate electrodes (3 mm diameter, located 9 mm apart in the pipe axis direction.

3.4.7. Capacitance sensor for void fraction measurement in water/steam flows (Jaworek et al (2004)).

1. **Results: accuracy and characteristics of the response**-Criteria 1-during the measurements the void fraction distribution along the mixing chamber was evaluated with an error estimated to be of the order of magnitude of 10%. The reference frequency ω_l with the steam injector full of water was measured just after all the measurements to guarantee the same temperature conditions. This is because water conductivity and permittivity depend on temperature variations. The authors claim that the sensors tested are a "simple, low cost and non invasive method, which allows determining void fraction and avoiding flow distortions".
2. **Installation constraints**-Criteria 2-No issues connected with the installation constraints.
3. **Dependence of the results on the phase distribution (flow regimes analyzed in the experiment)**-Criteria 3-During the calibration the void fraction was determined from an increase in the water level (due to the bubbles flowing upward) in the cylinder on which the electrodes were mounted. The authors calculated theoretically the relative frequency deviation of the oscillator based on the all five models of calculation of the relative permittivity of a mixture as a function of the void fraction (Figure 2(b), Jaworek et al. (2004)).

   Then they compared their results to the experimental values of frequency deviation shown in Figure 30.

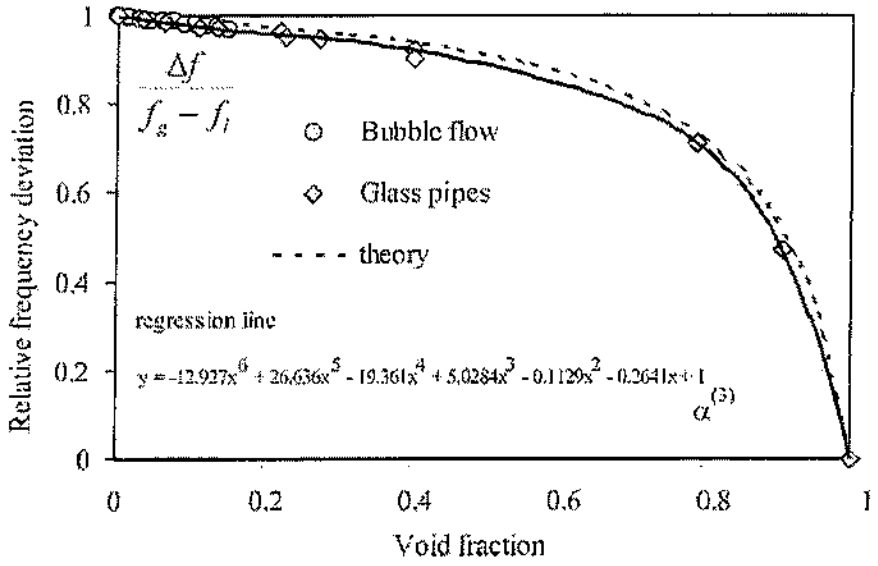

Figure 30: relative frequency deviations vs void fraction (continuous line in the 6th polynomial approximation), Jaworek et al. (2004), Figure 3

The authors concluded that the only model that can predict the real behavior of the void fraction is the parallel capacitance model. A calibration curve was obtained, fitting the experimental data, for both bubble flow (up to $\alpha = 15\%$) and annular flow up to $\alpha = 1$.

4. **Temperature range and pressure range**-Criteria 4 and Criteria 5-the test was performed in a steam injector, assembled of a steam nozzle, a mixing chamber and a diffuser (see Figure 4, Jaworek et al. (2004)). The steam temperature in the test circuit was 142°C. The three set of data were obtained with a throat pressure of 13.9, 64.1 and 130.3 kPa, respectively.
5. Time response-Criteria 6-NA
6. **Regulatory requirements**-Criteria 7-No issues related to the regulatory requirements.
7. **Disturbance to the flow**-Criteria 8-The probe does not cause any influence on the flow, since the electrode are mounted on the external surface of the pipe.
8. **Shape of the probe and configuration of the experimental circuit**-the evaluation of the capacitance of a two-phase steam-water mixture was realized using a high frequency (80 MHz) voltage to supply energy to the electrodes. This high frequency was chosen in order to cut off the influence of the resistive component of the impedance.

   The sensors were connected as a capacitance in a LC-resonant circuit (radio frequency oscillator). The oscillator is very sensitive to capacitance variations of the steam water

mixture causing frequency deviation. The comparison between the frequency of the oscillator and the reference value of an external oscillator lead to the capacitance measurement. The structure of the sensor and of the equivalent circuit is shown in Figure 1, Jaworek (2004).

The capacitance sensors were made in the form of two strips of 10 mm width, mounted outside of a pipe made by polycarbonate. They were monitoring the void fraction in a steam injector. Four pairs of electrodes were mounted across the mixing chamber and other four across the diffuser.

3.5. *References

Arnold, R. M., and Pitts, R. W., (1981)*, Fluid flow meter for mixed liquid and gas, *US patent 4,272,982, June16.*

Baker, C. R., (2000), Flow measurement handbook, *Cambridge University Press.*

Bearden, R. G., (1977)*, Progress on LOFT upgrade drag disk-turbine separate effects tests, *US Nuclear Regulatory Commission, Proceedings of Meeting of Review Group on Two Phase Flow Instrumentation,* NUREG-0375 (Paper No I.5).

Bergles, A. E. et al , (1981), Two-phase flow and heat transfer in the power and process industries, *Hemisphere, Washington, McGraw-Hill,* New York.

Bruggeman, D. A. G., (1935)* Berechnung verschiederen physikalischer Konstanten von heterogenen Substanzen, *Annalen phys.* 24(5), 636-664.

Chen, N.

C. J., Felde, D. K., (1982), Two phase mass flux uncertainty analysis for thermal-hydraulic test facility instrumented spool pieces, *ORNL.*

Coney, M. W. E., (1973)* The theory and the application of conductance probes for the measurement of liquid film thickness in two phase flow, *J. Phys. E: Scient. Instrum.*, 6:903-10.

Felde, D. K., (1982), Design concept and testing of an in-bundle gamma densitometer for subchannel void fraction measurements in the THTF electrically heated road bundle, *ORNL.*

Fossa, M., (1998), Design and performance of a conductance probe for measuring the liquid fraction in two-phase gas-liquid flows, *Flow Measurement and Instrumentation,* Volume 9, Issue 2, Pages 103-109.

Ginesi, D., (1991)*, Chosing the best flowmeter, *Chem. Eng.*, NY, 98(4):88-100.

Goodrich, L. D., (1979)*, Design and performance of the drag disk turbine transducer, *Int. Collq.*, Idaho Falls, ID, June.*

Hardy, J. E., (1982), Mass flow measurements under PWR reflood conditions in a downcomer and at a core barrel vent valve location, *ORNL*

* The references signed with * refer to publications that were not directly consulted.

* The references signed with * refer to publications that were not directly consulted.

Hardy, J. E. and Hylton , J. O., (1983), Electrical impedance string probes for two-phase void and velocity measurements, *ORNL, Int. J. Multiphase Flow,* Vol. 10, No. 5, pp. 541-556

Hardy, J. E. and Smith J. E., (1990), Measurement of two-phase flow momentum with fore transducers, Oak Ridge National Laboratory, Tennessee.

Hetsroni, G., (1982) Handbook of multiphase systems, *Hemisphere,* Washington.

Hewitt, G. F., (1978), Measurement of two phase flow parameters, *Academic Press Inc.,* London.

Hylton, J. O. and Muller, R. C., (1980)*, Impedance probe void fraction measurements, *Proc. Rewiev Group Conf. on Advanced Instrumentation Research For Reactor Safety,* pp. IV. 11-1 to 11-21, NUREG/CP-0015, Oak Ridge, Tennessee.

Hylton , J. O. and McGill, R. N., (1981)*, Measurement of velocity and void fraction in steam-water mixtures with electrical impedance probes, *Proc. OECD (NEA) CSNI 3rd Specialists Meeting on Transient Two-Phase Flow,* CSNI Rep. No. 61, Pasadena, California.

Hunter, J. J. and Green W. L., (1975)*, Blockage and its effect on a drag plate flowmeter, *Conf. on Fluid Flow Measurement in the Mid 1970's,* East Kilbride, Scotland: National Engineering Laboratory, Paper C-2.

Jaworek, A., Krupa, A. and Trela, M., (2004), Capacitance sensor for void fraction measurement in water/steam flows, *Flow Measurement and Instrumentation,* Volume 15, Issues 5-6, October-December 2004, Pages 317-324.

Kamath, P. S., and Lahey, R. T., (1977)*, A turbine meter evaluation model for two phase transients, *Rensselaer Polytechnic Institute,* NES-459.

Kratzer, W., and Kefer, V., (1988)*, Two phase flow instrumentation: a survey and operational experience with new and easy-to-handle devices, *Cranfield short course lecture.*

Makovsky, A., (1983)*, Medical imaging systems, Prentice Hall, Englewood Cliffs, NJ.

Maxwell, J. C., (1882)*, A treatise on electricity and magnetism, Oxford: *Clarendon Press.*

* The references signed with * refer to publications that were not directly consulted.

McPherson, G. D., (1977)*, Results of the first three non nuclear tests in the LOFT facility, *Nucl. Safety*, 18(3), 306-316.

Merilo, M., Dechene, R. L. and Cichowlas, W. M. (1977)*, Void fraction measurement with a rotating electric field conductance gauge, *J. Heat Transfer*, 99: 300-302.

Misawa, M., Ichikawa, N. Akai, M., Hori, K., Tamura, K. and Matsui, G., (1998), Development of fast X-ray system for transient two-phase flow measurement, *6th International Conference on Nuclear Engineering*, San Diego, California.

Petrick, M. and Swanson, B. S., (1958)*, Radiation attenuation method of measuring density of a two phase fluid, *Rev. Scient. Instrum.*, 29(12), 1079-1085.

Pietruske, H. and Prasser, H.-M. Wire-mesh sensors for high-resolving two-phase flow studies at high pressures and temperatures, *Flow Measurement and Instrumentation*, Volume 18, Issue 2, Pages 87-94.

Prasser, H. -M., Böttger, A. and Zschau, J., (1998), A new electrode-mesh tomograph for gas–liquid flows, *Flow Measurement and Instrumentation*, Volume 9, Issue 2, Pages 111-119.

Prasser, H.-M., Krepper, E., Lucas, D., Zschau, J., Peters,D., Pietzsch,. G., Taubert, W., Trepte, M., (2000), Fast wire-mesh sensors for gas-liquid flows and decomposition of gas fraction profiles according to bubble size classes, *2nd Japanese-European Two-Phase Flow Group Meeting*, Tsukuba, Japan

Prasser, H.-M., Zschau, J.,Peters, D., Pietzsch, G., Taubert, W., Trepte, M., (2002), Fast wire-mesh sensor for gas-liquid flows – Visualisation with up to 10000 frames per second, *ICAPP 2002*, Hollywood, Florida, Paper #1055.

Prasser, H.-M., Misawa, M. and Tiseanu, I., (2005), Comparison between wire-mesh sensor and ultra-fast X-ray tomograph for an air-water flow in a vertical pipe, *Flow Measurement and Instrumentation*, Volume 16, Issues 2-3, Pages 73-*83.

Priddy, W. J., (1994)*, Fields trial of multiphase metering systems at Prudoe Bay, Alaska, *SPE 69th Annu. Tech. Conf. Exhib.*, New Orleans, LA: 531-43.

Smorgav, A. E., (1990)*, Multiphase flow meter KO 300 MFM, *North Sea Flow Measurement Workshop*, East Kilbride: Scotland, National Engineering Laboratory.

* The references signed with * refer to publications that were not directly consulted.

Tsochatzidis, N. A., Karapantios, T. D., Kostoglou, M. V., Karabelas, A. J., (1992)*, A conductance method for measuring liquid fraction in pipes and packed beds, *Int. J. Multiphase Flow*, 5:653-657.

Turnage, K. G. and Jallouk, P. A., (1978)* Advanced Two Phase Instrumentation. Program Quart. Prog. Rep., for April-June 1978, NUREG/CR-0501 (ORNL/NUREG/TM-279).

Turnage, K. G., Davis, C. E. and Thomas, D. G., (1978)* Advanced Two Phase Instrumentation. Program Quart. Prog. Rep., for July-September 1978, NUREG/CR-0686 (ORNL/NUREG/TM-309).

Xiaozhang, Z., (1995)*, New multi meter system for flow measurement of water-oil-gas mixture, ISA Advances in Instrumentation and Control: Int. Conf. Exhib., 50(1):113-20.

www.engineeringtoolbox.com/target-flow-meters-d_497.html, 22 February 2008

www.glossary.oilfield.slb.com, 5 May 2008

www.aaliant.com, 5 May 2008

4. Conclusions

An analysis of instruments capable of measuring the two-phase mass flow rate inside the pipe lines of the SPES3 facility has been performed.

The most important accidental scenario is represented by the Direct Vessel Injection line break (DVI Lower Break). The main parameter that needs to be monitored during the simulation of the transient is the mass flow rate coming out of the Reactor Vessel into the containment. Since the density of each phase is not known, it is necessary to measure both the velocity of the two-phase flow (with a flow-meter) and the density of each phase (with a densitometer).

The measurement of the two-phase flow velocity is influenced by the velocity profile and by the phase distribution inside the pipe (i.e. by the flow pattern).

The next step will be to find the proper combination of instruments and the choice of the instruments will be based on the geometry of the DVI lines and DVI break lines and on the mass flow rates and void fractions expected in those lines, too.